1-1-2002

Polyelectrolyte electrophoresis : effects of molecular weight and molecular architecture.

Cynthia F. Welch
University of Massachusetts Amherst

POLYELECTROLYTE ELECTROPHORESIS: EFFECTS OF MOLECULAR WEIGHT AND MOLECULAR ARCHITECTURE

A Dissertation Presented

by

CYNTHIA F. WELCH

Submitted to the Graduate School of the
University of Massachusetts Amherst in partial fulfillment
of the requirements for the degree of

DOCTOR OF PHILOSOPHY

May, 2002

Polymer Science and Engineering

POLYELECTROLYTE ELECTROPHORESIS: EFFECTS OF MOLECULAR WEIGHT AND MOLECULAR ARCHITECTURE

A Dissertation Presented

by

CYNTHIA F. WELCH

Approved as to style and content by:

David A. Hoagland, Chair

Surita R. Bhatia, Member

M. Muthukumar, Member

Helmut H. Strey, Member

Thomas J. McCarthy, Department Head
Polymer Science and Engineering

DEDICATION

To Paul, for persuading me to undertake this task,

and to Tabitha, for persuading me to finish it.

ACKNOWLEDGMENTS

I would like to thank my advisor, David Hoagland, for his guidance, advice, and friendship. Without his contributions, my time at UMass would have been far less productive and fun. My committee members were also instrumental in helping me achieve this goal through many suggestions and discussions regarding my work. Surita Bhatia, M. Muthukumar, and Helmut Strey each played a significant role in the success of my work and in my professional growth.

I would also like to gratefully acknowledge the funding sources for this work, Nalco Chemical Company and the NSF-sponsored Materials Research Science and Engineering Center (MRSEC) at UMass. In addition to funding my work, both sources provided me with opportunities for professional growth.

Further thanks go to the entire PS&E faculty, staff, and students for maintaining such a high caliber department and encouraging the pursuit of science. I also received some much-appreciated help and useful discussions from the many members of the Hoagland, Strey, and Muthu groups, especially Brian Price, Doug Howie, Kingshok Ghosh, and Paul Welch. I would also like to express my appreciation to Griselda Bonilla and Vladimiros Nikolakis for assistance with some light scattering experiments.

Finally, I would like to acknowledge the untiring support and encouragement of my family. My parents, Ray and Gayle Farmer, not only provided me with an excellent foundation but have also demonstrated an unceasing belief in my abilities and judgment. And there are not enough words to express my thanks to my husband Paul, not just for his extensive help as a fellow student, but also for his gifts of friendship, motivation, and *agape*.

ABSTRACT

POLYELECTROLYTE ELECTROPHORESIS: EFFECTS OF MOLECULAR WEIGHT AND MOLECULAR ARCHITECTURE

MAY 2002

CYNTHIA F. WELCH, B.S., UNIVERSITY OF SOUTHERN MISSISSIPPI

M.S., UNIVERSITY OF SOUTHERN MISSISSIPPI

Ph.D., UNIVERSITY OF MASSACHUSETTS AMHERST

Directed by: Professor David A. Hoagland

The work described in this dissertation reveals the potential of electrophoretic techniques for the characterization and better understanding of polyelectrolyte solutions. The dependence of electrophoretic mobility μ on parameters such as solution ionic strength, polymer charge density, molecular weight, and chain architecture are explored. For oligomers, the free solution electrophoretic mobility μ_0 exhibits an unambiguous maximum with respect to molecular weight M; lowering solution ionic strength I accentuates this poorly understood phenomenon. Though the dependence of μ_0 on M disappears at higher M, electrophoretic migration through dilute neutral polymer solutions will give M-dependent μ-distributions for high M polyelectrolytes. Until now, this capillary electrophoresis technique was limited to polyanion analysis; a method of overcoming the technological challenges of analyzing polycations with this technique is presented here. The new ability to analyze polycations via capillary electrophoresis opens the door to many new investigations into polyelectrolyte solution behavior. This capability is demonstrated by a comprehensive study of protonated dendrimers; μ_0 is investigated as a function of I, dendrimer charge, and dendrimer radius. The results match predictions of the standard electrokinetic model for a dielectric sphere, revealing that the relaxation effect dominates the electrophoretic behavior of highly charged dendrimers.

TABLE OF CONTENTS

LIST OF TABLES

Table

Page

LIST OF FIGURES

Figure

Page

CHAPTER 1

INTRODUCTION

Electrophoresis, or the migration of a charged solute in an applied electric field, can be a powerful tool for the analysis of polyelectrolytes. Electrophoretic techniques have revolutionized the fields of biochemistry and molecular biology, allowing for the molecular weight analysis of proteins and the sequencing/sizing of DNA. The advances in electrophoretic methods have even played a significant role in the success of the human genome project. While the biopolymer community has realized the great potential of electrophoretic techniques, these same techniques have played only a limited role in the investigations of synthetic polymers. Unlike biopolymers, most synthetic polymers are neither charged nor water-soluble; without these properties, electrophoretic characterization is generally impossible. Polyelectrolytes, which possess both of these properties, are only seldom characterized via electrophoretic methods. However, investigators have achieved impressive results for some polyelectrolytes by adapting protocols established for biopolymers. Such adaptations usually require much trial and error, and none have made the routine analysis of polycations possible. The difficulties arise from shortcomings in both scientific and technological areas. On scientific grounds, the existing theories for polyelectrolyte electrophoresis generally fail to capture the experimentally observed behavior; worse yet, experimental results reported by various authors show large discrepancies, even for the same polymer system. On technological grounds, the inability to directly copy established biopolymer protocols results from issues ranging from detection difficulties to undesirable interactions between the polyelectrolyte and the electrophoresis medium (i.e., capillary or gel).

The goal of this dissertation is to address both types of difficulties. First, we will use model polyelectrolytes to systematically test the existing electrophoresis theories,

thereby improving the molecular-level understanding. Because some of these experiments may best be accomplished with polycations, we also aim to overcome the technological challenges associated with capillary electrophoresis of polycations. The end results should begin to unleash the potential of electrophoretic methods for the analysis and understanding of synthetic polyelectrolyte solutions.

1.1 The Technique: Capillary Electrophoresis

Historically, the primary electrophoretic method has been gel electrophoresis. However, capillary electrophoresis experiments became feasible about two decades ago, and the advantages of using a capillary system have steadily increased since that time. These advantages include shorter analysis times, easy automation of both the experiment and data collection, and truly quantitative detection of solutes.

Figure 1.1 shows the simple instrumentation required for capillary electrophoresis. A fused silica capillary is positioned between positive and negative electrodes in two buffer reservoirs. Because the capillary is composed of silica, negative siloxy charges exist along its walls. The positive counterions for these surface charges move toward the cathode when an electric field is applied. This motion drags the rest of the solvent along as well, creating an electroosmotic flow which essentially has a plug flow profile. This flat profile differs from pressure-driven parabolic flows and has the advantage of less severe broadening effects on sample bands. Sample injection occurs electrokinetically by placing the sample solution at the appropriate electrode and applying the electric field for a short period of time. The buffer reservoir then replaces the sample solution and the field is reestablished. The sample begins to migrate toward the in-line concentration detector (usually a UV absorbance detector) at a rate determined by both electroosmosis and electrophoresis. The experimentally measured variable is the electrophoretic mobility μ, defined as the ratio of the solute velocity V to the applied

electric field E. When E is low, μ can be regarded as a fundamental physico-chemical property that reflects the equilibrium properties of the polymer and its environment. Essentially, μ characterizes the polymer's motion down a gradient of electrical potential.

In this dissertation, the capillary technique is used to investigate three problems in polyelectrolye electrophoresis. The first two deal with molecular weight effects, and the last examines the issue of molecular architecture.

1.2 Oligomer Electrophoresis in Free Solution

Chapter 2 describes the dependence of the free solution electrophoretic mobility μ_0 on molecular weight M for linear polyelectrolytes. For the first time, a maximum in μ_0 with respect to M is clearly demonstrated. The maximum occurs in the oligomer range for poly(deoxythymidine) and is strongly affected by solution ionic strength. This maximum was previously suggested by experiments with poly(styrene sulfonate); however, no physical basis for a maximum in μ_0 is currently known. Rather, theory predicts a rise in μ_0 in the low M range and then a plateau in the high M range. The observed maximum will clearly be an enormous hindrance to the use of free solution electrophoresis for separating polyelectrolyte oligomers.

1.3 Polycation Electrophoresis in Neutral Polymer Solutions and Gels

As mentioned above, μ_0 is independent of M for high molecular weight linear polyelectrolytes. To impart a size-dependent μ_0 and allow for separations by molecular weight, a relatively new capillary electrophoresis technique may be used. In this technique, a dilute solution of neutral polymers acts as a tenuous matrix of obstacles that entangle the migrating polyelectrolytes. The entanglement reduces the electrophoretic mobility μ according the the molecular weight of the polyelectrolyte (and of the neutral polymer). Thus far, however, fractionation of polyelectrolytes by capillary

electrophoresis has been limited to negatively charged polymers. Application to polycations poses a major technological challenge, as strong electrostatic interactions will cause adsorption of the polycation to the negatively charged capillary. In Chapter 3, we show how a cationic surfactant can be used to create a dynamic capillary coating that will eliminate adsorption problems. This approach enables robust and high-resolution polycation analysis, as demonstrated by the separation of three protonated or quaternized poly(2-vinylpyridine)s. Further, electrophoretic analyses by the new method give information regarding molecular weight distributions and suggest how poly(2-vinylpyridine)s degrade/crosslink when exposed to quaternizing conditions for an excessive period.

Appendix A describes the extension of the above work to high molecular weight commercial polycations. These polycations present further challenges because they possess varying degrees of charge and are difficult to detect via UV absorbance. Efforts to fractionate these polymers began with the capillary electrophoresis technique and evolved into the initial development of a gel electrophoresis method for cationic polymers.

1.4 Cationic Dendrimer Electrophoresis in Free Solution

Dendrimers define a class of structurally symmetric, highly branched polymers whose configurational and solution properties differ substantially from those of analogous linear polymers. Polyelectrolyte dendrimers contain charged sites at their termini, at their branch points, or at both positions. Chapter 4 focuses on how the electrophoretic motion of polypropylenimine dendrimers compares to that of a comparably sized sphere or flexible linear polymer. The dendrimer serves as a model system due to its well-defined charge properties and uniform degree of branching. As the degree of charge α is varied, the dendrimer's electrophoretic behavior resembles that of a

linear polymer: μ_0 increases sharply at low α and begins to plateau in the intermediate α range. However, the data also agree with predictions for a charged sphere when nonlinear electrostatic effects are included. Quantitative agreement with this same sphere model is achieved as ionic strength is varied for solutions of fully charged dendrimers. The overall results show that nonlinear electrostatics dominate the behavior of charged dendrimers and suggest that similar mechanisms may be operative for linear polyelectrolytes.

1.5 Summary

This dissertation reveals the potential of electrophoretic techniques for the characterization and better understanding of polyelectrolyte solutions. The overall goal is to provide comprehensive experimental results that can be compared to existing theories; in doing so, we aim to increase our understanding of polyelectrolyte solution behavior and demonstrate where the theories may be improved. Chapter 5 gives an overview of the results and discusses possible future investigations, specifically with polycations in nonaqueous or mixed solvent systems. Such studies would give additional insight into the manner in which counterions affect the electrophoretic mobility of charged polymers.

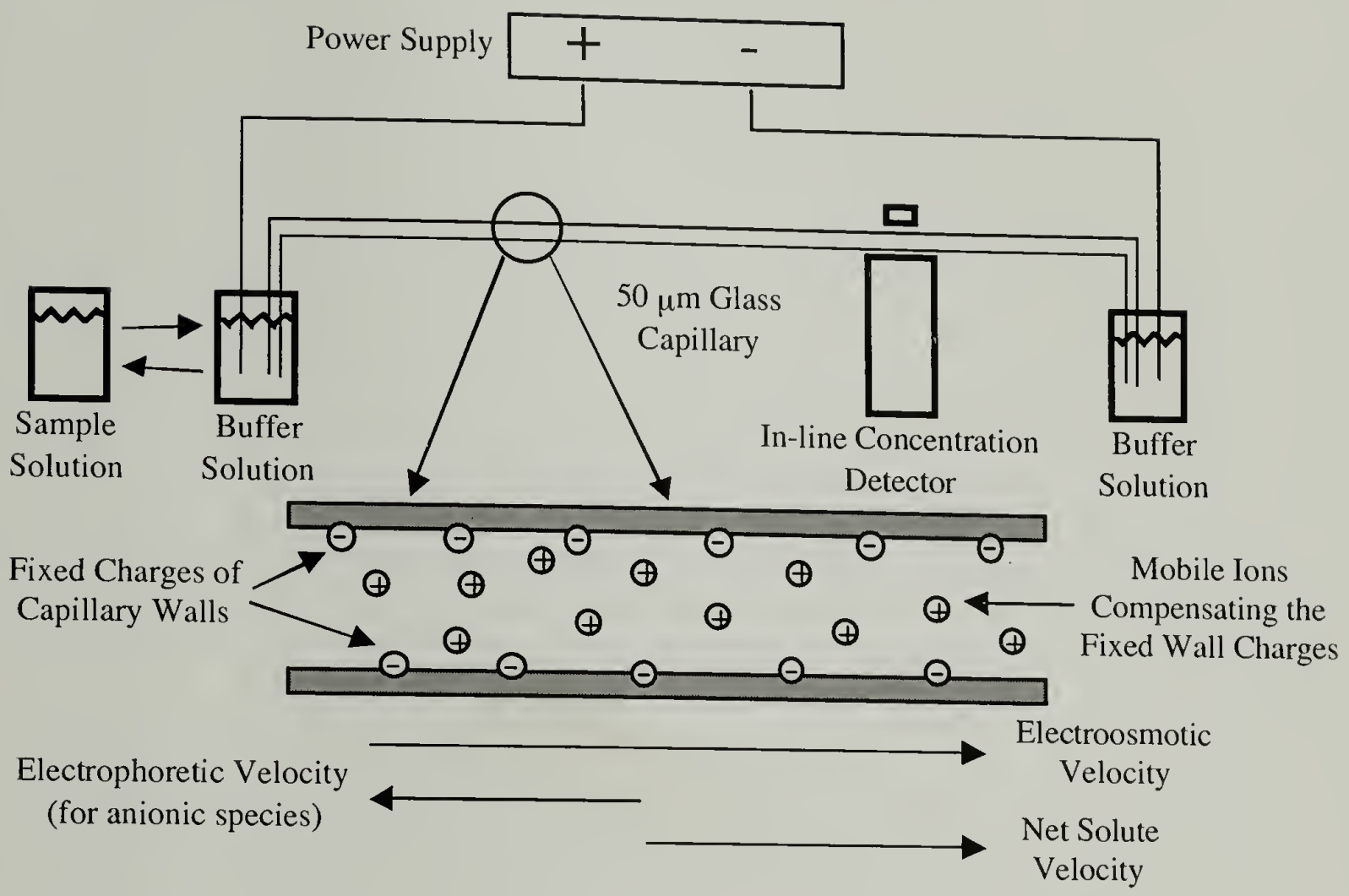

Figure 1.1. Schematic of capillary electrophoresis instrumentation.

CHAPTER 2

FREE SOLUTION MOBILITY OF OLIGOMERS

2.1 Abstract

An unambiguous maximum of the free solution electrophoretic mobility μ_0 with respect to molecular weight M is discovered in the oligomer range for poly(deoxythymidine); lowering ionic strength I accentuates this phenomenon. Previous experiments with poly(styrene sulfonate) implied the possibility of a maximum; however, no physical basis for a maximum in μ_0 is currently known. Rather, theory predicts a logarithmic M dependence at low M that flattens to M independence at high M. The observed maximum will complicate any electrophoretic analysis of oligomers, whether in free solution, neutral polymer solutions, or gels.

2.2 Background: Molecular Weight Dependence of Free Solution Electrophoretic Mobility

The biopolymer community depends heavily on electrophoretic techniques to characterize and separate proteins and DNA by molecular weight M; these techniques also hold great potential for the analysis of synthetic polyelectrolytes. The most common methods, gel electrophoresis and capillary electrophoresis in neutral polymer solutions, assume that the free solution electrophoretic mobility μ_0 is independent of M and that all of the M dependence comes from the matrix material (either the gel or the neutral polymer solution). Both theory and experiment indicate this assumption is valid for high molecular weight polymers, but a strongly M-dependent μ_0 persists in the oligomer range. Most published data for uniformly charged polymers show that μ_0 increases to M independence for M greater than about 10-40 monomer (or base) units [1-6]. Recently,

however, Stellwagen et al. [7] reported that μ_0 for duplex DNA rises with M for chains containing up to 400 base pairs; in an earlier report, Cohen et al. [8] showed that differences in μ_0 allow duplex DNA restriction fragments of up to 23,000 base pairs to be separated electrophoretically in a complex, free solution environment. The situation may be even more complicated, as previous experiments in our laboratory with oligomeric poly(styrene sulfonate) imply a maximum in μ_0 with respect to M [9]. We believe disagreement about the M dependence of μ_0 may be resolved by systematic experiments with lower M polyelectrolytes.

2.2.1 Theory

When an electric field is applied to a charged solute, four forces will govern the solute's motion through the solution. The direct electric force F_e felt by the charged solute is given by $F_e = QE$, where Q is the charge and E is the applied field. As the solute moves through the viscous medium of the surrounding solvent, it also experiences a hydrodynamic drag force F_h which slows its motion. If a polyelectrolyte can be modeled as a cylinder, F_h can be approximated by $F_h = 3\pi\eta VL/ln(L/2a)$, where η is the solvent viscosity, V is the cylinder's steady-state velocity, and L and a are the cylinder's length and radius, respectively.

The remaining two forces acting on the solute result from effects of the electric field on the charged solute's counterions. As the counterions experience an electric force in the opposite direction of the charged solute, they will create hydrodynamic disturbances that exert a retardation force F_r to slow the motion of the charged solute. Though the total charge magnitude of the counterion cloud matches that of the solute, $F_r \neq -F_e$ because some of the effect is dampened by the surrounding viscous medium. Because the amount of dampening depends on the distance between the solute and its counterions, F_r is a strong function of solution ionic strength. The distribution of counterions around the solute is needed to calculate F_r; this information may be derived

from the nonlinear Poisson-Boltzmann equation or, in some cases, estimated by the Debye-Hückel approximation.

The calculation of F_c assumes that the polyelectrolyte and its counterion cloud retain their equilibrium conformations in the presence of the applied electric field. While typical electric field strengths used in electrophoresis are orders of magnitude too low to affect the polyelectrolyte's conformation, the structure of the counterion cloud is likely to be distorted if the solute charge density is high. Distortion of the counterion cloud leads to a combination of electric and hydrodynamic effects which give rise to the fourth force, termed the relaxation force F_r. More specifically, as the counterion cloud's center of charge moves away from that of the solute, a local dipole field oriented opposite to the applied field is created. In addition, since the counterion cloud will be distorted such that more counterions are on the downstream side of the solute, the hydrodynamic drag on the solute will increase. Under conditions where F_r is important, the distribution of counterions must be calculated from the nonlinear Poisson-Boltzmann equation.

The force balance on a charged solute in dilute solution may be written as

$$F_e - F_h - F_c - F_r = 0 \tag{2.1}$$

Henry [10] first solved this equation within the Debye-Hückel approximation to predict the electrophoretic behavior of cylinders with low charge density. In this case, F_r vanishes and the dimensionless mobility μ_0' is given by

$$\mu_0' = \frac{2\xi K_0(a\kappa)}{a\kappa K_1(a\kappa)}\beta(a\kappa) \tag{2.2}$$

where ξ is the dimensionless charge density parameter, a is the cylinder radius, κ is the inverse Debye length, K_0 and K_1 are Bessel functions, and $\beta(a\kappa)$ varies smoothly from 1.0 ($a\kappa = 0$) to 1.5 ($a\kappa = \infty$). The electrophoretic mobility is defined as the ratio of solute

velocity V to electric field magnitude E, and μ_0 is made dimensionless through division by $2\varepsilon_0\varepsilon kT/3\eta e$; such a dimensionless parameter provides for easier and more meaningful comparisons between experiments and theories. The charge density parameter is given as

$$\xi = \frac{e^2}{4\pi\varepsilon_0\varepsilon kTb} = \frac{l_b}{b} \tag{2.3}$$

where e is the electron charge, ε_0 is the permittivity of a vacuum, ε is the dielectric constant, k is the Boltzmann constant, b is the average axial distance between charges, and l_b is the Bjerrum length.

The Henry result indicates that μ_0 should not depend on cylinder length L, which seems to contradict the Einstein relationship, $\mu_0 = DQ/kT$. For a cylinder, $D \sim ln(L)/L$ and $Q \sim L$, implying that μ_0 should increase logarithmically with L. However, the Einstein equation does not account for F_c; Henry's derivation shows that the long range hydrodynamic disturbances generated by the counterions exactly cancel those generated by the cylinder. This cancellation of forces only occurs over long length scales, so μ_0 should display the logarithmic dependence on L for short cylinders but not for long ones. To capture this expected length dependence, Muthukumar [11,12] models a linear polyelectrolyte as a connected assembly of point-like charges. Using the Debye-Hückel approximation and considering F_e, F_h, and F_c, he obtains

$$\mu_0' = \frac{2\xi}{\pi}\int_0^\infty \frac{(kl)^2}{(kl)^2 + (\kappa l)^2} S(kR_g)\,l\,dk \tag{2.4}$$

where l is the segment size, R_g is the radius of gyration, and $S(k)$ is the structure factor. An exact expression for $S(k)$ is available for rod-like chains, allowing an explicit evaluation of the integral. This approach leads to the formula

$$\mu_0' = 2\xi \left\{ E_1(\kappa l) - E_1(\kappa L) - \left(\frac{1}{\kappa L}\right)\left[1 - \exp(-\kappa L)\right] \right\} \qquad (2.5)$$

where E_1 is the exponential integral. The equation provides the expected logarithmic L dependence for short enough chains, as shown in Figure 2.1. Völkel and Noolandi[4,13] and Allison and Mazur[14] used more structurally realistic models to derive the same type of molecular weight dependences for single-stranded DNA.

2.2.2 Experimental Evidence

Previous experimental studies establish an undisputed M-independent μ_0 for high M polymers [1,7,9]. Figure 2.2 gives an example of this for poly(styrene sulfonate) (PSS), but similar results have been noted for both single-stranded and double-stranded DNA. Though the expected logarithmic M dependence for shorter chains has also been reported [1,7], prior work in our laboratory implies an unexplained maximum in μ_0 in the oligomer range for PSS [9]. Figure 2.3 shows an electropherogram for a PSS oligomer with nominal degree of polymerization $N = 8$. The presence of multiple peaks can most readily be interpreted as an electrophoretic separation by N. Surprisingly, some of the peaks correspond to μ_0 greater than that of either the styrene sulfonate monomer or high M PSS. The combination of these results and those obtained for other oligomeric PSS samples indicates that μ_0 passes through a maximum somewhere in the range $5 < N < 25$. As an unambiguous assignment of N values to the peaks in Figure 2.3 is impossible, the maximum and its location remain speculative. Later work by Cottet et al. [15] reproduces these results and attempts to model the behavior with a semiempirical approach.

2.3 Experimental

2.3.1 Materials

The polymer chosen for this study is phosphorylated poly(deoxythymidine) (poly(dT), Sigma), which is available in monodisperse oligomeric fractions of $N = 2, 4, 6, 8$, and 16 and as a polydisperse polymer with $N > 650$. Poly(dT) samples were dissolved in DI H_2O at an initial concentration of 0.5 mg/ml for the highest I (= 0.1 M) experiments; more dilute samples were required as I decreased, with the lowest I (=0.001 M) experiment using poly(dT) concentrations of 0.05 mg/ml. All capillary electrophoresis experiments were conducted with dibasic sodium phosphate (Fisher) running buffers; the buffer concentration effectively dictates I for the experiment. To validate I for each buffer, the conductivity σ is measured in a gold dip cell attached to a conductivity meter (Cole-Parmer). Then, during the capillary electrophoresis experiments, we routinely monitor the current i of the solvent-filled capillary and use it to calculate the conductivity of the solution:

$$\sigma = \frac{i}{\pi r^2 E} \tag{2.6}$$

where r is the capillary radius and E is the electric field strength. We generally find σ values which closely match those measured in the conductivity cell, with the current remaining stable over the whole set of experiments. If the current drifts, indicating a change in σ (and I), a new solution or capillary is prepared.

2.3.2 Capillary Electrophoresis

Capillary electrophoresis experiments are performed in a home-built apparatus [9] that encloses the capillary in a cooled environmental chamber. Two fans in combination with an air-water heat exchanger maintain the inner capillary temperature at 20 ± 0.5°C and eliminate undesirable Joule heating effects at electric field strengths less than 250 V/cm. The voltage is applied with a 0-30 kV power supply from Glassman High

Voltage. Samples are injected electrokinetically (2-10 s), and an ISCO CV^4 UV/Vis absorbance detector monitors sample elution at 260 nm. To eliminate anomalous signals from dust, all solutions are prefiltered through 0.22 or 0.45 μm Millex-GV or –HV syringe filters (Millipore).

Fused silica capillaries of 50 μm internal diameter are purchased from Polymicro Technologies and cut to the appropriate length, typically 60 cm. Poly(dT) does not adsorb to the negatively-charged walls of the capillary, and measurement reproducibility can be enhanced by oxidizing the capillary's bare glass surface, creating the maximum possible fraction of negative silanol groups. Using a microsyringe for injection, each new capillary is flushed with 1.0 M KOH (1 hr.) and then rinsed briefly with DI H_2O (5 min.) and the run buffer (≥ 10 min.). Final equilibration of the capillary with the buffer occurs in the presence of an applied field (≤ 250 V/cm). When reproducibility becomes poor, the conditioning sequence is repeated.

Electrokinetic sample injection occurs at the anode (positive polarity), despite the negative charge of poly(dT), because the negative capillary surface drives an electroosmotic velocity V_{osm} exceeding the sample's opposing electrophoretic velocity V_{el}. The injected material migrates under the combined influence of electrophoresis and electroosmosis, with the net solute velocity V_{net} given by

$$V_{net} = V_{osm} - V_{el} \qquad (2.7)$$

Since V_{el} values are the experimental objective, V_{osm} is separately measured using a coinjected neutral tracer (acetone). After obtaining V_{el}, μ_0 is calculated according to its definition ($\mu_0 = V_{el}/E$).

2.4 Results and Discussion

The availability of absolutely monodisperse fractions of oligomeric ss-DNA now allows for a more systematic investigation of μ_0 in the low N range. The poly(dT) used for this study has similar properties to those of PSS: the intrinsic persistence length and ξ for PSS are roughly 1.2-1.4 nm [16,17] and 2.50-2.78 [17], respectively, while for poly(dT) the corresponding values will be similar to those reported for ss-DNA, roughly 1.0 nm and 1.65, respectively [18,19]. Incorporating electrostatic contributions, the persistence length at lower I will be larger for both polymers.

Figure 2.4 plots $\mu_0(N)$ for poly(dT), using I as a parameter. The data show a strong N dependence of μ_0 for short chains, with the observed behavior highly dependent on I. As expected from the introductory discussion, μ_0 rises with N in the low N range, reflecting an increasing compensation of hydrodynamic effects as the chain size grows relative to κ^{-1}. The difference between μ_0 of polymer and dimer reduces with I; the difference at the lowest I examined (I = 0.001 M) is 24%, a value roughly consistent with the difference previously seen between polymer and monomer for PSS mobility. At low I, the maximum in μ_0 for poly(dT) is unambiguous. For I = 0.001M, the mobility at N = 16 is roughly 20% greater than for the high molecular weight polymer. Figure 2.5 establishes that the mobility difference sufficiently allows for a baseline separation of a mixture of the two samples. The magnitude of the mobility maximum appears to diminish at larger I, although data for these conditions are more limited. A lack of monodisperse samples in the range $16 < N < 600$ prevents a more accurate location of the mobility maximum.

One possible explanation for the maximum in $\mu_0(N)$ could arise from perturbations from end groups on the oligomers. As the poly(dT) samples are phosphorylated, an extra phosphate group resides at one chain end (in addition to the phosphate for each repeat unit). To compare to the PSS oligomers, we analyzed MALDI mass spectroscopy data to find end groups of a butyl group and a proton for the PSS

chains. We have been unable to formulate a simple chain model that would predict a mobility maximum when an extra charge or frictional unit is placed at the chain end(s). In addition, since PSS and poly(dT) differ so greatly in end group structure and yet show the same oligomer behavior, we do not believe the functionality on the chain end is responsible for the mobility maximum we observe.

The only data in the literature that might be compared to ours are those of Grossman [1], who studied poly(dT) by capillary electrophoresis as well. Although his data are roughly comparable to those presented here, with mobility rising with N in the range $2 < N < 10$, no maximum in μ_0 is noted. We believe that a combination of Joule heating and high ionic strength in his study suppressed the maximum we see; also, the composition of Grossman's buffer was totally different than the one employed here. For duplex-DNA, Stellwagen [7] also did not report a maximum. However, the large stiffness of duplex-DNA probably invalidates any comparison to results for ss-DNA.

2.5 Summary

The experimental results presented above conclusively establish that μ_0 for flexible polymers has a complex dependence on N in the oligomer range. The mobility for oligomers generally rises with N, saturating when this parameter reaches approximately 20-50. A maximum in μ_0 exists at intermediate N and will clearly be an enormous hindrance to the use of free solution electrophoresis for separating polyelectrolyte oligomers. Unfortunately, the presence of the maximum may not always be immediately obvious, and no physical basis for it is currently known.

2.6 References

1. Grossman, P. D. *Free-Solution Capillary Electrophoresis*; Grossman, P. D. and Colburn, J. C., Ed.; Academic Press: San Diego, CA, 1992.

2. Dolnik, V.; Liu, J.; Banks, J. F., Jr.; Novotny, M. V.; Bocek, P. *J. Chrom.* **1989**, *480*, 321.

3. Carney, S. L.; Osborne, D. J. *Anal. Biochem.* **1991**, *195*, 132.

4. Völkel, A. R.; Noolandi, J. *Macromolecules* **1995**, *28*, 8182.

5. Braud, C.; Vert, M. *Polym. Bull.* **1992**, *29*, 177.

6. Cohen, A. S.; Terabe, S.; Smith, J. A.; Karger, B. L. *Anal. Chem.* **1987**, *59*, 1021.

7. Stellwagen, N. C.; Gelfi, C.; Righetti, P. G. *Electrophoresis* **1997**, *42*, 687.

8. Cohen, A. S.; Najarian, D.; Smith, J. A.; Karger, B. L. *J. Chrom.* **1988**, *458*, 323.

9. Hoagland, D. A.; Arvanitidou, E.; Welch, C. *Macromolecules* **1999**, *32*, 6180.

10. Henry, D. C. *Proc. Roy. Soc., Ser. A* **1931**, *133*, 106.

11. Muthukumar, M. *Macromol. Theory Simul.* **1994**, *3*, 61.

12. Muthukumar, M. *Electrophoresis* **1996**, *17*, 1167.

13. Völkel, A. R.; Noolandi, J. *J. Chem. Phys.* **1995**, *102*, 5506.

14. Allison, S. A.; Mazur, S. *Biopolymers* **1998**, *46*, 359.

15. Cottet, H.; Garcil, P.; Theodoly, O.; Williams, C. E. *Electrophoresis* **2000**, *21*, 3529.

16. Nierlich, M.; Boué, F.; Lapp, A.; Oberthur, R. *J. Physique* **1985**, *46*, 649.

17. Davis, R. M.; Russel, W. B. *Macromolecules* **1987**, *20*, 518.

18. Record, M. T.; Woodbury, C. P.; Lohman, T. M. *Biopolymers* **1976**, *15*, 893.

19. Tinland, B.; Pluen, A.; Sturm, J.; Weill, G. *Macromolecules* **1997**, *30*, 5763.

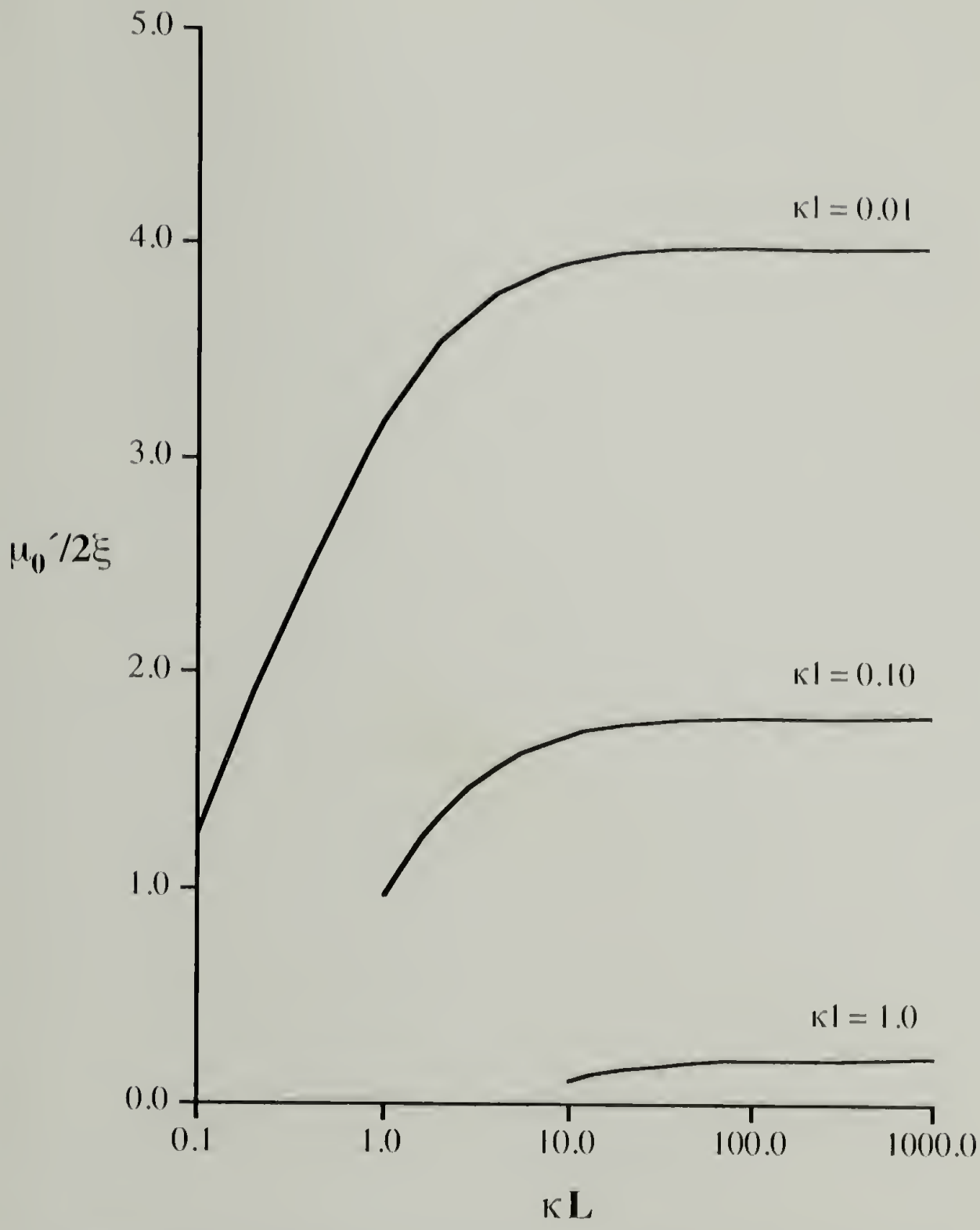

Figure 2.1. The dimensionless mobility $\mu_0'(\kappa L)$ given by the Muthukumar solution for rod-like chains (Eq. 2.5).

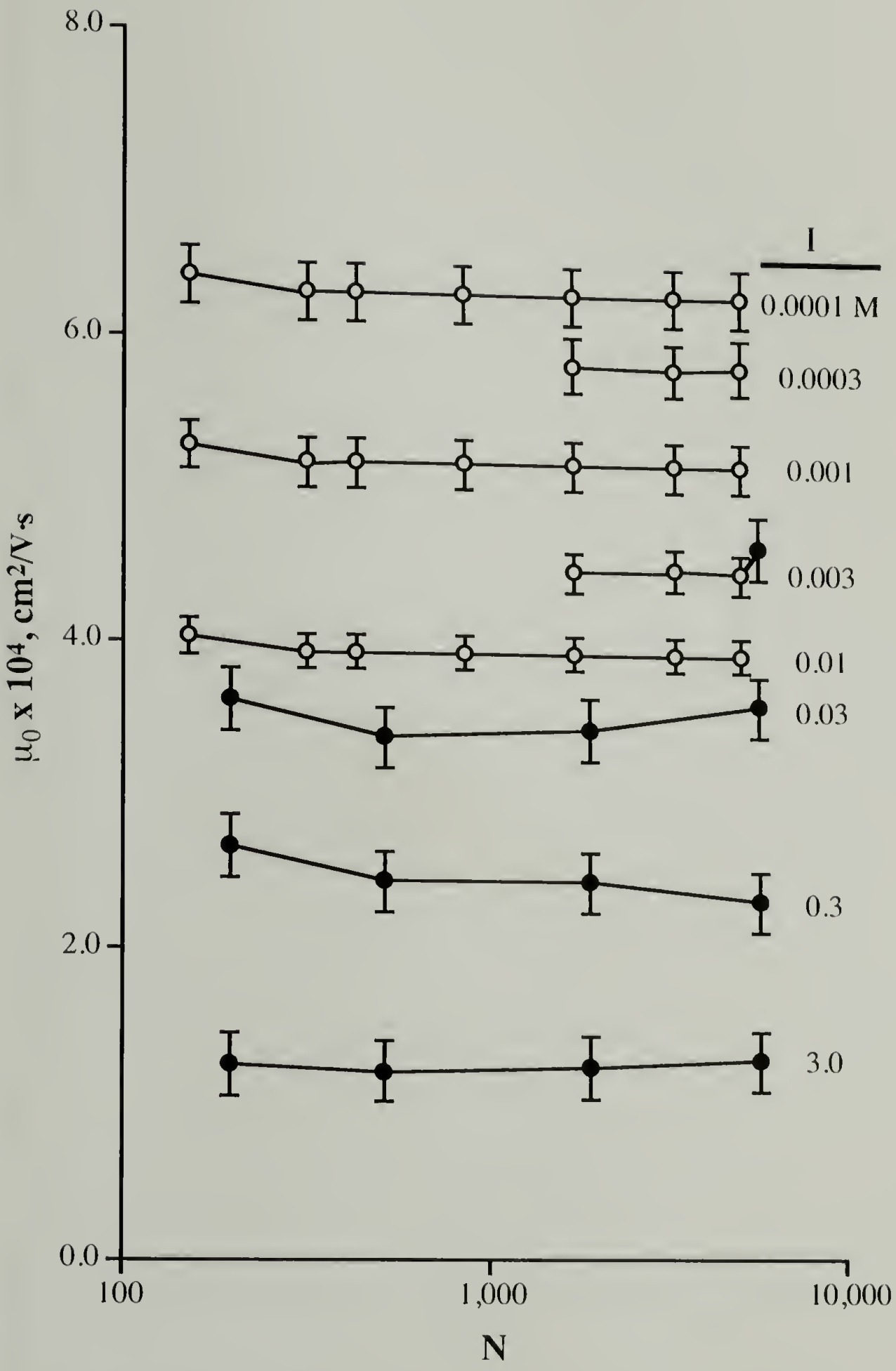

Figure 2.2. The electrophoretic mobility $\mu_0(N)$ for PSS in aqueous NaCl with $N > 100$. (Open circles represent data collected via capillary electrophoresis, while the data with filled circles come from electrophoretic light scattering.) Figure reproduced from ref. [9].

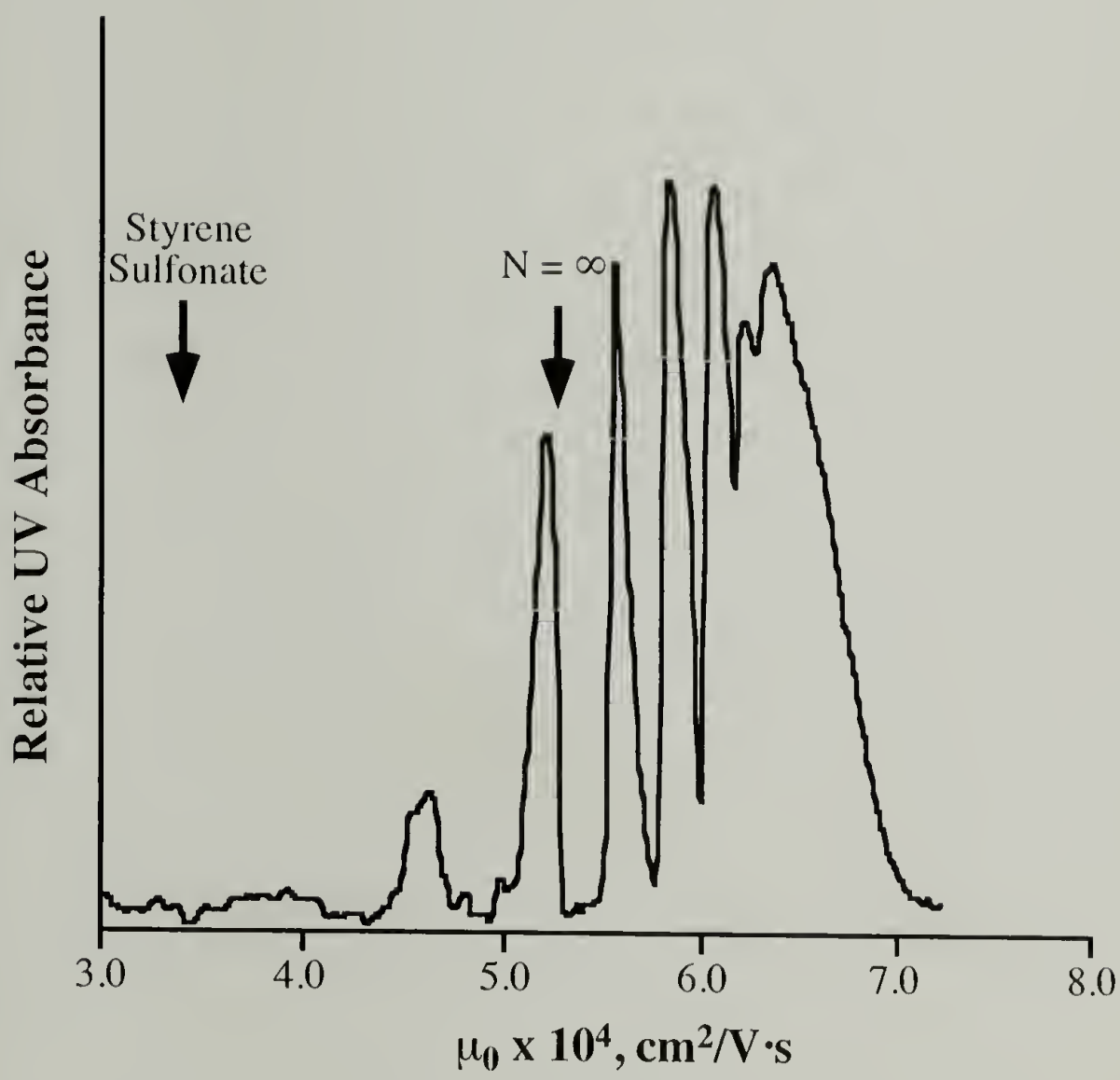

Figure 2.3. The mobility distribution for PSS with nominal $N = 8$ and $I = 0.001$M in aqueous NaCl. Arrows indicate mobilities measured for styrene sulfonate ($N = 1$) and high molecular weight PSS ($N = \infty$) when co-injected with the $N = 8$ PSS; these mobility values were verified in separate runs of individual styrene sulfonate and high molecular weight PSS, using identical run conditions. Figure reproduced from ref. [9].

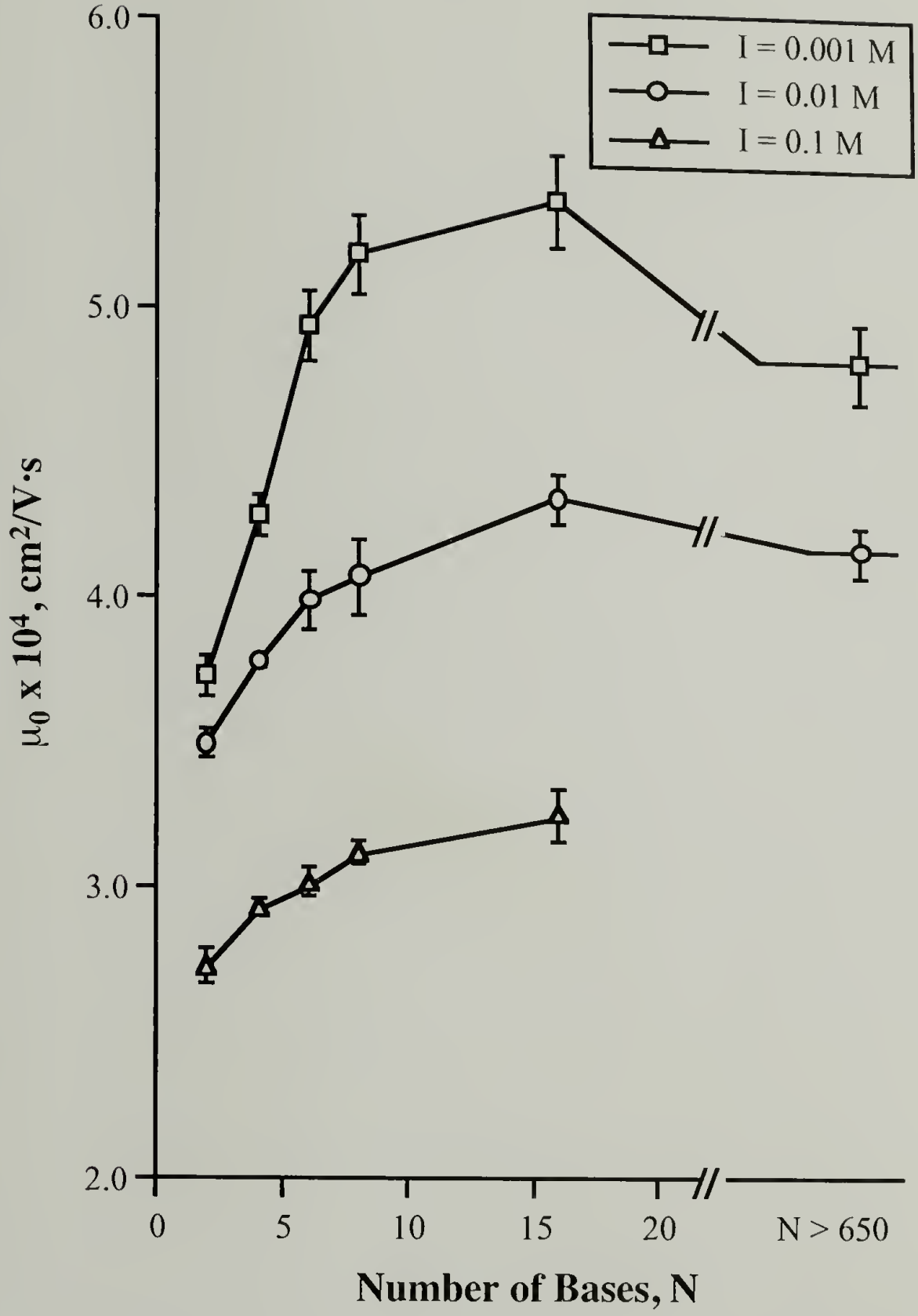

Figure 2.4. The mobility $\mu_0(N)$ for poly(dT) in aqueous Na_2HPO_4. Reproducibility of sequential runs is reflected in ±1.0 standard deviation error bars.

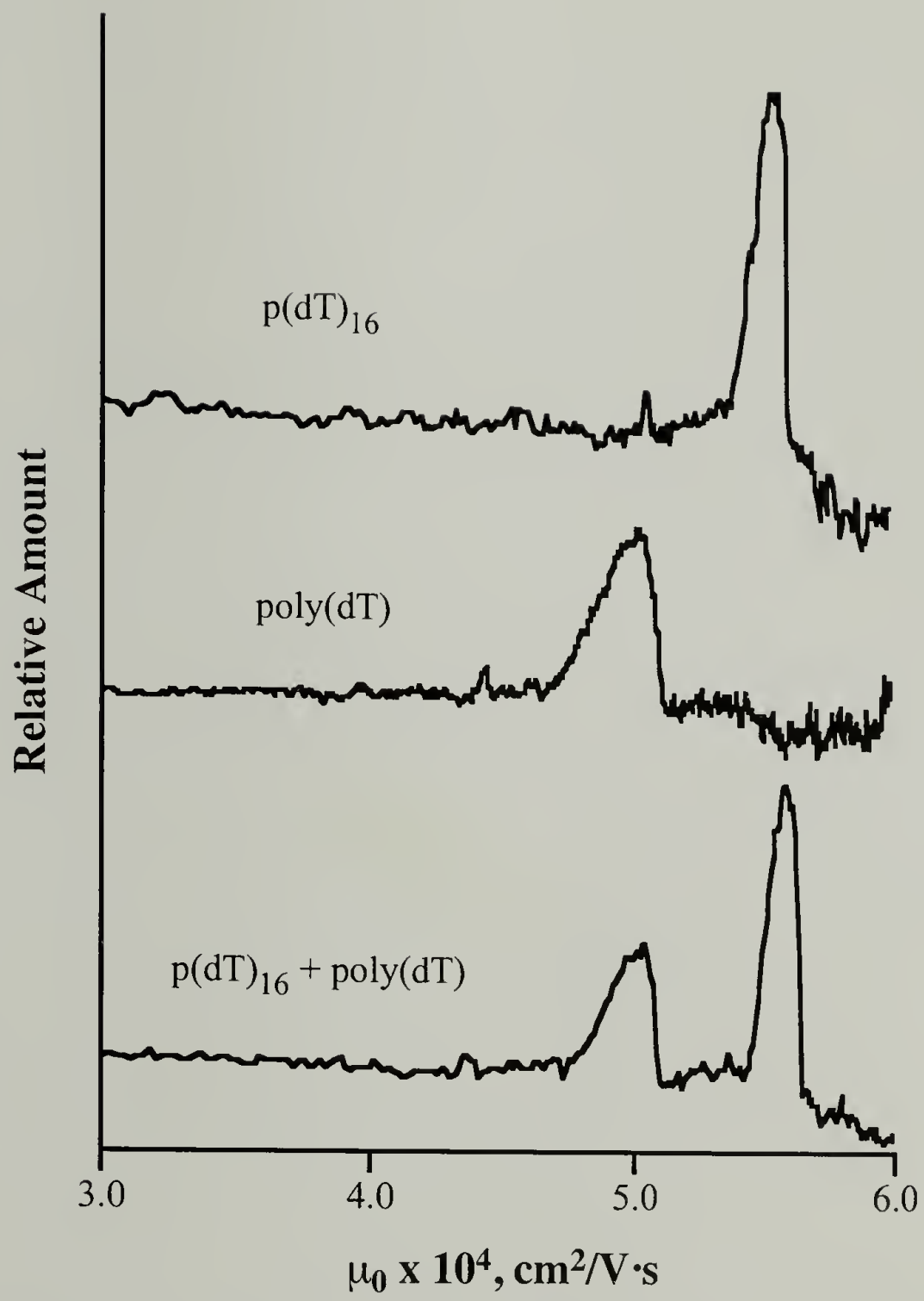

Figure 2.5. Mobility distributions at $I = 0.001$M for monodisperse oligomeric poly(dT) with $N = 16$, high molecular weight poly(dT) ($N > 650$), and a mixture of the two.

CHAPTER 3

MOLECULAR WEIGHT ANALYSIS OF POLYCATIONS BY CAPILLARY ELECTROPHORESIS IN DILUTE NEUTRAL POLYMER SOLUTIONS

3.1 Abstract

Under appropriate conditions, polyelectrolytes separate according to molecular weight during their electrophoretic migration through a dilute solution of inert neutral polymers. These separations facilitate a new capillary electrophoresis-based approach for high resolution and high throughput polyelectrolyte molecular weight analysis, one theoretically applicable to both polyanions and polycations. Although pioneered for DNA, a polyanion, the new method is discussed here in the context of synthetic polycations. Numerous experimental difficulties evolve from the introduction of positive solute charge, not the least of which is a strong tendency for solute adsorption on the negative capillary walls. The adsorption can be overcome by using a run buffer with a cationic surfactant that forms a dynamic yet stable positive wall coating. Feasible at nearly any pH, the surfactant approach enables robust and high-resolution polycation analysis. For illustration, we compare the separation at low pH of three protonated poly(2-vinylpyridine)s to the separation at neutral pH of the same polymers after quaternization. A good match is found. Further, electrophoretic analyses by the new method suggest how poly(2-vinylpyridine)s degrade/crosslink when exposed to quaternizing conditions for an excessive period.

3.2 Introduction

Synthetic polycations find extensive industrial application in technologies such as flocculation, coatings, and sludge-dewatering. Polycations with quaternized ammonium functionality also serve as model systems for probing polyelectrolyte phenomena in nonaqueous media and for following the impact of linear charge density on polyelectrolyte properties. Unfortunately, the strong electrostatic interaction of these positively charged polymers with most hydrophilic surfaces hinders their molecular weight analysis. Development of a molecular weight characterization method that overcomes this obstacle not only would benefit model studies but also could improve commercial processes that rely on these materials. Targeting polymer charge as a driving force for improved characterization methods, we previously explored the analysis of synthetic polyanions by various electrophoretic methods [1-3]. Here, we demonstrate a method to determine polycation molecular weight distributions via capillary electrophoresis. The electrophoretic measurements are then compared to size exclusion chromatography (SEC) measurements.

As nearly all surfaces in contact with water develop negative surface charge, to characterize polycations by conventional methods necessitates special efforts to control surface interactions. SEC packings for polycations, for example, are chemically modified to limit electrostatically driven solute adsorption. Even so, adsorption on the high surface area packings can still occur, making SEC tedious, expensive, and unreliable as compared to its application with polyanions or neutral polymers [4]. Another disadvantage of SEC is its limited molecular weight range; many polycations of commercial importance possess molecular weights above the SEC method's upper limit, roughly 2 to 5 x 10^6 g/mol. Standard electrophoretic methods can easily handle polymers of much larger size. Gel electrophoresis, typically applied in this capacity for anionic biopolymers such as DNA, remains unexplored for cationic polymers. However, both polyacrylamide and agarose gels, the traditional supports for gel electrophoresis, contain

residual negative charges that irreversibly bind most polycations. Because of these sorts of experimental difficulties, molecular weight distributions for commercially produced synthetic polycations are generally unavailable.

Beyond the oligomer size range, capillary electrophoresis in a free solution containing only electrolyte does not provide a size-based separation of uniformly charged polyelectrolytes [5-11]. Rather, polymer migration depends on each chain's linear charge density as well as the solution's ionic strength. Adding a low concentration of neutral polymer to the electrolyte alters this undesirable state in a fundamental and positive way. Now, efficient separations by molecular weight can be achieved for a variety of both synthetic and biological polyanions [3,12-17]. A match of polyelectrolyte and neutral polymer chain length seems to optimize polyelectrolyte molecular weight separation.

When dilute, the neutral chains can be viewed as isolated molecular-sized obstacles that transiently entangle in pairwise fashion with the migrating polyelectrolytes; entangled pairs may then drift downfield some distance before the two disentangle. Polyelectrolyte molecular weight strongly affects the processes of entanglement and drift, explaining how separation by this parameter occurs [18,19]. When semidilute or concentrated, the neutral polymers may act more in the manner of a conventional gel support, and reptation-based migration models have been suggested [20]. The degree to which the neutral polymers modulate electrophoretic mobility depends not only on polyelectrolyte molecular weight but also on additional factors such as neutral polymer molecular weight and concentration [3,6,15,16,18,19]. With many of these factors poorly understood from a theoretical perspective, a molecular weight analysis by this approach necessarily relies on calibration by polyelectrolyte molecular weight standards, a significant drawback. Nevertheless, the neutral polymer approach is faster than gel electrophoresis, and unlike SEC, apparently does not encounter an upper molecular weight bound. For polycations, the tenuous nature of the neutral polymer separation

media would suggest reduced aggregation and adsorption problems as compared to gel electrophoresis and SEC. The purpose of the current study is to evaluate this hypothesis.

With the neutral polymer solutions, polycation adsorption problems are certainly not eliminated, as negative siloxy charges populate the surface of the usual fused silica capillaries employed in capillary electrophoresis. However, various techniques for coating capillary surfaces have proven effective in preventing adsorption of ampholytic biopolymers (i.e., proteins) in free solution experiments [21-26]. These coatings render the capillary surface either positively charged or neutral, and several of the coatings can be cheaply and easily prepared. Coated capillaries can also be purchased from commercial vendors.

We have thus combined two advances in capillary electrophoresis, coated capillaries to prevent polycation adsorption and neutral polymer solutions to impart size-dependent mobilities, for the study of synthetic polycations. Preliminary publications by our group [27] and Clos and Engelhardt [28] reported the feasibility of this approach by demonstrating that separations of nearly monodisperse protonated poly(2-vinylpyridine)s (P2VPs) could be obtained in coated capillaries. The previous studies, however, were limited to low pH (in the range 2.5-3.0), a condition needed to achieve the protonation of an otherwise neutral polymer. Here, we extend the technique to include the examination of quaternized P2VPs at neutral pH, development of a more robust capillary coating procedure, and comparison of separations for protonated and quaternized polycations of the same chain length. Further, we illustrate the usefulness of the new method by examining broad molecular weight distribution samples produced by degradation/ crosslinking of a narrow polydispersity starting polycation. Our efforts to apply the new method to commercial polycations are described in Appendix A.

3.3 Experimental

3.3.1 Materials

Three nearly monodisperse P2VP samples (Scientific Polymer Products) and their quaternized counterparts are examined in this study. The nominal weight-average molecular weights of the P2VPs are 3.6 x 10^4, 4.0 x 10^5, and 1.2 x 10^6 g/mol, and $M_w/M_n \leq 1.1$ characterizes each. The neutral matrix polymer is pullulan (polymaltotriose) at a molecular weight of either 1.7 x 10^6 ($M_w/M_n = 1.14$) or 8.5 x 10^5 g/mol ($M_w/M_n = 1.14$) (Shodex standards available through Phenomenex). Buffer solutions are prepared from potassium hydrogen phthalate (KHP, Fisher Scientific), HCl (Fisher Scientific), and tris(hydroxymethyl)aminomethane (Tris, Sigma). For the non-quaternized P2VPs, water-solubility and a degree of protonation of ~35% [29,30] are ensured by use of KHP-HCl buffer at pH = 2.8 and $I = 0.01$ M. The quaternized P2VPs are examined at neutral pH, so a Tris-HCl buffer at pH = 7 and $I = 0.01$ M is selected.

3.3.2 Quaternization of P2VP with Benzyl Bromide

The three narrow polydispersity P2VPs were quaternized with benzyl bromide, following the method of Schmidt et al. [31]. Here, the P2VP is dissolved in a 1:3 benzyl bromide:nitromethane solution at a concentration of 2.0 wt%. The reaction proceeds at room temperature for 4 weeks in the dark to give a milky white mixture. The solvent is partially evaporated prior to the dropwise precipitation of the polyelectrolyte in toluene. The precipitate is vacuum filtered and washed three times with ethyl ether. A second purification is achieved through dissolution in 1:1 methanol:ethanol followed by dropwise precipitation in 1:1 toluene:ethyl acetate. The recovered poly(N-benzyl-2-vinylpyridinium bromide) (PBVP-Br) is subjected to this step twice more and then dissolved in DI H_2O. This polyelectrolyte solution is dialyzed extensively against DI H_2O, filtered, and freeze-dried. Elemental analysis reveals that all three polymers have a degree of quaternization of 73%.

3.3.3 Quaternization of P2VP with Dimethylsulfate

This quaternization procedure follows Noda et al. [32], using dimethylsulfate (Aldrich, 99+%) as the quaternizing reagent and dimethylformamide (Aldrich, 99.8%) as the solvent. The reaction proceeds at room temperature in a 2.0 wt% polymer solution prepared at a 10:1 molar ratio of dimethylsulfate to monomer repeat unit; all reactants and products are soluble in the homogeneous reaction medium. After a period of 1 to 24 hours, the quaternized polymer is precipitated into stirring acetone and dissolved in DI H_2O. The electrolyte level is raised to 1.0 M by addition of NaCl, and this salt solution of polymer is dialyzed extensively against 1.0 M NaCl to exchange the methylsulfate counterion with chloride. Further dialysis against DI H_2O provides a virtually salt-free poly(N-methyl-2-vinylpyridinium chloride) (PMVP-Cl) solution, as verified by conductivity measurements. The PMVP-Cl solution is then freeze-dried to produce a white, fluffy product. In order of increasing molecular weight, the degrees of quaternization for the three narrow polydispersity test polymers are 59%, 54%, and 50% (by elemental analysis); these values correspond to a quarternization reaction period of 1 hr. In addition, the 400,000 g/mol polymer is subject to quaternization periods of 4 and 24 hr., producing degrees of quaternization of 60% and 64%, respectively.

3.3.4 Capillary Electrophoresis

Capillary electrophoresis experiments are performed in the manner described in Chapter 2. The temperature is maintained at 20 ± 0.5°C, and the electric field strength is always < 250 V/cm to avoid undesirable Joule heating. P2VP and PMVP-Cl samples (0.2–1.0 mg/mL) are injected electrokinetically (1-5 s at 200 V/cm), and the ISCO CV^4 UV/Vis absorbance detector monitors sample elution at 265 nm. Acetone is co-injected as a neutral tracer to monitor the electroosmotic velocity. To eliminate anomalous signals from dust, all solutions are prefiltered through 0.22 or 0.45 μm Millex-GV or –HV syringe filters (Millipore).

The fused silica capillaries (50 μm internal diameter, Polymicro Technologies) must be modified to prevent polycation adsorption to the negatively charged inner silica surface. We employ for this task a cationic surfactant, cetyltrimethylammonium bromide (CTAB, Aldrich), which forms a bilayer or hemimicellar coating on the capillary wall, reversing the wall's charge [23]. To form the CTAB layer, the capillary is first treated with 1.0 M KOH (≥ 30 min.), rinsed with DI H_2O (5 min.), and then filled with a 0.5 mM CTAB/buffer solution (≥ 30 min.). Finally, the coated capillary is equilibrated with this surfactant-containing buffer solution during application of an electric field, usually at 200 V/cm. The dynamic nature of the coating requires CTAB to be present at concentrations greater than its critical micelle concentration in the running buffer and sample solution vials. For the reported experiments, the CTAB concentration is 0.5 mM. The CTAB layer produces an electroosmotic velocity V_{osm} larger than the electrophoretic velocity V_{el} of the polycation but opposite in direction. To calculate V_{el}, the measured solute velocity is simply subtracted from V_{osm}. The electrophoretic mobility μ is then calculated according to its definition, $\mu = V_{el}/E$, where E is the applied electric field. Results are presented as properly normalized distributions of μ by converting the relative absorbance A from a function of time t to a function of μ:

$$A(\mu)d\mu = A(t)dt \tag{3.1}$$

$$A(\mu) = \frac{A(t)}{d\mu/dt} \tag{3.2}$$

Since

$$\mu = \frac{L_c l}{V}\left(\frac{1}{t_m} - \frac{1}{t}\right), \tag{3.3}$$

$$\frac{d\mu}{dt} = \frac{L_c l}{V t^2} \tag{3.4}$$

and

$$A(\mu) = \frac{A(t)t^2 V}{L_c l} \tag{3.5}$$

where L_c = total capillary length, l = capillary length from injection end to detector, V = applied voltage, and t_m = elution time of neutral marker. Figure 3.1 shows an example of this transformation.

Fractions of the neutral and nearly monodisperse polysaccharide pullulan are prepared in the surfactant-containing buffer at pullulan concentrations below the critical overlap concentration c^*, a parameter defining the upper concentration limit of the dilute regime. Literature values [33] for both intrinsic viscosity, $[\eta]$, and radius of gyration, R_g, are employed to calculate c^* ($c^* = [\eta]^{-1}$ or $c^* = 3M_w/4\pi R_g^3 N_A$); either approach yields c^* $\approx$ 5.6 mg/ml for the 8.5 x 10^5 g/mol pullulan and $c^* \approx$ 3.5 mg/ml for the 1.7 x 10^6 g/mol pullulan.

3.3.5 Size Exclusion Chromatography

Following the procedures of Kato et al. [34], PMVP-Cl samples are examined by size exlusion chromatography with a single TSK gel GMPW column. To preclude undesired solution-packing interactions, these samples are eluted in an aqueous mobile phase containing 0.5 M acetic acid and 0.3 M sodium sulfate. Detection is by refractive index.

3.4 Results and Discussion

Initial work [27] on protonated P2VPs was conducted in a commercial, poly(ethylene glycol)-grafted capillary (J & W Scientific, μSil-DB Wax) at low pH. Restricted in pH (2.5 – 5) and degraded with use, this capillary was of marginal utility for polycation studies. Searching for a more robust capillary, we followed several coatings procedures reported previously in the literature, including one based on chemical modification of siloxy groups [21] and one based on the physical adsorption of a cationic polymer [22]. Although the resulting coatings were perhaps suitable for analysis of small molecules or lightly charged proteins, neither proved reliable for the analysis of highly

charged polycations. Searching further, the CTAB coating [23] was considered next. The dynamic and renewable nature of a surfactant coating could potentially ease capillary preparation and extend capillary lifetime. The pH stability of such a coating is another advantage, one allowing study, under other otherwise analogous conditions, of both protonated P2VPs at low pH and quaternized P2VPs at neutral pH.

3.4.1 Protonated P2VPs

Figure 3.2 shows the μ distributions measured both in free solution and in a dilute pullulan solution for a mixture of the three protonated P2VPs. As expected, the samples elute simultaneously in free solution, reflecting the independence of μ on molecular weight in this environment. In a dilute ($c = c^*/2$) solution of high molecular weight (1.7 x 10^6 g/mol) pullulan, on the other hand, three distinct μ peaks are observed. The value of μ for each polycation decreases from its free solution value as a result of electric field-induced entanglements of the polycations with pullulan chains, a process affecting the migration of the highest molecular weight P2VP the most. Experiments performed on individual polycation solutions confirm the identification of peaks and that P2VP fractions migrate independently. Each peak is narrow, reflecting the low polydispersity of these polymers and the high resolution of the analysis. An analysis of parameters controlling peak width has not been attempted.

Clos and Engelhardt [28] also employed neutral polymer solutions to separate solutions of nearly monodisperse protonated P2VPs. The main differences between their study and ours are the molecular weight and concentration range of the neutral polymer. For their neutral polymer, they used higher, nondilute concentrations (5–9 wt.%) of a 7 x 10^4 g/mol dextran possessing a broad polydispersity. In a 5 wt.% solution of this material, they achieved good separation for P2VPs with molecular weights in the range 1 to 12 x 10^4 g/mol but poorer results at higher and lower molecular weight. Employing larger dextran concentrations, they increased resolution at lower molecular weights but never achieved good separation over the entire range studied (0.15 to 173 x 10^4 g/mol).

In contrast, we use a higher molecular weight and more dilute neutral polymer, thereby obtaining a better separation for the higher molecular weight P2VPs. These features are in accord with those described for polyanions in the literature [3,6,15,16,18,19] and recently highlighted in a model study with monodisperse polyelectrolytes and neutral polymers [3]. As the neutral polymer concentration approaches or exceeds c^*, lower molecular weight polyelectrolytes are hindered increasingly by entanglements with the neutral polymer, a factor that enhances polyelectrolyte separation. A comprehensive understanding of these molecular interactions is lacking.

3.4.2 Quaternized Polymers: PBVP-Br

Figures 3.3 and 3.4 give the μ distributions for the three PBVP-Br samples in free solution and in a 8.5 x 10^5 g/mol pullulan solution, respectively. Figure 3.3 shows that in free solution, a mixture of the three polymers elutes as a single peak with a μ value similar to that seen for the protonated P2VPs in Figure 3.2. Again, μ is independent of molecular weight in this environment. Surprisingly, μ also seems insensitive to polymer charge density, as the protonated and quaterized polymers possess widely different degrees of charge (35% vs. 73%, respectively). This type of behavior has been noted before, and its explanation remains an area of active debate. Some attribute the effect to relaxation forces due to the counterions (described in Chapter 2), while others invoke the concept of counterion condensation [35]. According to the counterion condensation hypothesis, these highly charged polymers possess large enough charge densities to induce the condensation on the chain backbone of a sufficient number of small ions to yield an effective backbone charge density of one charge per Bjerrum length [35]. Neither the counterion condensation concept nor the models empolying the relaxation effect explicitly predicts the equivalence of protonated and quaternized polymers, but the structural differences between the two systems apparently are small enough to produce little discernable impact on μ. These trends reinforce the reliability of the new method

for measuring polycation molecular weight in spite of minor variations in chain structure or charge density.

In a pullulan solution (Figure 3.4), the mixture of the three PBVP-Brs gives a complex μ distribution which is quite different from the three narrow peaks seen for the protonated polymers in Figure 3.2. Experiments with the individual PBVP-Brs reveal that while the lowest molecular weight sample yields a narrow peak in this environment, the two higher molecular weight samples possess much broader μ distributions. Though the data shown here were obtained in a c^* solution of 8.5 x 10^5 g/mol pullulan, similar electropherograms resulted from pullulan solutions that were either more dilute or of higher molecular weight. These results imply that the quaternization reaction significantly altered the molecular weight distributions of the two higher molecular weight samples. Though the quaternization procedure used here was previously reported to give no noticeable change in molecular weight distribution (by SEC) [31], similar procedures have been shown to cause degradation of P2VP [32]. Figure 3.4 demonstrates the sensitivity of the capillary electrophoresis technique to molecular weight; as these experiments were easily accomplished without any sign of polycation adsorption problems, this technique offers a powerful new method for the analysis of polycation molecular weight distributions.

3.4.3 Quaternized Polymers: PMVP-Cl

Searching for a quaternization reaction that would not alter the starting polymer's molecular weight distribution, we turned to the method of Noda et al. [32] with dimethylsulfate as the quaternizing reagent. Figure 3.5 shows that the three P2VP samples subjected to quaternization for 1 hr. produce electrophoresis data similar to those for the same (protonated) polymers prior to quaternization. In free solution, all three PMVP-Cl samples elute as a single peak, whereas the dilute 1.7 x 10^6 g/mol pullulan solution causes a mixture to separate and yield three peaks. Except in buffer composition and polymer quaternization, these experiments are identical to the ones employed for the

separations displayed in Figure 3.2. As with the PBVP-Br samples, the PMVP-Cl samples in free solution possess nearly the same values of μ as their protonated counterparts, regardless of the differences in polymer charge density, either between protonated and quaternized polymer or between quaternized polymers of different molecular weight.

The three PMVP-Cl peaks produced by electrophoresis in the pullulan solution exhibit comparable widths and possess μ values similar to those of their protonated counterparts; therefore, we conclude that the quaternization reaction did not significantly alter the average molecular weight or broaden the polydispersities of these samples. However, the situation changes when quaternization reaction times are larger. To further investigate the ability of our fractionation method to distinguish between polycations possessing broad molecular weight distributions, three samples of the 4.0×10^5 g/mol P2VP quaternized for reaction times of 1, 4, and 24 hours are compared. Degrees of quaternization are similar despite the differences in reaction time. In free solution experiments, all three samples provide narrow peaks of similar μ, as shown in Figure 3.6. However, in dilute ($c = c^*/2$) solutions of 8.5×10^5 g/mol pullulan, the detrimental effect of longer quaternization reaction time is plainly evident. Figure 3.7 shows that at a reaction period of 1 hour the μ peak remains nearly as narrow as in Figure 3.2. However, as reaction time increases to 4 and then 24 hours, the peak broadens and μ shifts to higher values.

The broadened μ peak and the higher μ values indicate that the PMVP-Cl samples are significantly altered as reaction time increases. Additional insight into the alteration is offered by SEC. Figure 3.8 displays chromatograms for the same polymer samples, and surprisingly, reveals that more lengthy quaternization times can produce chains with sizes both larger and smaller than the original chains. The most plausible explanation for this broadening is the presence of a crosslinking side reaction, one that acts intramolecularly to reduce chain size and intermolecularly to increase chain size. A

possible mechanism for crosslinking is the nucleophilic attack by an unsubstituted pyridine on a pyridine previously activated by quaternization [36]. Other quaternization reactions cause similar degradation/crosslinking of P2VP, although the mechanisms for the effect have not been specified [32]. Investigators relying on PMVP-Cl as a model polyelectrolyte rarely have checked for the presence of degradation/crosslinking.

The comparison of electrophoretic and chromatographic data indicates that the two methods manifest degradation/crosslinking differently. An insensitivity of the electrophoretic approach to the larger size of crosslinked aggregates can be understood in terms of the proposed entanglement model for the separation mechanism [19]. Briefly, computer simulations reveal that when the polyelectrolyte and neutral polymer entangle, they form a double hairpin conformation with four hairpin arms extending from the locus of contact. Disentanglement occurs preferentially when the shortest hairpin arm is released. In the case of a lightly crosslinked polyelectrolyte, we would expect an entanglement with the neutral polymer to involve up to six hairpin arms; here, the rate of disentanglement should depend on the length of the shortest arm (belonging to either the crosslinked polyelectrolyte or the neutral polymer), rather than the molecular weight of the crosslinked polyelectrolyte.

3.5 Summary

Two recent advances in capillary electrophoresis techniques enable us to separate water-soluble polycations according to molecular weight. Using cationic surfactant coatings that block adsorption of the polycations to the negatively charged capillary surface, reproducible and high resolution experiments can be performed at low and intermediate pH. We believe these developments make possible the routine molecular weight characterization of highly charged polycations. The biggest remaining challenge

lies in detection, facilitated here by the strong intrinsic UV absorptions of P2VP and PMVP-Cl.

To produce molecular weight dependent values of μ, we perform electrophoresis in dilute solutions of a nearly monodisperse neutral polymer. At fixed neutral polymer molecular weight and concentration, quaternized P2VPs possess the same electrophoretic mobilities as their protonated counterparts. Either the relaxation effect or counterion condensation apparently suppresses μ shifts due to small changes of structure or charge density. Different choices of neutral polymer and cationic surfactant are obviously possible, perhaps allowing for greater optimization than achieved here. Analysis of the degraded/crosslinked PMVP-Cl samples illustrates the type of application that might be expected. Subtle changes in the molecular weight distribution resulting from different reaction conditions are clearly discerned with these materials.

3.6 References

1. Smisek, D. L.; Hoagland, D. A. *Macromolecules* **1989**, *22*, 2270.

2. Hoagland, D. A.; Smisek, D. L.; Chen, D. Y. *Electrophoresis* **1996**, *17*, 1151.

3. Starkweather, M. E.; Hoagland, D. A.; Muthukumar, M. *Macromolecules* **2000**, *33*, 1245.

4. Dubin, P. L. *Electrostatic Effects*; Dubin, P. L., Ed.; Elsevier: Amsterdam, 1988, pp 55-75.

5. Hoagland, D. A.; Arvanitidou, E.; Welch, C. *Macromolecules* **1999**, *32*, 6180.

6. Muthukumar, M. *Electrophoresis* **1996**, *17*, 1167.

7. Barrat, J.-L.; Joanny, J.-F. *Theory of Polyelectrolyte Solutions*; Prigogine, I. and Rice, S. A., Ed.: New York, 1996, pp 1-62.

8. Grossman, P. D. *Free-Solution Capillary Electrophoresis*; Grossman, P. D. and Colburn, J. C., Ed.; Academic Press: San Diego, CA, 1992, pp 111-132.

9. Völkel, A. R.; Noolandi, J. *Macromolecules* **1995**, *28*, 8182.

10. Braud, C.; Vert, M. *Polym. Bull.* **1992**, *29*, 177.

11. Stellwagen, N. C.; Gelfi, C.; Righetti, P. G. *Electrophoresis* **1997**, *42*, 687.

12. Chin, A. M.; Colburn, J. C. *Am. Biotech. Lab., News Ed.* **1989**, *7*, 16.

13. Zhu, M.; Hansen, D. L.; Burd, S.; Gannon, F. *J. Chromatogr.* **1989**, *480*, 311.

14. Poli, J. B.; Schure, M. R. *Anal. Chem.* **1992**, *64*, 896.

15. Barron, A. E.; Soane, D. S.; Blanch, H. W. *J. Chromatogr. A* **1993**, *652*, 3.

16. Barron, A. E.; Blanch, H. W.; Soane, D. S. *Electrophoresis* **1994**, *15*, 597.

17. Barron, A. E.; Blanch, H. W. *Separation and Purification Methods* **1995**, *24*, 1.

18. Starkweather, M. E.; Muthukumar, M.; Hoagland, D. A. *Macromolecules* **1998**, *31*, 5495.

19. Starkweather, M. E.; Muthukumar, M.; Hoagland, D. A. *Macromolecules* **1999**, *32*, 6837.

20. Cottet, H.; Gareil, P.; Viovy, J.-L. *Electrophoresis* **1998**, *19*, 2151.

21. Hjertén, S. *J. Chromatogr.* **1985**, *347*, 191.

22. Towns, J. K.; Regnier, F. E. *J. Chromatogr.* **1990**, *516*, 69.

23. Lucy, C. A.; Underhill, R. S. *Anal. Chem.* **1996**, *68*, 300.

24. Engelhardt, H.; Cuñat-Walter, M. A. *J. Chromatogr. A* **1995**, *716*, 27.

25. Schmalzing, D.; Piggee, C. A.; Foret, F.; Carrilho, E.; Karger, B. L. *J. Chromatogr. A* **1993**, *652*, 149.

26. Chiari, M.; Nesi, M.; Sandoval, J. E.; Pesek, J. J. *J. Chromatogr. A* **1995**, *717*, 1.

27. Welch, C. F.; Hoagland, D. A. *Polymer Preprints* **1998**, *39(2)*, 771.

28. Clos, H. N.; Engelhardt, H. *J. Chromatogr. A* **1998**, *802*, 149.

29. Muller, G.; Ripoll, C.; Selegny, E. *European Polym. J.* **1971**, *7*, 1373.

30. Ripoll, C.; Muller, G.; Selegny, E. *European Polym. J.* **1971**, *7*, 1393.

31. Förster, S.; Schmidt, M.; Antonietti, M. *Polymer* **1990**, *31*, 781.

32. Yamaguchi, M.; Yamaguchi, Y.; Matsushita, Y.; Noda, I. *Polymer J.* **1990**, *22*, 1077.

33. Kato, T.; Okamoto, T.; Tokuya, T.; Takahashi, A. *Biopolymers* **1982**, *21*, 1623.

34. Kato, Y.; Matsuda, T.; Hashimoto, T. *J. Chromatogr.* **1985**, *332*, 39.

35. Manning, G. S. *J. Phys. Chem.* **1981**, *85*, 1506.

36. Schofield, K. *Hetero-Aromatic Nitrogen Compounds: Pyrroles and Pyridines*; Butterworths: London, 1967.

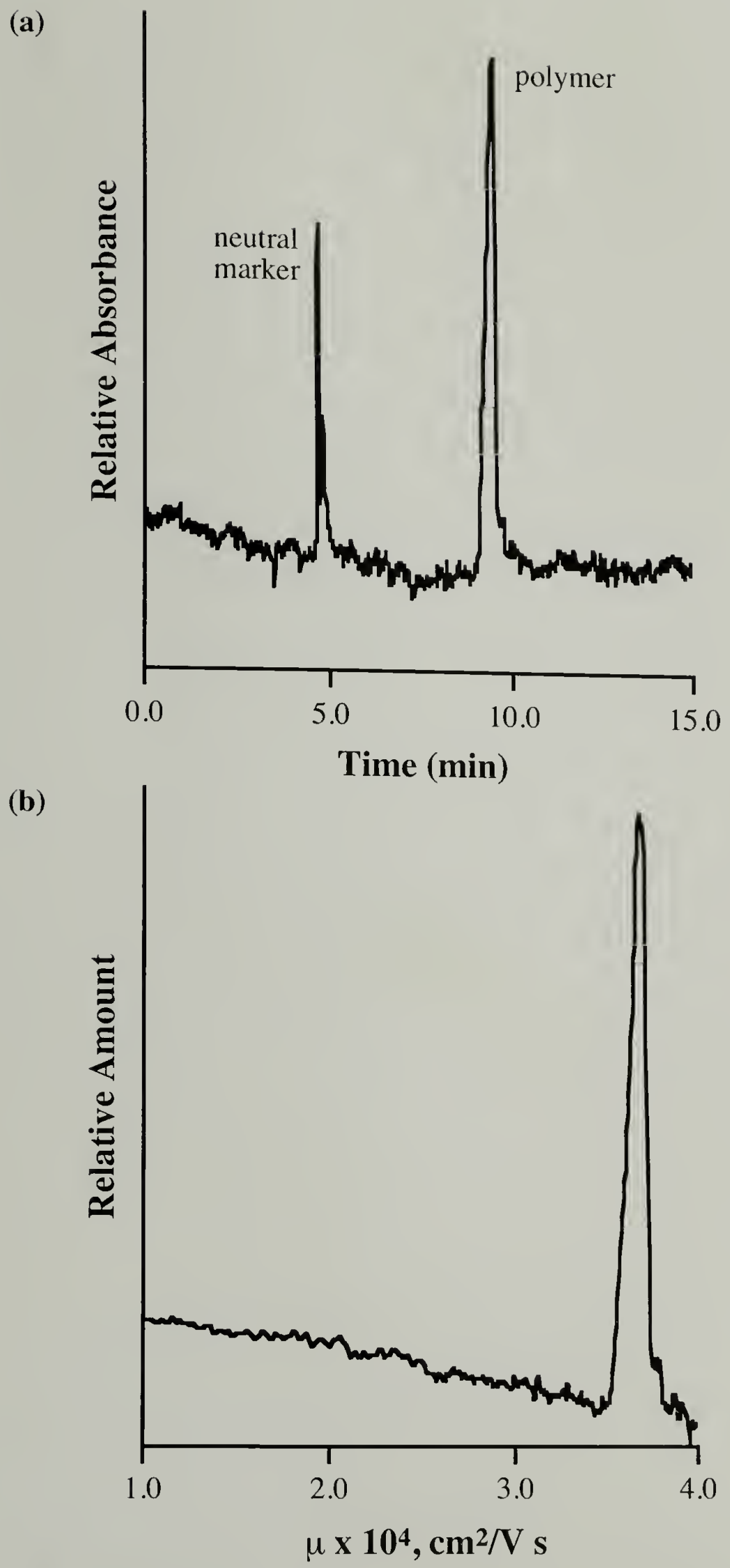

Figure 3.1. Transformation of (a) *A(t)* to (b) *A(μ)*, shown for a mixture of protonated P2VPs in free solution.

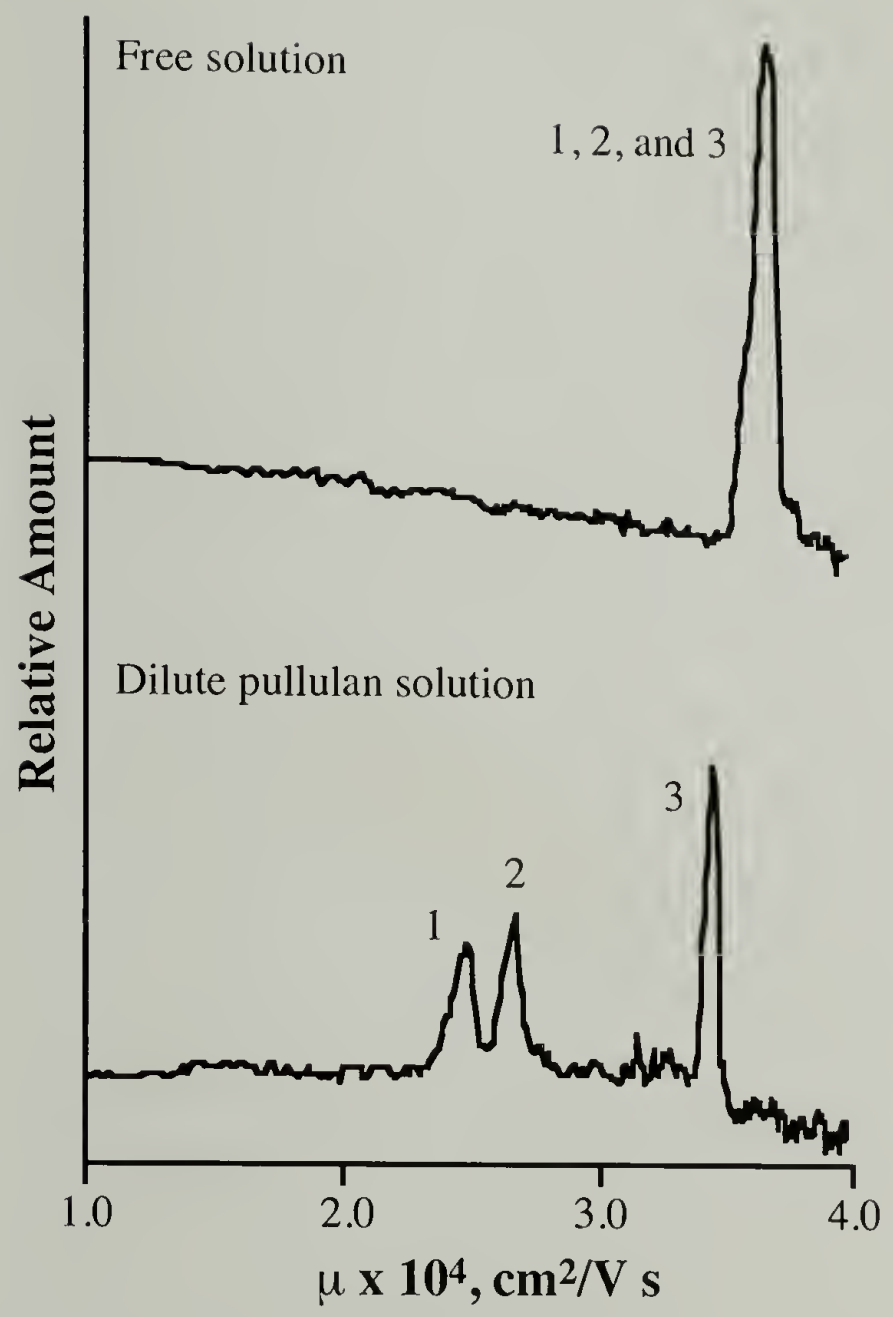

Figure 3.2. Electrophoretic mobility μ for three protonated P2VPs, in free solution and in 1.7 x 10^6 g/mol $c^*/2$ pullulan solution; **1** = 1.2 x 10^6 g/mol, **2** = 4.0 x 10^5 g/mol, **3** = 3.6 x 10^4 g/mol.

Figure 3.3. Electrophoretic mobility μ for a mixture of the three PBVP-Brs in free solution.

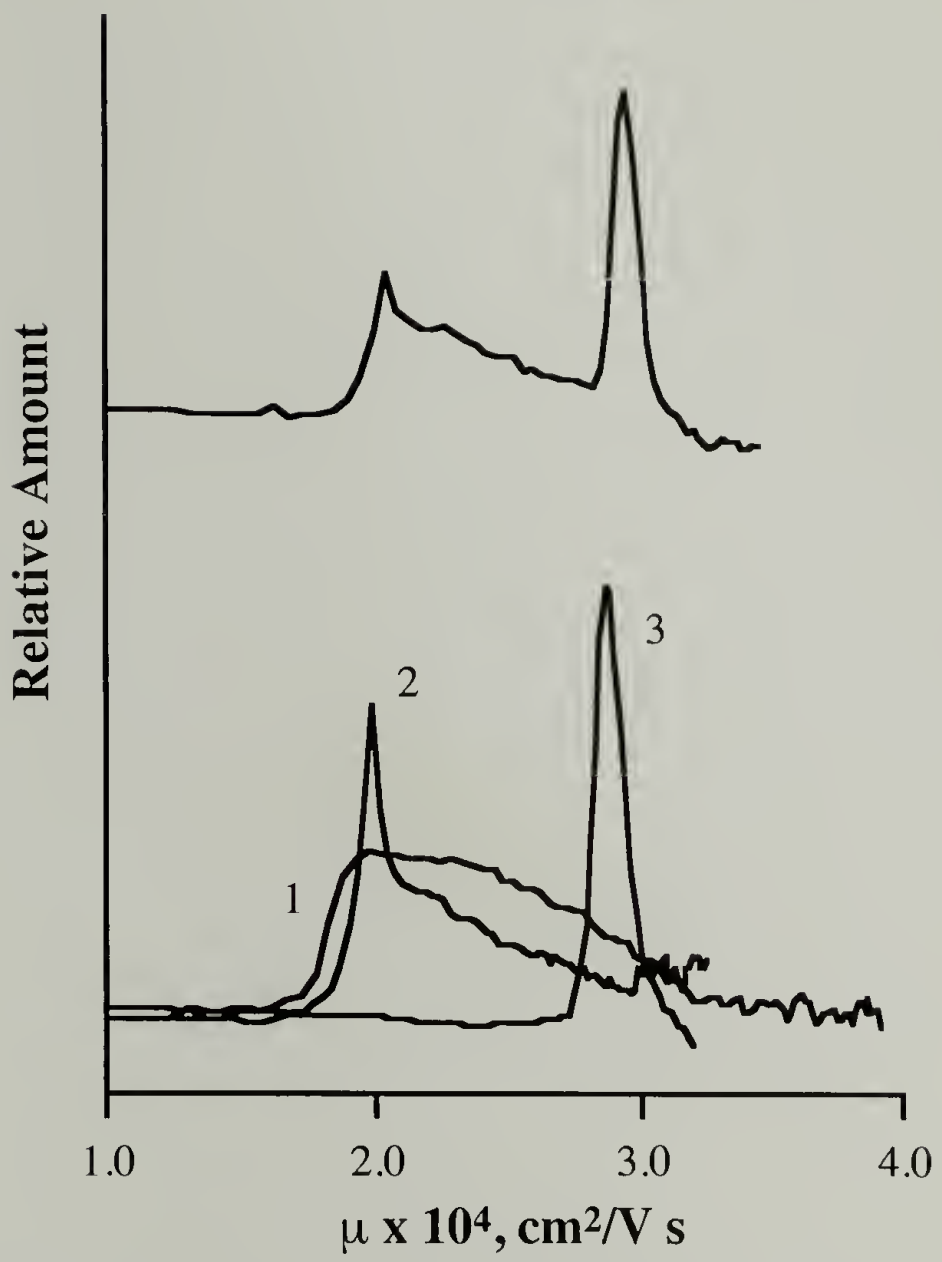

Figure 3.4. Electrophoretic mobility μ for three PBVP-Brs in 8.5 x 10^5 g/mol c^* pullulan solution. The upper electropherogram results from a mixture of the three PBVP-Brs, while the lower one overlays the traces obtained for the individual polymers; **1** = 1.2 x 10^6 g/mol, **2** = 4.0 x 10^5 g/mol, **3** = 3.6 x 10^4 g/mol.

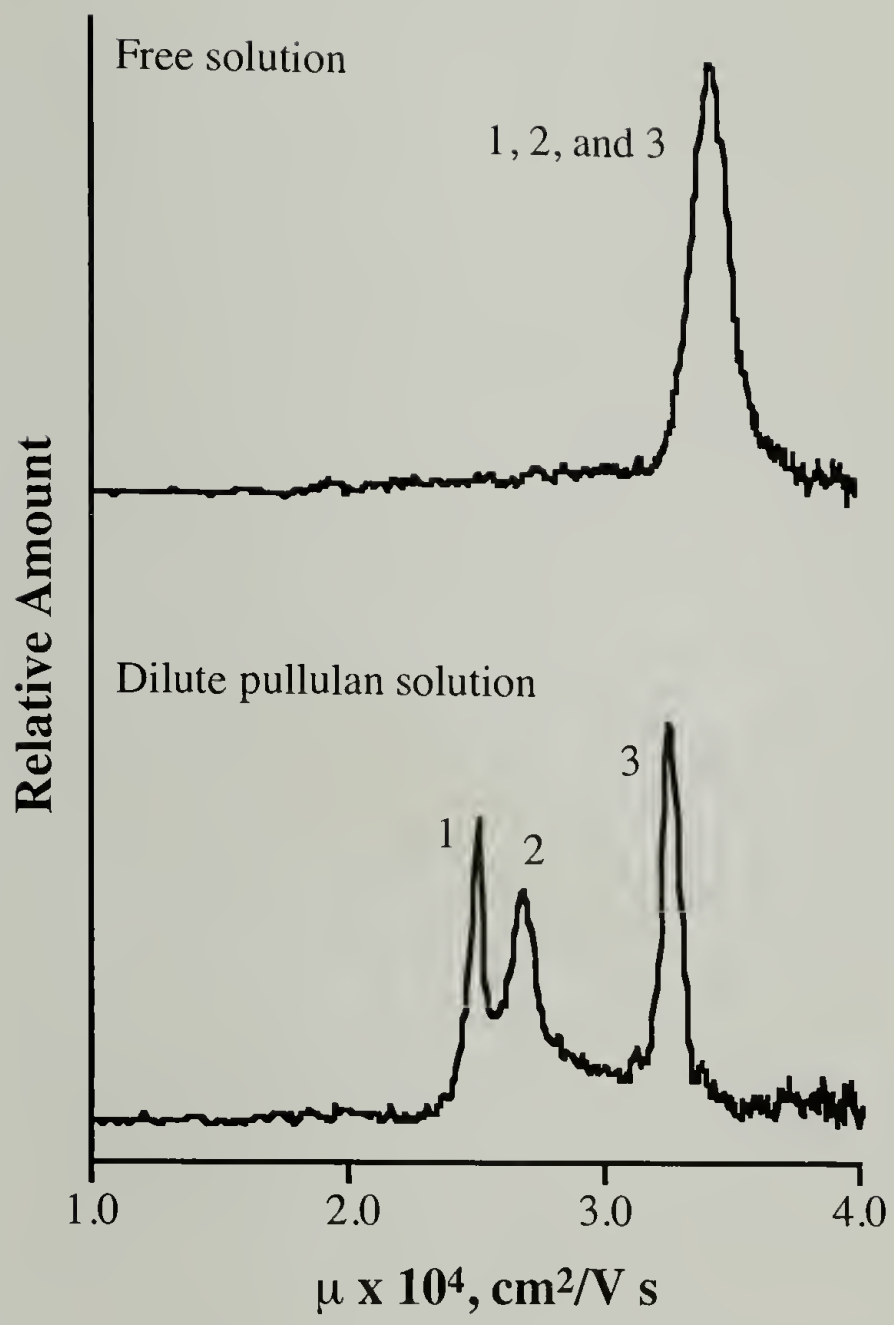

Figure 3.5. Electrophoretic mobility μ for three PMVP-Cl samples, in free solution and in 1.7 x 10^6 g/mol $c^*/2$ pullulan solution; **1** = 1.2 x 10^6 g/mol, **2** = 4.0 x 10^5 g/mol, **3** = 3.6 x 10^4 g/mol.

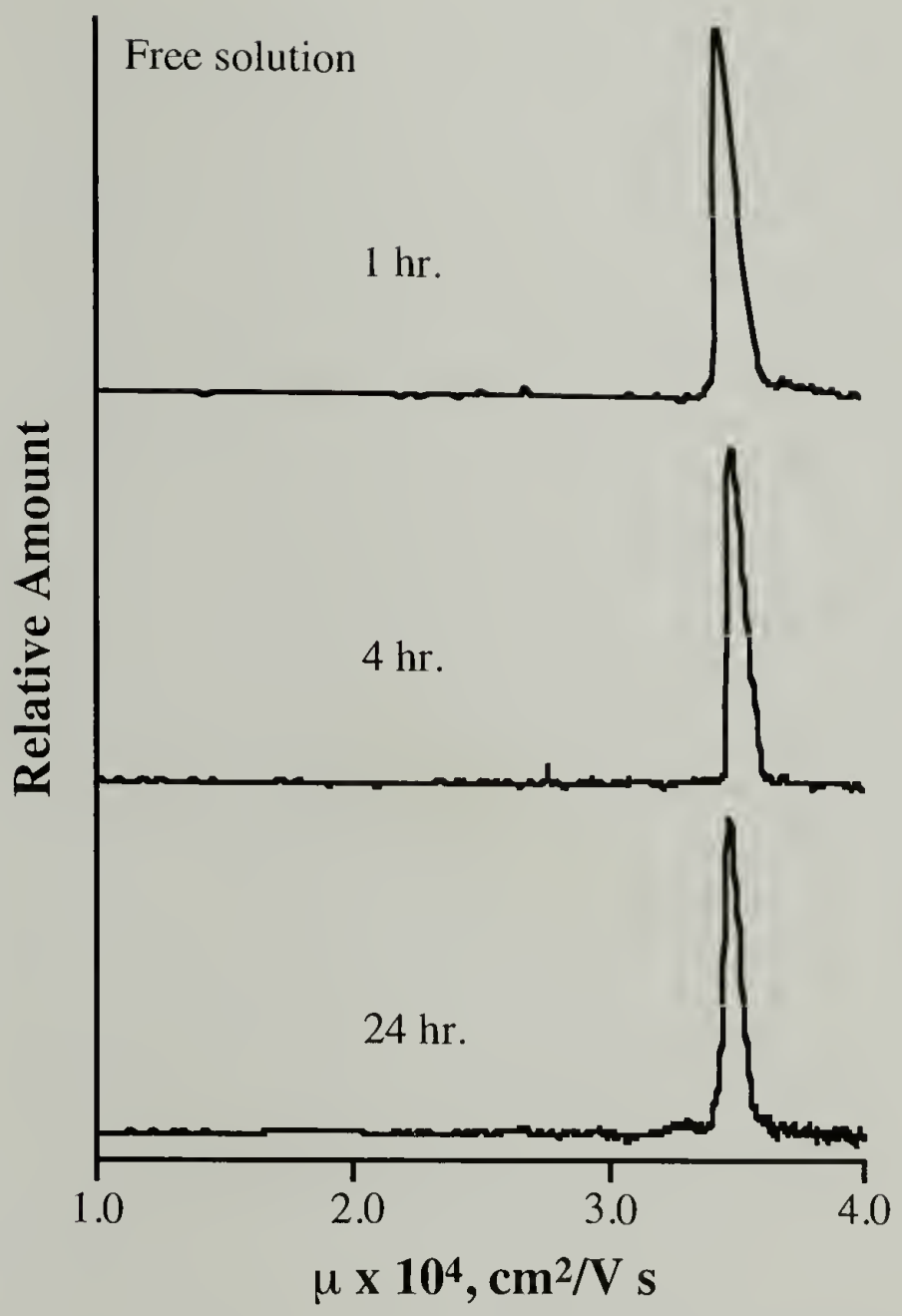

Figure 3.6. Electrophoretic mobility μ for three 4.0 x 10^5 g/mol PMVP-Cls in free solution.

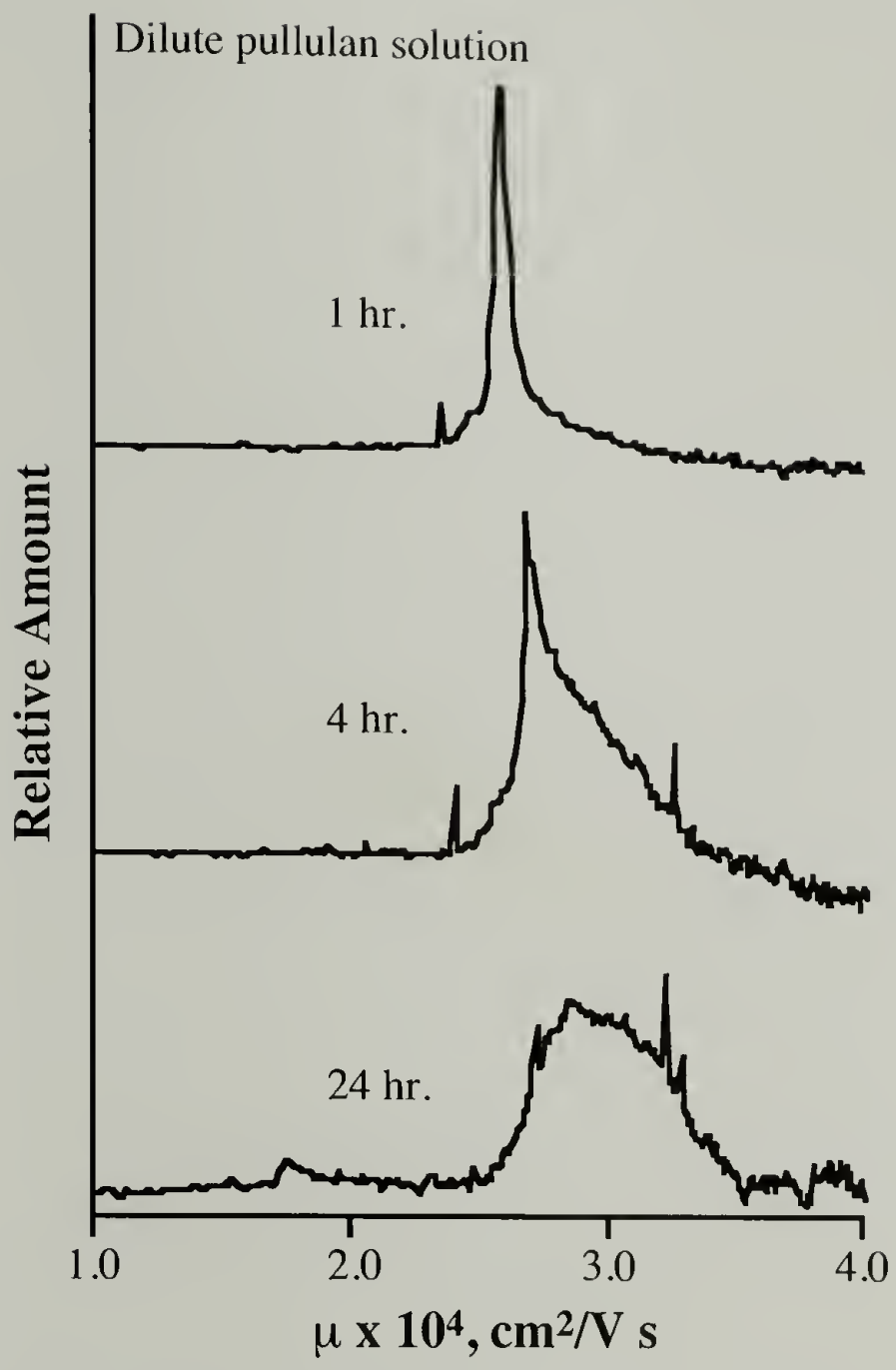

Figure 3.7. Electrophoretic mobility μ for three 4.0 x 10^5 g/mol PMVP-Cls in 8.5 x 10^5 g/mol $c^*/2$ pullulan solution.

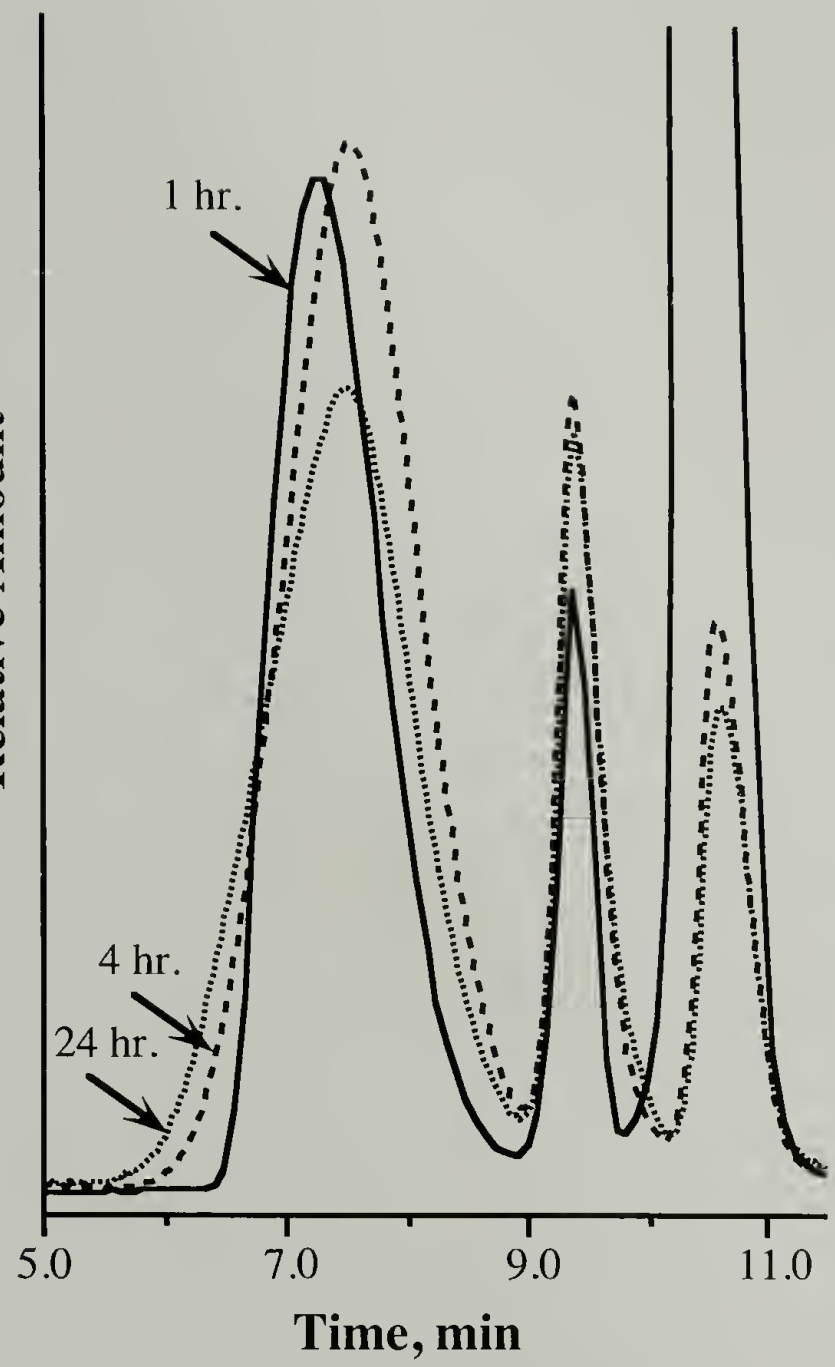

Figure 3.8. SEC chromatograms for the three PMVP-Cls of Figures 3.6 and 3.7. The peaks associated with polymer appear in the range of 6 to 9 minutes; extraneous peaks at times beyond 9 minutes are artifacts characteristic of the mobile phase.

CHAPTER 4

FREE SOLUTION MOBILITY OF DENDRIMERS

4.1 Abstract

The free solution electrophoretic mobility μ_0 of protonated polypropylenimine dendrimers has been investigated by capillary electrophoresis as a function of ionization α, ionic strength I, and hydrodynamic radius a. When dendrimer electrophoretic behavior is compared to that of linear polyelectrolytes, similar trends are noted for α but not for I or a. However, near quantitative agreement is observed for all of the dendrimer data when compared to standard electrokinetic model predictions for a dielectric sphere of radius a. This successful match of experiment and theory is achieved without the use of any fitting parameters. The results show that the electrophoretic behavior of highly charged dendrimers with $a\kappa$ near unity is dominated by the relaxation effect.

4.2 Introduction

Charged dendrimers may be considered as a model system to gain insight into two areas of research. First, due to their precisely known, uniform degree of branching, they offer an ideal means to investigate the topological effects of polyelectrolyte electrophoresis. Second, charged dendrimers may act as a model system to test electrophoresis theories for spheres, as the charge density of a dendrimer is more well-defined and easily controlled than that of a spherical colloid. In this study, we take advantage of the well-defined nature of the dendrimer's charge properties and degree of branching to compare its electrophoretic behavior to that of linear polyelectrolytes and charged spheres, as a function of both degree of charge and solution ionic strength.

Previous dendrimer electrophoresis studies vary widely from the characterization of dendrimer properties [1-3] to the use of dendrimers as transport agents in chromatographic [4] or drug delivery applications [5]. One previous investigation even discusses fundamental counterion-polyelectrolyte interactions for dendrimers with chargeable terminal groups [6]. However, a systematic study that reveals the role of topology in dendrimer electrophoresis is lacking. Such a study would not only aid the interpretation of the types of experiments mentioned above but would also contribute to the general understanding of topological effects in polyelectrolyte electrophoresis.

Colloid scientists routinely compare a particle's free solution electrophoretic mobility μ_0 to theoretical predictions for a sphere to characterize the particle's surface charge or potential. Though these theoretical predictions are relied upon heavily, serious questions regarding the validity of the standard electrokinetic model [7] remain. Rarely do the results obtained from electrophoresis measurements match those from other techniques (i.e., conductivity, streaming potential, dielectric response), and many studies end with rationalizations involving ion adsorption, particle surface "hairiness," or conduction processes behind the shear plane [8-15]. At the heart of the problem is the inability to rigorously test the theory with a model system. Spherical colloids generally have a heterogeneous surface which gives an ill-defined surface charge. As such, they can hardly be considered as a model with which to test the validity of the theories. Even when the somewhat better-defined latex particles have been employed, significant deviations from the predicted behavior have been observed. Dendrimers behave hydrodynamically as spheres [16], and unlike typical spherical colloids, they have a well-defined and easily controlled charge density. A charge may be induced in commercially available dendrimers by simple pH variation, and the nature of the charge (chemical group and location) is given by the chemical structure of the dendrimer. Furthermore, dendrimers are in the right size range (order of nm) to investigate the relaxation effect, a key element of the standard electrokinetic model for spheres.

4.3 Theory

When an electric field is applied to a charged solute, four forces will govern the solute's motion through the solution. The direct electric force F_e felt by the charged solute is given by $F_e = QE$, where Q is the charge and E is the applied field. As the solute moves through the viscous medium of the surrounding solvent, it also experiences a hydrodynamic drag force F_h which slows its motion. For a sphere, F_h is given by Stokes' law, $F_h = 6\pi\eta aV$, where η is the solvent viscosity, a is the sphere radius, and V is its steady-state velocity. Linear polyelectrolytes may be more appropriately modeled as cylinders, and in this case F_h can be approximated by $F_h = 3\pi\eta VL/ln(L/2r)$, where L and r are the cylinder's length and radius, respectively.

The remaining two forces acting on the solute result from effects of the electric field on the charged solute's counterions. As the counterions experience an electric force in the opposite direction of the charged solute, they will create hydrodynamic disturbances that exert a retardation force F_c to slow the motion of the charged solute. Though the total charge magnitude of the counterion cloud matches that of the solute, $F_c \neq -F_e$ because some of the effect is dampened by the surrounding viscous medium. Because the amount of dampening depends on the distance between the solute and its counterions, F_c is a strong function of solution ionic strength. The distribution of counterions around the solute is needed to calculate F_c; this information may be derived from the nonlinear Poisson-Boltzmann equation or, in some cases, estimated by the Debye-Hückel approximation.

The calculation of F_c assumes that the counterion cloud remains undistorted in the presence of the applied electric field. This assumption becomes invalid if the solute charge density is high and if the solute radius is of the same order of magnitude as the Debye length κ^{-1} (κ^{-1} characterizes the distance between the solute and it counterions). Distortion of the counterion cloud leads to a combination of electric and hydrodynamic effects which gives rise to the fourth force, termed the relaxation force F_r. More

specifically, as the counterion cloud's center of charge moves away from that of the solute, a local dipole field oriented opposite to the applied field is created. In addition, since the counterion cloud will be distorted such that more counterions are on the downstream side of the solute, the hydrodynamic drag on the solute will increase. Under conditions where F_r is important, the distribution of counterions must be calculated from the nonlinear Poisson-Boltzmann equation.

The force balance on a charged solute in dilute solution may be written as

$$F_e - F_h - F_c - F_r = 0 \tag{4.1}$$

Henry [17] first solved this equation within the Debye-Hückel approximation to predict the electrophoretic behavior of spheres with low surface potential ζ. In this case, F_r vanishes and the dimensionless mobility μ_0' is given by

$$\mu_0' = \zeta'\beta(a\kappa) \tag{4.2}$$

where ζ' is the dimensionless surface potential ($= e\zeta/kT$; e is the electron charge, k is the Boltzmann constant) and $\beta(a\kappa)$ varies smoothly from 1.0 ($a\kappa = 0$) to 1.5 ($a\kappa = \infty$). His result confirms the earlier predictions of Hückel [18] in the limit of small $a\kappa$ and Smoluchowski [19] at large $a\kappa$.

Later, Wiersema et al. [20] and O'Brien and White [7] used the full Poisson-Boltzmann equation and employed numerical techniques to solve Eq. 4.1, including the effects of F_r. Both solutions extend to spheres with higher ζ, with the O'Brien and White solution being the more accurate of the two. Figure 4.1 compares these results to the Henry solution over a large range of $a\kappa$ for several ζ' values. For small and large values of $a\kappa$, the numerical solutions agree with Henry's result, implying that even for large ζ' the relaxation effect is not important in these regimes. However, for moderate $a\kappa$ the

Henry and numerical solutions deviate, with the deviation becoming more pronounced as ζ' increases. Clearly for this range of $a\kappa$, the numerical solutions predict a large relaxation effect for spheres with high ζ.

Figure 4.1 appropriately plots μ_0'/ζ' as a function of $a\kappa$ to show the predicted behavior for spheres at constant ζ'. Alternatively, predictions for spheres with a constant Q and a ζ' which varies with $a\kappa$ are more correctly plotted as shown in Figure 4.2 [21]. Here, Q is transformed to the dimensionless charge σ' (= $Qe/4\pi a\varepsilon\varepsilon_0 kT$; $\varepsilon\varepsilon_0$ is the fluid permittivity), and μ_0'/σ' is plotted as a function of $a\kappa$. Consistent with Figure 4.1, Figure 4.2 shows increasing deviations from the Henry result with increasing σ'.

Equation 4.1 has also been solved for linear polyelectrolytes, with the polyelectrolyte most often modeled as a charged rod or cylinder. To our knowledge, no solution has ever been attempted specifically for a highly branched structure such as the dendrimer. However, Muthukumar's solution [22] (described in Chapter 2) for a polyelectrolyte modeled as a connected assembly of point-like charges may be applied to any polyelectrolyte with fractal dimension d_f. In this case, the structure factor $S(k)$ is approximated by an interpolation formula, and the resulting dimensionless mobility μ_0' is given by

$$\mu_0' = \sigma' \frac{4}{\pi}\left(\frac{3d_f}{2}\right)^{1/2} \int_0^\infty \frac{t^2}{t^2 + \left(2\kappa^2 R_g^2/3d_f\right)} \frac{dt}{\left(1+t^2\right)^{d_f/2}} \tag{4.3}$$

where the radius of gyration R_g replaces a in the equation for σ'. Because the Muthukumar solution employs the Debye-Hückel approximation (and therefore neglects F_r), it predicts behavior similar to that of the Henry solution.

4.4 Experimental

4.4.1 Materials

The dendrimers chosen for our model studies are the well-studied polypropylenimine (PPI) dendrimers (DAB-Am-16 and DAB-Am-64, Aldrich). The 3rd generation dendrimer (G3, DAB-Am-16) can be used as received, but the 5th generation dendrimer (G5, DAM-Am-64) requires a purification procedure to remove nitrile end group dendrimers. The procedure, recommended by the manufacturer (DSM), involves vacuum filtration of a 15 wt% G5 aqueous solution over Celite filter aid (Fisher). This method transforms the original, cloudy solution to a clear one. The purified G5 dendrimer is recovered through rotary evaporation with a SpeedVac Plus 110 (Savant).

Buffer solutions for the capillary electrophoresis experiments are prepared from potassium hydrogen phthalate (KHP, Fisher), hydrochloric acid (HCl, Fisher), glycine (Gly, Sigma), formic acid (Fisher), sodium hydroxide (NaOH, Fisher), acetic acid (HOAc, Fisher), sodium acetate (NaOAc, Fisher), tris(hydroxymethyl)aminomethane (Tris, Sigma), and sodium chloride (NaCl, Sigma). Several buffer systems were used to cover a large pH range (2.8-11.5) at I=0.01 M: Gly-HCl-NaCl (2.8-3.5), NaOAc-HOAc (4.5-5.5), Tris-HCl (7-9), Gly-NaOH-NaCl (9.5-11.5). Additionally, ionic strength studies were conducted with two different buffers at pH 2.8: KHP-HCl and formic acid-NaOH.

4.4.2 Titrations

PPI dendrimers become charged as the pH of their aqueous solutions is lowered. Both the primary amine terminal groups and the tertiary amine branch points acquire protons, though the primary amines have been shown to protonate preferentially at higher pHs since they have a higher pK_a [23]. Full protonation of all amine groups occurs between pH 3 - 4, depending on solution ionic strength [24]. Titration of each dendrimer with HCl reveals the degree of protonation α as a function of pH, as demonstrated in Figure 4.3. Because solution ionic strength affects α, our titrations maintain a constant

ionic strength of 0.01M by addition of 0.01M HCl or 0.01M NaOH to a 0.01M NaCl solution of the dendrimer. The condition of electroneutrality permits the calculation of α as ([HCl] – [NaOH] – [H^+] + [OH^-])/[amine], where [H^+] and [OH^-] are given by the measured pH and [amine] is the concentration of amine groups (both primary and tertiary). Figure 4.3 reveals that at I=0.01 M, full protonation ($\alpha = 1$) occurs at pH = 3.3.

4.4.3 Capillary Electrophoresis

Capillary electrophoresis experiments are performed in the manner described in Chapter 2. The temperature is maintained at 20 ± 0.5°C, and the electric field strength is always < 250 V/cm to avoid undesirable Joule heating. PPI sample solutions (1 – 10 mg/ml) are injected electrokinetically (2 - 5 s), and the ISCO CV^4 UV/Vis absorbance detector monitors sample elution at 205 nm. Prior to use, all solutions are filtered through 0.22 μm syringe filters (Millex-GV, Millipore).

The fused silica capillary typically used in capillary electrophoresis must be modified to prevent adsorption of the cationic dendrimers. Two types of coated capillaries were used here: one with a neutral polymer coating and one with a cationic surfactant coating. The neutral polymer-coated capillary has polyvinylalcohol (PVOH) permanently attached to the fused silica surface to mask its negative charge; this 50 μm I.D. capillary was purchased from Agilent Technologies. The cationic surfactant-coated capillary can be easily and reproducibly prepared, as described in Chapter 3; we use cetyltrimethylammonium bromide (CTAB, Aldrich) to create a positive surface charge on 50 μm I.D. fused silica capillaries (Polymicro Technologies). The dynamic nature of this coating requires the inclusion of CTAB in all running buffer and sample solutions; the CTAB concentration for all experiments reported here is 0.5 mM. For pH > 9, the CTAB apparently associates with the dendrimer to give it a higher degree of charge; therefore, PVOH capillaries are used for all experiments with pH > 9.

Regardless of which capillary is used, any contribution from the electroosmotic velocity V_{osm} to the solute's net velocity must be subtracted when calculating the correct

electrophoretic velocity V_{ep} of the dendrimer. The positive surface charge on the CTAB capillary produces a V_{osm} towards the anode, while the PVOH serves to drastically reduce V_{osm} towards the cathode. V_{osm} may be measured by co-injecting a small molecule solute with known μ_0; we use acetone (Fisher, $\mu_0 = 0$) for CTAB-coated capillaries and phenyltrimethylammonium chloride (PTMAC, Aldrich, $\mu_0 = 2.91 \times 10^{-4}$ cm^2/Vs at 20°C) for PVOH-coated capillaries. After obtaining V_{ep}, μ_0 is calculated according to its definition ($\mu_0 = V_{ep}/E$).

4.4.4 Comparison to Theory

To compare the electrophoretic behavior of dendrimers to that predicted for charged spheres, ζ' must be calculated for each dendrimer at each ionic strength and pH studied. The relationships between ζ', $a\kappa$ and σ' for spherical particles have been tabulated by Loeb et al. [25]. Stigter [26] has numerically fit these tabulations with a summation formula, and Yoon [27] has reproduced the Loeb results by solving an integral equation. We employ all three methods to calculate ζ' values for the dendrimers, using the dendrimer's hydrodynamic radius as a (sphere radius) and α to calculate σ'. Here, $Q = \alpha Ne$ and N = total number of amine groups in the dendrimer ($N = 30$ for G3; $N = 126$ for G5). Mapping the dendrimer's parameters to a sphere in this way effectively puts all of the charge at the "surface" of the dendrimer's hydrodynamic radius. To investigate the importance of this assumption, we calculated ζ' using two different values of σ' for each $a\kappa$ at $\alpha = 1$ (with $Q = 16e$ or $30e$ for G3 and $Q = 64e$ or $126e$ for G5).

The hydrodynamic radii of the dendrimers are taken from Scherrenberg et al. [16], with $a = 1.18$ nm for PPI G3 and $a = 1.98$ nm for G5. Though these values are for nearly neutral PPI dendrimers in water, our dynamic light scattering measurements (Brookhaven Instruments) indicate no discernable deviations due to changes in solution pH or ionic strength.

The MOBILITY computer program based on O'Brien and White's solution for sphere electrophoresis is commercially available (University of Melbourne) and is used

here to calculate μ_0' for a sphere with parameters (ζ', $a\kappa$ and σ') matching those of the dendrimer under various experimental conditions.

To compare the electrophoretic behavior of dendrimers to that predicted by the Muthukumar solution for a fractal polyelectrolyte, we use Mathematica to evaluate Eq. 4.3 with $d_f = 2$, 3, or 4, and with the appropriate values for σ' and κR_g for PPI G3 and G5 under various experimental conditions. The values for R_g are taken from Scherrenberg et al. [16], with $R_g = 0.93$ nm for PPI G3 and $R_g = 1.39$ nm for PPI G5.

4.5 Results and Discussion

4.5.1 Function of α

Figures 4.4 and 4.5 show the dependence of μ_0 on α for PPI G3 and G5; the $\mu_0(\alpha)$ plots result from the combination of $\alpha(pH)$ and $\mu_0(pH)$ data. The behavior observed is similar to that of linear polyelectrolytes [28-30]: μ_0 initially rises sharply with α and then increases more slowly at larger α. For linear polyelectrolytes, some have attributed the onset of nonlinearity to Manning's "counterion condensation" hypothesis [29-31]. This concept asserts that when the distance between charges along the polymer backbone is less than the Bjerrum length, the charge density is large enough to cause condensation on the chain backbone of a sufficient number of small ions to yield an effective backbone charge density of one charge per Bjerrum length [32,33]. Electrophoretic behavior would then depend on the effective charge density, a constant above a certain critical charge density. For fully ionized PPI dendrimers, the distance between charges along the "backbone" corresponds to the distance between branch points, about 0.37 nm. In aqueous solutions, the Bjerrum length is about 0.71 nm, giving a crude approximation for the onset of counterion condensation at $\alpha \approx 0.5$. However, the dendrimer data shown in Figures 4.4 and 4.5 reveal μ_0 as varying smoothly with α, rather than a distinct break in the $\mu_0(\alpha)$ curve at $\alpha \approx 0.5$. Application of the counterion condensation model to highly

branched objects such as dendrimers is questionable at best, as its application to linear polyelectrolyte electrophoresis lacks theoretical justification.

To compare the $\mu_0(\alpha)$ behavior to that expected for a sphere, this data is plotted along with the theoretical predictions in a dimensionless format in Figures 4.6 and 4.7. In Figure 4.6, the dendrimer data is compared to the Henry result for I=0.01 M solutions with1:1 electrolyte and to the O'Brien and White result for I=0.01 M KCl solutions. The Henry result does not depend on properties of the small ions, while the O'Brien and White calculation requires the equivalent conductivity λ_i^0 of each counter- and co-ion as input parameters. Though the collection of the dendrimer data required various buffer systems (rather than KCl solutions), the comparison shown in Figure 4.6 is a useful first approximation. For low values of α, both the Henry result and the O'Brien and White predictions agree well with the dendrimer data. As α increases and the Debye-Hückel approximation becomes invalid, the Henry solution greatly overestimates the mobility of the dendrimers. Not surprisingly, the use of the full Poisson-Boltzmann equation in the O'Brien and White model enables a much closer match to the data in this region. The O'Brien and White calculation not only shows qualitative agreement but also comes remarkably close quantitatively, in spite of the difference in electrolyte systems.

To determine if the O'Brien and White model could match the data more closely, the calculations were re-evaluated using the buffer systems employed for the dendrimer experiments. To cover the broad pH range (2.8 – 11.5), four different buffer systems were required. Table 4.1 lists the buffer composition at each pH, and Table 4.2 gives λ_i^0 values of the various counter- and co-ions. Figure 4.7 compares the dendrimer data to the O'Brien and White results for both KCl solutions (as in Fig. 4.6) and the specific buffer systems used in the experiments. Little difference is noted between the two sets of O'Brien and White calculations. Previous calculations show that differences in the counterion's λ_i^0 can have a significant effect on μ_0', while variations in the co-ion's λ_i^0 play a much smaller role [20]. This observation is in agreement with the results shown in

Figure 4.7; the identity of the counterion (Cl^-) is usually the same for both sets of calculations, while the identity of the co-ion is always different (K^+ vs. Na^+ or $Tris^+$). In fact, the one buffer system that produces any real differences in μ_0' values from those for KCl is NaOAc-HOAc (pH 4.5-5.5), which employs an acetate counterion rather than a chloride one. Furthermore, this buffer seems to be the source of the small "dip" in μ_0' seen in the dendrimer data in the plateau region ($0.6 < \alpha < 1.0$): the acetate counterion has a lower λ_i^0.value than chloride, which leads to a lower value for μ_0'.

The exceptional success of the O'Brien and White solution argues strongly that the relaxation effect dominates the electrophoretic behavior of the dendrimers as α increases. Furthermore, the ability to predict the plateau region by incorporating the relaxation effect dissolves any need to invoke the "counterion condensation" argument so often used to explain similar behavior of linear polyelectrolytes.

To compare the $\mu_0(\alpha)$ behavior to that predicted by the Muthukumar solution for a fractal polyelectrolyte, we must first choose a fractal dimension for the dendrimer. Some experimental evidence indicates that dendrimers are not truly fractal [34]; however, other studies report that R_g does appear to scale with molecular weight M ($R_g^{d_f} \sim M$). The reported values of d_f include 2 for a charged dendrimer [35], 3 for the neutral PPI dendrimer in D_2O [16], and 4 for a random-walk dendrimer [36]. Figure 4.8 uses each of these d_f values to compare the results of Eq. 4.3 to the experimental $\mu_0'(\alpha)$ data for the PPI dendrimers. As for the Henry predictions, the agreement between the Muthukumar solution and the dendrimer data is limited to the low α region. The different d_f values give practically no difference in μ_0' in this range.

The only fundamental study on dendrimer electrophoresis which could be compared to this work is that of Dubin et al [6]. Using dendrimers with chargeable terminal groups (carboxyl-terminated polyamidoamine (PAMAM)), they present limited $\mu_0(\alpha)$ data ($\alpha > 0.4$) for generations 2 and 5. In the intermediate α range, they observe a steady increase in μ_0, with a comparable difference in μ_0 to that seen above for the same

α range. Further, they note higher μ_0 values for the smaller dendrimer for $\alpha > 0.5$; this result can also be seen in our data, though to a slightly lesser extent as we are comparing dendrimers which are closer in size than in the Dubin study. Interestingly, they observe one feature which is absent from our $\mu_0(\alpha)$ data: a maximum in μ_0 for both dendrimers in the high α range. A maximum in $\mu_0(\alpha)$ is predicted by O'Brien and White for $a\kappa > 3$. Though Dubin et al. observed a maximum for $a\kappa$ as small as 1.25, their maximum in μ_0 may still be a consequence of the relaxation effect. Anyway, our data were collected at much lower $a\kappa$ (= 0.387 and 0.649 for G3 and G5, respectively), and the nearly quantitative agreement with the O'Brien and White theory over the full range of α argues strongly for the dominance of the relaxation effect.

4.5.2 Function of Ionic Strength

Figures 4.9 and 4.10 examine the effect of ionic strength I on μ_0 for fully protonated ($\alpha = 1$) PPI G3 and G5 for two different buffer systems: formic acid/NaOH and KHP/HCl, respectively. While both buffers give the same qualitative $\mu_0(I)$ behavior, the formic acid/NaOH system yields higher μ_0 values. This observation will be discussed in more detail below.

Qualitatively, the dendrimers' behavior differs from that previously observed for linear polyelectrolytes in two ways. First, regardless of chemical structure or backbone flexibility, μ_0 decreases nearly logarithmically with increasing I for linear polyelectrolytes [37]. While μ_0 also decreases with I for the dendrimers, the dependence is not logarithmic; rather, the I dependence is strong at low I and begins to lessen as I increases. Second, high molecular weight linear polyelectrolytes exhibit a molecular weight-independent mobility at a given I [37]. Conversely, the PPI G3 dendrimer consistently displays a higher mobility than that of G5. The relatively low molecular weight of these dendrimers may make a comparison to charged linear oligomers more appropriate. Unfortunately, the electrophoretic behavior of charged oligomers is not well understood. Previous experimental investigations (see Chapter 2 and ref. [37] reveal a

complex dependence of μ_0 on chain length N, with a maximum occuring in $\mu_0(N)$ in the oligomer range. As the physical basis for this maximum is not known, any attempt to attribute the observed molecular weight dependence in the dendrimer data to the same phenomenon is fruitless. Additionally, diffusion coefficient and intrinsic viscosity data suggest that dendrimers behave hydrodynamically differently than linear polymers or oligomers. The dendrimer's high degree and uniformity of branching gives a denser structure and may limit hydrodynamic effects of the surrounding solvent on the interior of the molecule. A dendrimer, then, may be more appropriately modeled hydrodynamically as a sphere, while the linear polyelectrolyte behaves more like a cylinder. This difference in hydrodynamic behavior may be enough to explain the differences noted above in electrophoretic behavior.

To compare to theoretical predictions for charged spheres, we convert the data of Figure 4.9 to its dimensionless form of μ_0'/σ' vs. $a\kappa$ for Figure 4.11. Here, the Henry theory greatly overestimates the dendrimer mobility for the whole $a\kappa$ range studied, with its deviations from the G5 data being greater than that of G3. Since the dendrimers are fully charged and a is close to κ^{-1}, the large departure of the Henry theory from the data is not surprising. On the other hand, the O'Brien and White model provides quantitative agreement to within the experimental error for the entire measurement range, $0.2 < a\kappa < 2.0$, without using any fitting parameters. As with the $\mu_0'(\alpha)$ data, the relaxation effect dominates the electrophoretic behavior and successfully accounts for the reduction of mobility as compared to the Henry result. Further, the O'Brien and White model predicts lower μ_0' values for the G5 dendrimer than for G3 at all $a\kappa$; thus, the combination of sphere hydrodynamics and the relaxation effect captures the experimentally observed molecular weight dependence.

The O'Brien and White model was developed for a solid sphere with all of its charge at the surface. PPI dendrimers, of course, have their charges distributed throughout the molecule. In mapping the dendrimer to a sphere, we have effectively put

all of its charge at its hydrodynamic radius. Perhaps more importantly, this treatment does not account for small counterions which may partition into the dendrimer and lower the effective charge at the dendrimer (or sphere) "surface." Though the above results seem to show that our solid sphere approximation is valid, a question arises regarding the sensitivity of the O'Brien and White predictions to σ'. To answer this question, we compared the data of Figure 4.9 to predictions for spheres with σ' values corresponding to dendrimers which were only charged at the terminal groups. In this case $Q = 16e$ and $64e$ for G3 and G5, respectively (in the above analysis for Figure 4.11, $Q = 30e$ and $126e$ for G3 and G5, respectively). Figure 4.12 shows that these results match the data just as well as the predictions for the fully charged dendrimers, implying that the model is not sensitive to σ' at these relatively high σ' values. This insensitivity to σ' is not unexpected, however, given that the $\mu_0'(\alpha)$ data show very little increase in μ_0' for $\alpha > \sim 0.4$ ($Q = 12e$) for G3 and $\alpha > \sim 0.3$ ($Q = 38e$) for G5. Indeed, in re-examining the $\mu_0'(\alpha)$ data, the ability of the O'Brien and White model to match $\mu_0'(\alpha)$ for $\alpha << 1$ implies that the number of partitioned ions must be small for the system studied here.

A desire to explain the differences in $\mu_0(I)$ for the two different buffer systems (Figures 4.9 and 4.10) prompted us to compare the O'Brien and White predictions for these two systems. Figure 4.13 reveals that differences in λ_i^0 for the small ions cannot account for the lower μ_0 values in the KHP/HCl buffer. In fact, the model predicts slightly higher μ_0 values for the KHP/HCl buffer than for the formic acid/NaOH system. The lower μ_0 values of the KHP/HCl system may instead result from specific ion interactions with the dendrimer.

To compare the $\mu_0(I)$ data of Figure 4.9 to the Muthukumar predictions, a plot of $\mu_0'/\sigma'(R_g\kappa)$ is presented in Figure 4.14. As with Figure 4.8, the Muthukumar solution is given for three different values of d_f: 2, 3, and 4. For these highly charged dendrimers, the Muthukumar results greatly overestimate the behavior of the dendrimers, just as the Henry theory does. As d_f increases, the curves shift to lower μ_0'/σ' values and come

closer to the values measured for the dendrimers; however, the shape of the curve given by the Muthukumar theory is somewhat different from that of the dendrimer data. The major source of the discrepancy is probably in the neglect of the relaxation effect; however, the treatment of dendrimers as fractal objects may also be questionable [34].

Dubin et al. [6] also investigated $\mu_0(I)$ for dendrimers with fully charged terminal groups. Generations 2,3,4, and 5 all show an I dependence similar to that seen above for the PPI dendrimers, and the same molecular weight dependence at a given I is observed as well. Dubin et al. attribute the molecular weight trend to nonspecific ion binding effects; we see no reason to make such arguments for the PPI dendrimers, as their behavior matches that predicted by the O'Brien and White model.

Finally, a comparison between our dendrimer $\mu_0(I)$ data and that of typical spherical particles is needed. Much effort has been devoted to producing well-defined spherical colloids for the purpose of testing the O'Brien and White model. Though the resulting data is quite extensive, none has yet shown the quantitative agreement we see with the PPI dendrimers without using adjustable parameters. In fact, the only claims to "reasonable" quantitative agreement have involved assuming either a surface charge which differs from that measured by other techniques or a shear plane which is displaced from the particle's surface [38,39]. Dendrimers, however, have a well-defined and easily-controlled charge density; taking advantage of this feature results in unprecedented quantitative agreement with the O'Brien and White predictions and verifies the dominance of the relaxation effect when surface charge is high and $a \approx \kappa^{-1}$.

4.6 Summary

The results presented above compare the electrophoretic motion of a dendrimer to that of a comparably sized sphere or flexible linear polymer. Dendrimers can serve as a model system due to their well-defined charge properties and uniform degree of

branching. As the degree of charge α is varied, the dendrimer's electrophoretic behavior resembles that of a linear polymer: μ_0 increases sharply at low α and begins to plateau in the intermediate α range. However, the data also agree with predictions for a charged sphere when nonlinear electrostatic effects are included. Quantitative agreement with this same sphere model is achieved as ionic strength is varied for solutions of fully charged dendrimers. Such agreement with the sphere model is somewhat surprising, as ions can penetrate into the dendrimer interior and dendrimers are not truly spherical. The overall results show that nonlinear electrostatics dominate the behavior of charged dendrimers and suggest that similar mechanisms may be operative for linear polyelectrolytes.

4.7 References

1. Pesak, D. J.; Moore, J. S.; Wheat, T. E. *Macromolecules* **1997**, *30*, 6467.

2. Brothers, H. M.; Piehler, L. T.; Tomalia, D. A. *J. Chromatogr. A* **1998**, *814*, 233.

3. Li, J.; Swanson, D. R.; Qin, D.; Brothers, H. M.; Piehler, L. T.; Tomalia, D.; Meier, D.J. *Langmuir* **1999**, *15*, 7347.

4. Khaledi, M. G. *Micellar Electrokinetic Chromatography*; Khaledi, M. G., Ed.; John Wiley & Sons: New York, 1998; Vol. 146, pp 77.

5. Ruponen, M.; Yla-Herttuala, S.; Urtti, A. *Biochim. Biophys. Acta - Biomembranes* **1999**, *1415*, 331.

6. Huang, Q. R.; Dubin, P. L.; Moorefield, C. N.; Newkome, G. R. *J. Phys. Chem. B* **2000**, *104*, 898.

7. O'Brien, R. W.; White, L. R. *J. Chem. Soc. Faraday Trans. II* **1978**, *74*, 1607.

8. Elimelech, M.; O'Melia, C. R. *Coll. Surf.* **1990**, *44*, 165.

9. Fernández Barbero, A.; Martínez García, R.; Cabrerizo Vílchez, M. A.; Higaldo-Alvarez, R. *Coll. Surf. A* **1994**, *92*, 121.

10. Seebergh, J. E.; Berg, J. C. *Coll. Surf. A* **1995**, *100*, 139.

11. Barchini, R.; Saville, D. A. *Langmuir* **1996**, *12*, 1442.

12. Tuin, G.; Senders, J. H. J. E.; Stein, H. N. *J. Coll. Int. Sci.* **1996**, *179*, 522.

13. Folkersma, R.; van Diemen, A. J. G.; Stein, H. N. *Langmuir* **1998**, *14*, 5973.

14. Rasmusson, M.; Wall, S. *J. Coll. Int. Sci.* **1999**, *209*, 312.

15. Vorwerg, L.; Antonietti, M.; Tauer, K. *Coll. Surf. A* **1999**, *150*, 129.

16. Scherrenberg, R.; Coussens, B.; van Vliet, P.; Edouard, G.; Brackman, J.; de Brabender, E. *Macromolecules* **1998**, *31*, 456.

17. Henry, D. C. *Proc. Roy. Soc., Ser. A* **1931**, *133*, 106.

18. Hückel, E. *Phys. Z.* **1924**, *25*, 204.

19. von Smoluchowski, M. *Z. Phys. Chem.* **1918**, *92*, 129.

20. Wiersema, P. H.; Loeb, A. L.; Overbeek, J. T. G. *J. Coll. Int. Sci.* **1966**, *22*, 78.

21. Russel, W. B.; Saville, D. A.; Schowalter, W. R. *Colloidal Dispersions*; Cambridge University Press: Cambridge, 1989.

22. Muthukumar, M. *Electrophoresis* **1996**, *17*, 1167.

23. Koper, G. J. M.; van Genderen, M. H. P.; Elissen-Román, C.; Baars, M. W. P. L.; Meijer, E. W.; Borkovec, M. *J. Am. Chem. Soc.* **1997**, *119*, 6512.

24. van Duijvenbode, R. C.; Borkovec, M.; Koper, G. J. M. *Polymer* **1998**, *39*, 2657.

25. Loeb, A. L.; Overbeek, J. T. G.; Wiersema, P. H. *The Electrical Double Layer Around a Spherical Colloid Particle*; MIT Press: Cambridge, 1961.

26. Stigter, D. *J. Electroanal. Chem.* **1972**, *37*, 61.

27. Yoon, B. J. *J. Coll. Int. Sci.* **1997**, *192*, 503.

28. Hoagland, D. A.; Smisek, D. L.; Chen, D. Y. *Electrophoresis* **1996**, *17*, 1151.

29. Whitlock, L. R. *Isotachophoresis of Synthetic Ion-Containing Polymers*; Jorgenson, J. W. and Phillips, M., Ed.; American Chemical Society: Washington, DC, 1987, pp 222-245.

30. Gao, J. Y.; Dubin, P. L.; Sato, T.; Morishima, Y. *J. Chrom. A* **1997**, *766*, 233.

31. Klein, J. W.; Ware, B. R. *J. Chem. Phys.* **1984**, *80*, 1334.

32. Manning, G. S. *Q. Rev. Biophys.* **1978**, *11*, 179.

33. Manning, G. S. *J. Phys. Chem.* **1981**, *85*, 1506.

34. Rietveld, I. B.; Smit, J. A. M. *Macromolecules* **1999**, *32*, 4608.

35. Welch, P.; Muthukumar, M. *Macromolecules* **1998**, *31*, 5892.

36. Zimm, B.; Stockmayer, W. *J. Chem. Phys.* **1949**, *17*, 1301.

37. Hoagland, D. A.; Arvanitidou, E.; Welch, C. *Macromolecules* **1999**, *32*, 6180.

38. Borkovec, M.; Behrens, S. H.; Semmler, M. *Langmuir* **2000**, *16*, 5209.

39. Gittings, M. R.; Saville, D. A. *Langmuir* **1995**, *11*, 798.

40. Lide, D. R. *CRC Handbook of Chemistry and Physics*; 76 ed.; CRC Press: Boca Raton, 1995.

pH	Counterions	Co-ions
2.8	100% Cl^-	70% Na^+,16% H^+,14% Gly^+
3.5	100% Cl^-	91.5% Na^+,3.2% H^+,5.3% Gly^+
4.5	100% $acetate^-$	100% Na^+
5.5	100% $acetate^-$	100% Na^+
7.0	100% Cl^-	100% $Tris^+$
7.8	100% Cl^-	100% $Tris^+$
8.7	100% Cl^-	100% $Tris^+$
9.5	87.3% Cl^-, 12.7% Gly^-	100% Na^+
10.3	65.4% Cl^-, 32.7% Gly^-, 1.9% OH^-	100% Na^+
10.7	56.1% Cl^-, 39.2% Gly^-, 4.7% OH^-	100% Na^+
11.5	32.5% Cl^-, 40.8% Gly^-, 26.7% OH^-	100% Na^+

Table 4.1. Buffer compositions for the $\mu_0(\alpha)$ study. Gly = glycine; Tris = tris(hydroxymethyl)aminomethane.

Cations	λ (10^{-4} m^2S/mol)	Anions	λ (10^{-4} m^2S/mol)
K^+	73.48	Cl^-	76.31
Na^+	50.08	$Acetate^-$	40.9
H^+	349.65	OH^-	198
Gly^+	40*	Gly^-	35*
$Tris^+$	40*	$Formate^-$	54.6
		HP^-	53.5

Table 4.2. Equivalent ionic conductivities of buffer ions [40]. Gly = glycine; Tris = tris(hydroxymethyl)aminomethane; HP = hydrogen phthalate; * = estimated value.

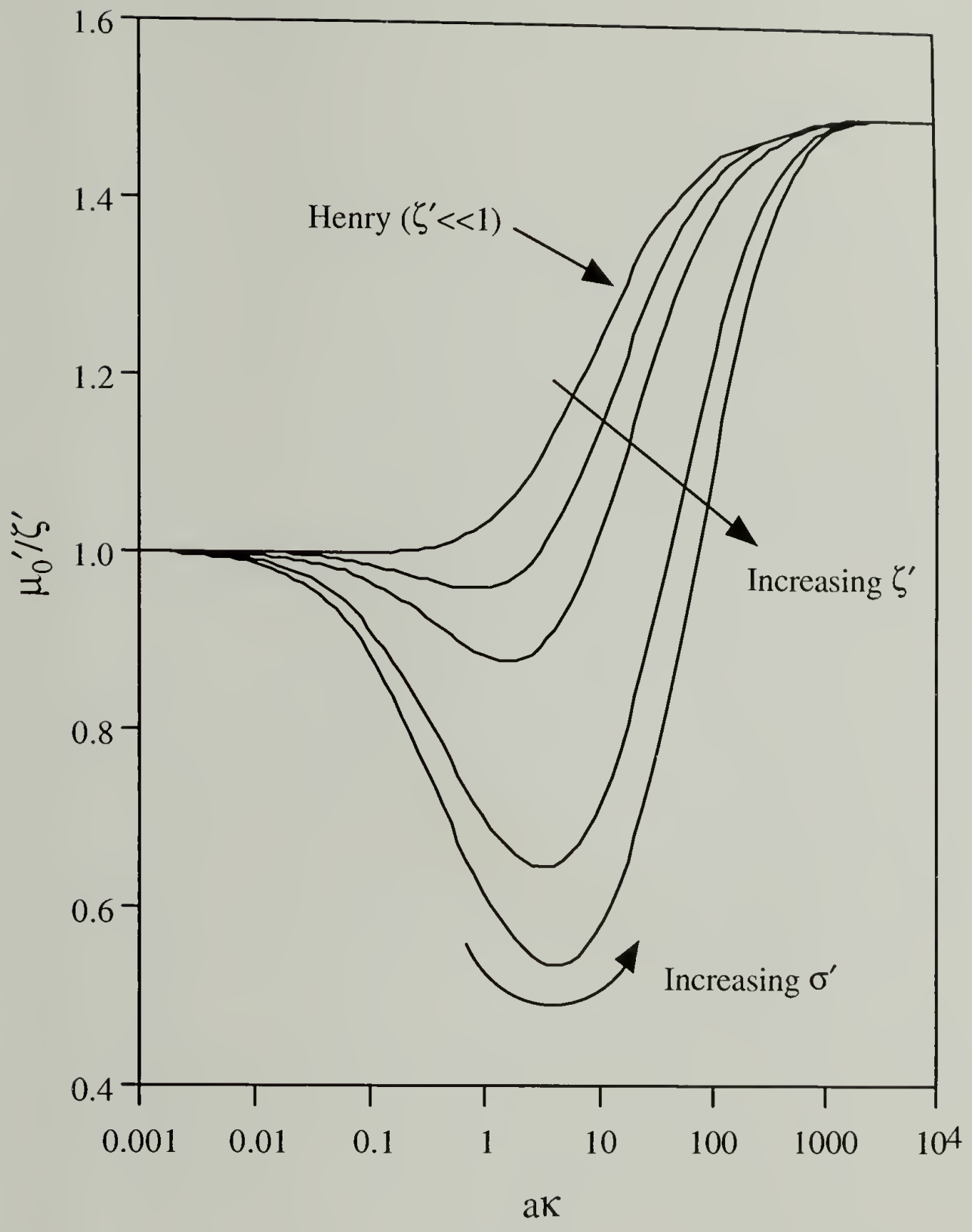

Figure 4.1. Comparison of theories for charged spheres at constant surface potential: $\mu_0'/\zeta'(a\kappa)$. All curves below the Henry curve are from Wiersema et al [20].

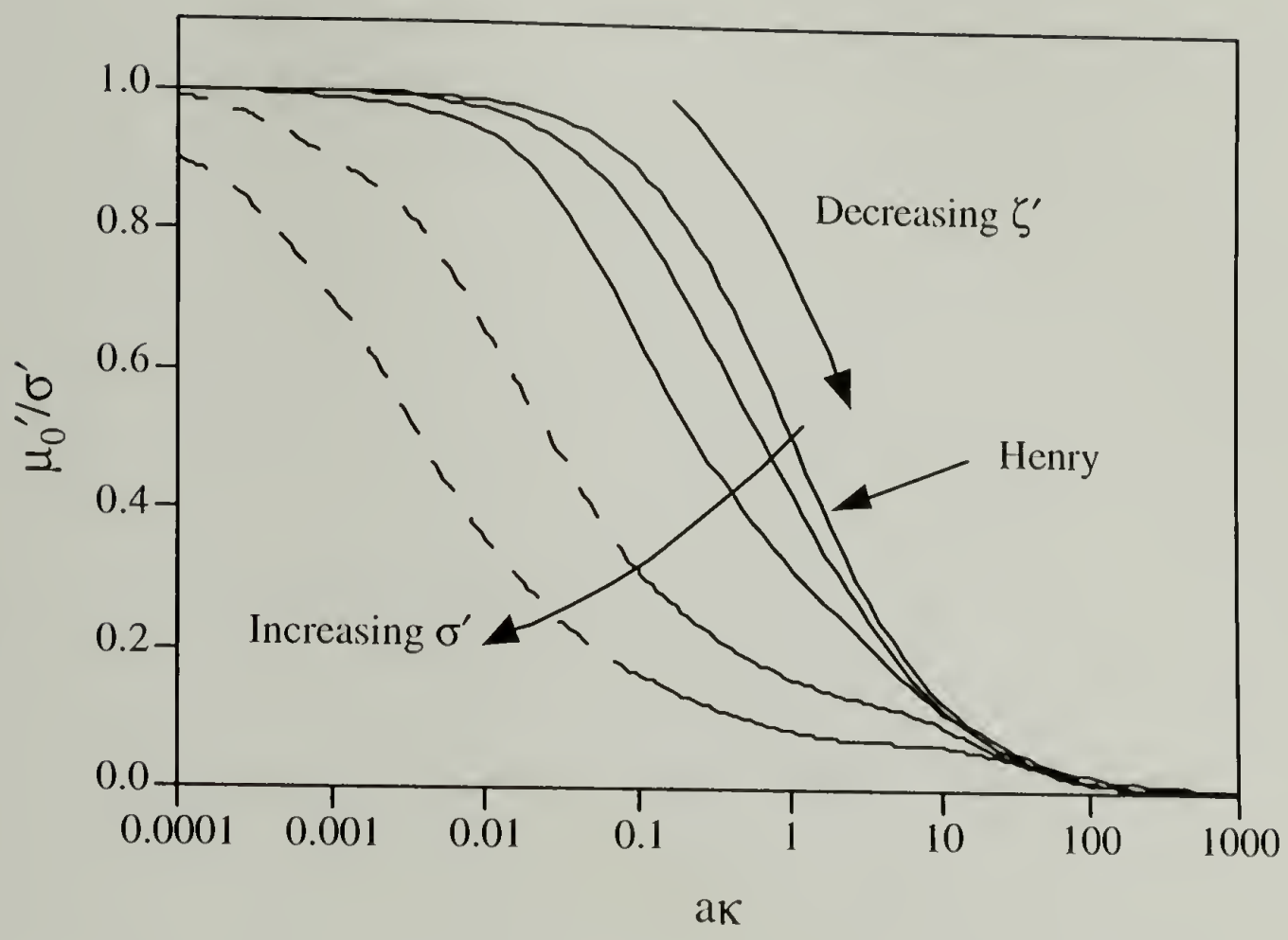

Figure 4.2. Comparison of theories for charged spheres at constant charge: $\mu_0'/\sigma'(a\kappa)$. All curves below the Henry curve are from the O'Brien and White model [7].

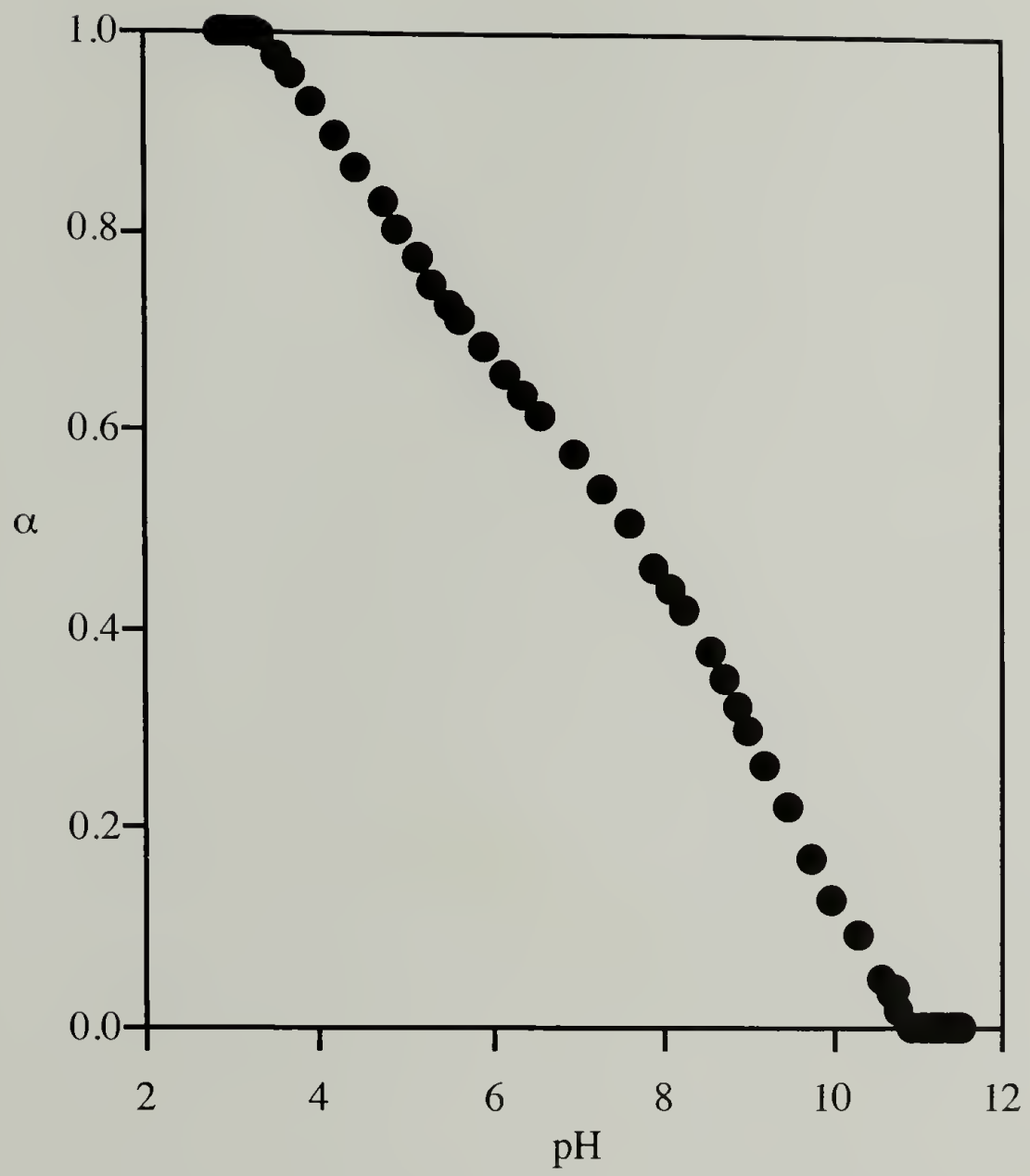

Figure 4.3. Titration of PPI G3 in 0.01M NaCl, using 0.01M HCl and 0.01M NaOH.

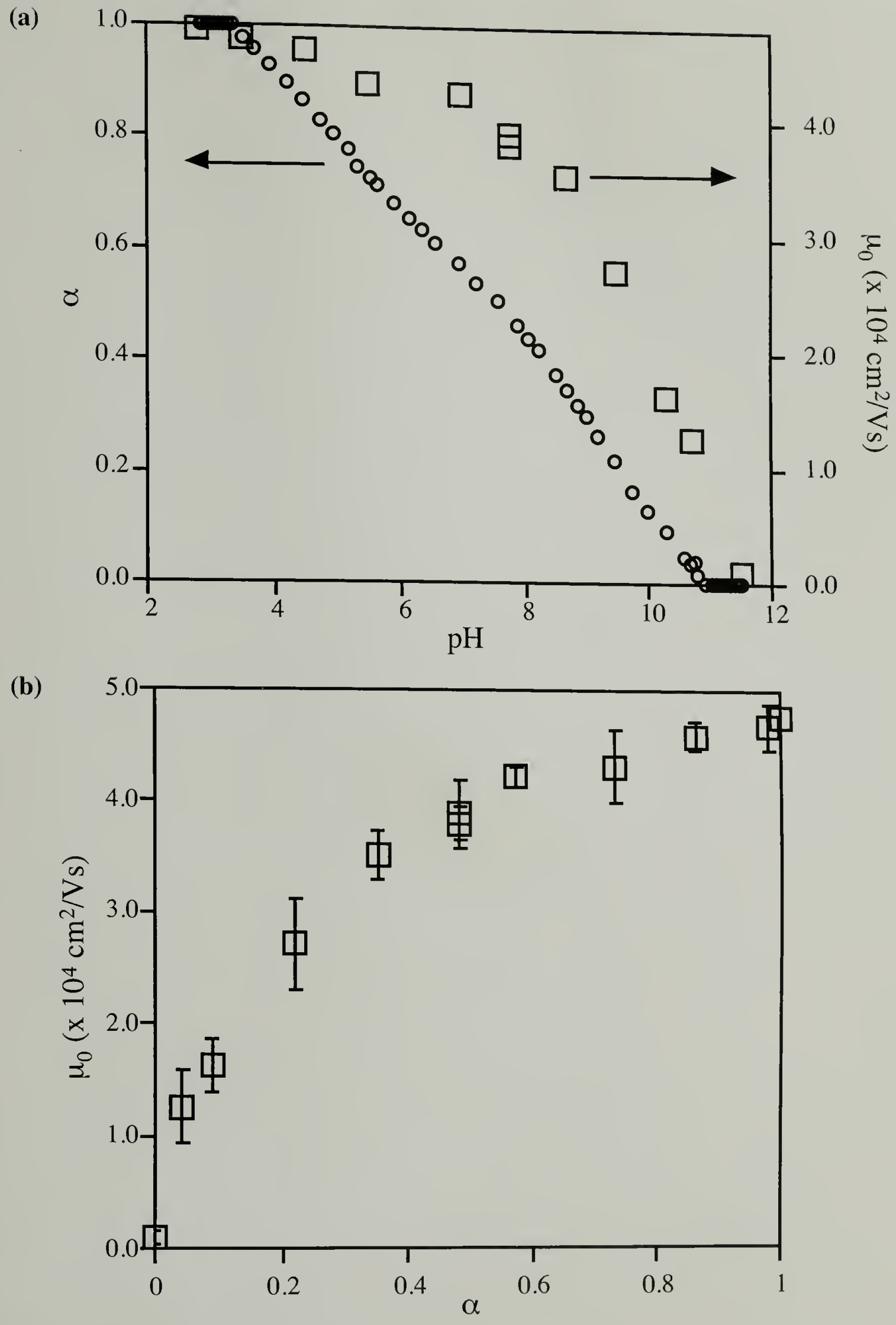

Figure 4.4. (a) pH dependence of α and μ_0 for PPI G3. (b) Electrophoretic mobility $\mu_0(\alpha)$ for PPI G3. For all data, ionic strength I is constant at 0.01M.

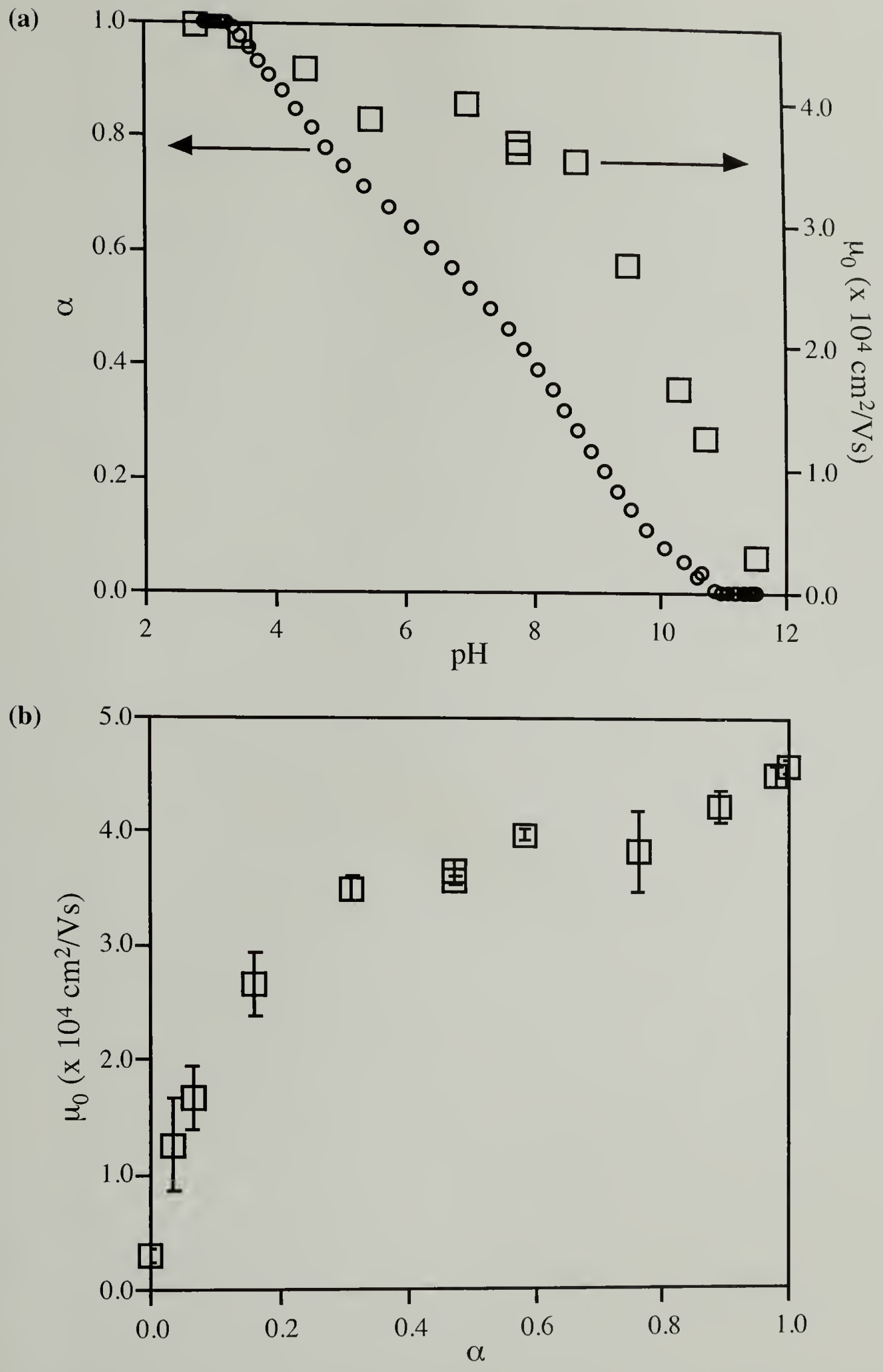

Figure 4.5. (a) pH dependence of α and μ_0 for PPI G5. (b) Electrophoretic mobility $\mu_0(\alpha)$ for PPI G5. For all data, ionic strength I is constant at 0.01M.

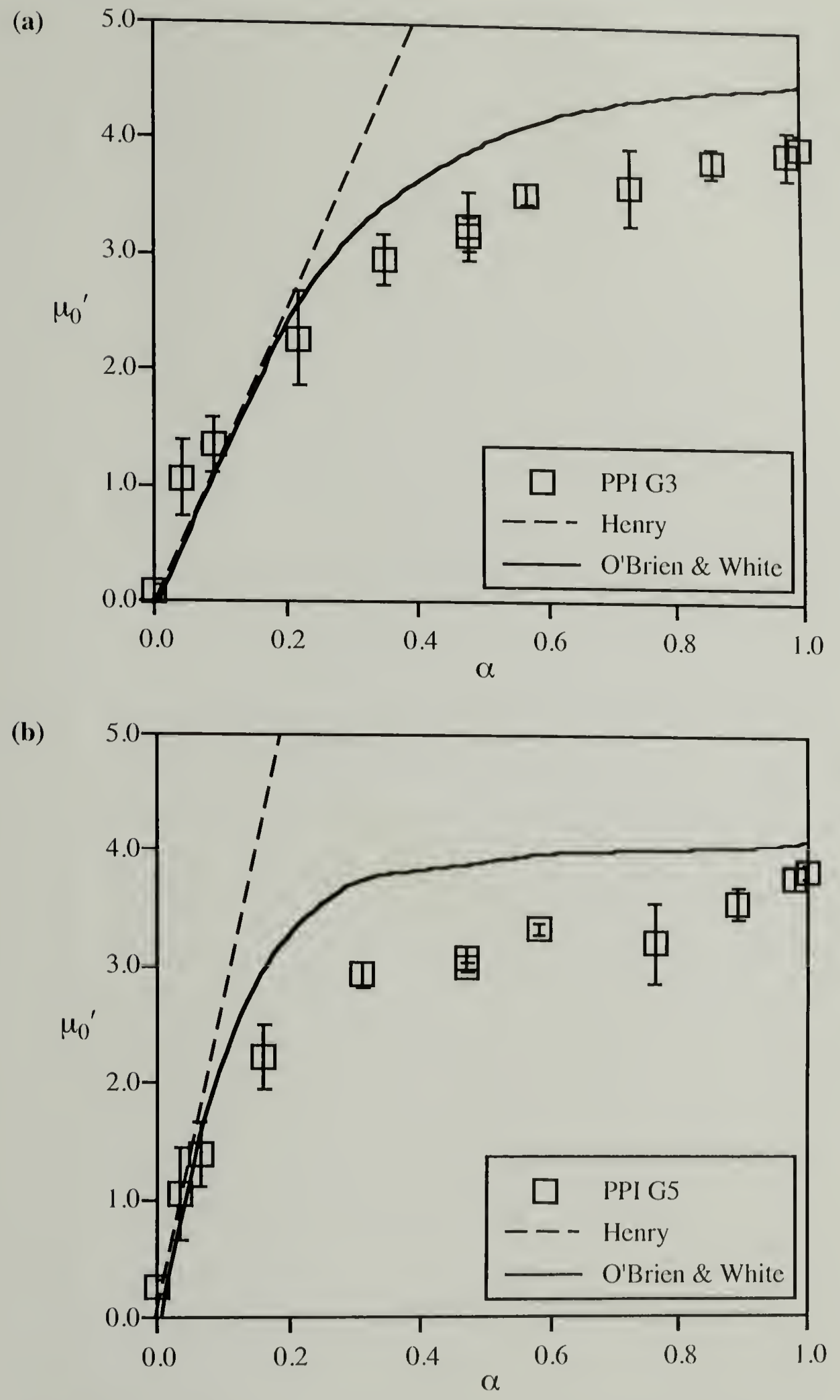

Figure 4.6. The dimensionless mobility $\mu_0'(\alpha)$ for (a) PPI G3 and (b) PPI G5, compared to predictions for charged spheres by Henry and O'Brien & White (see text).

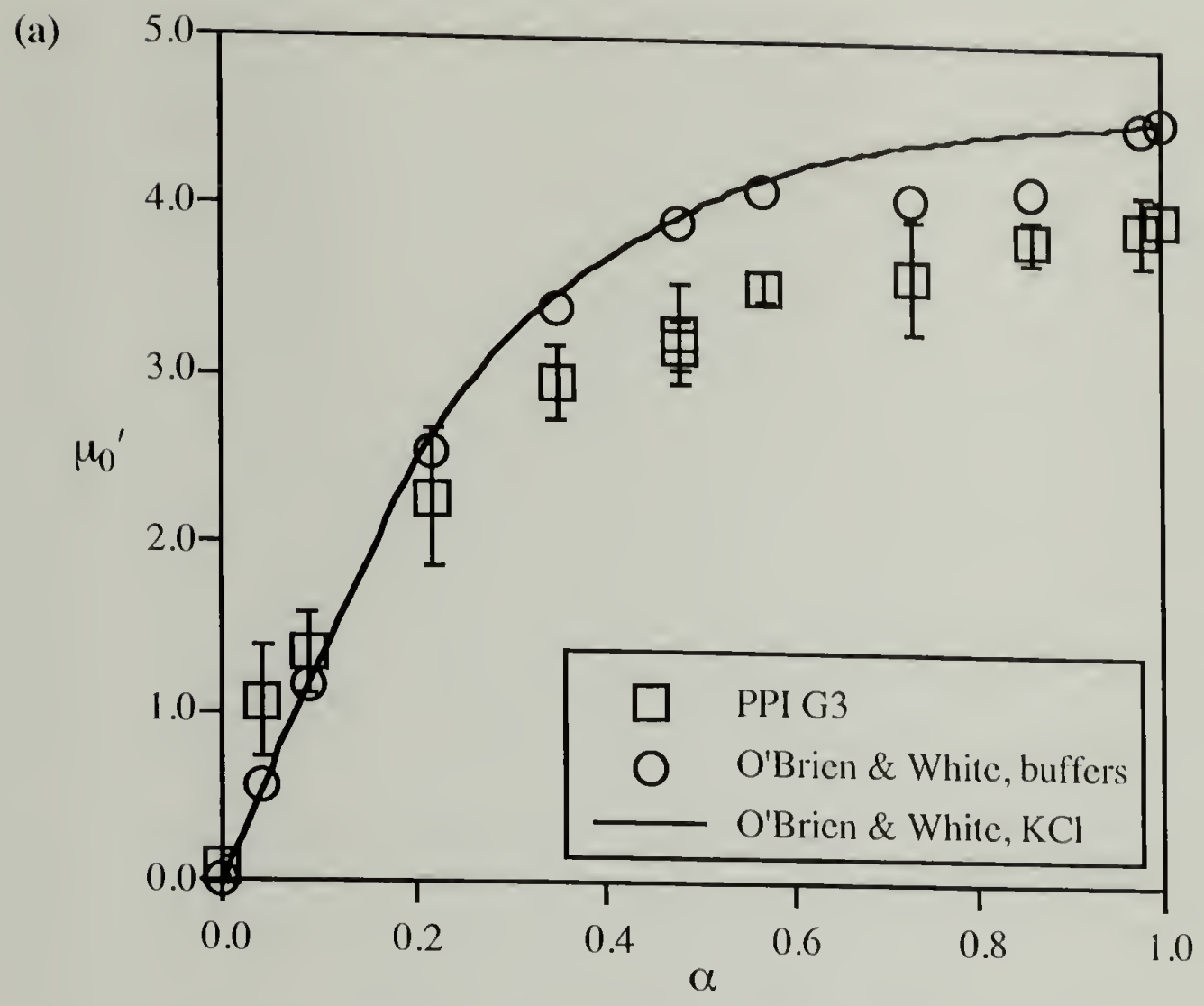

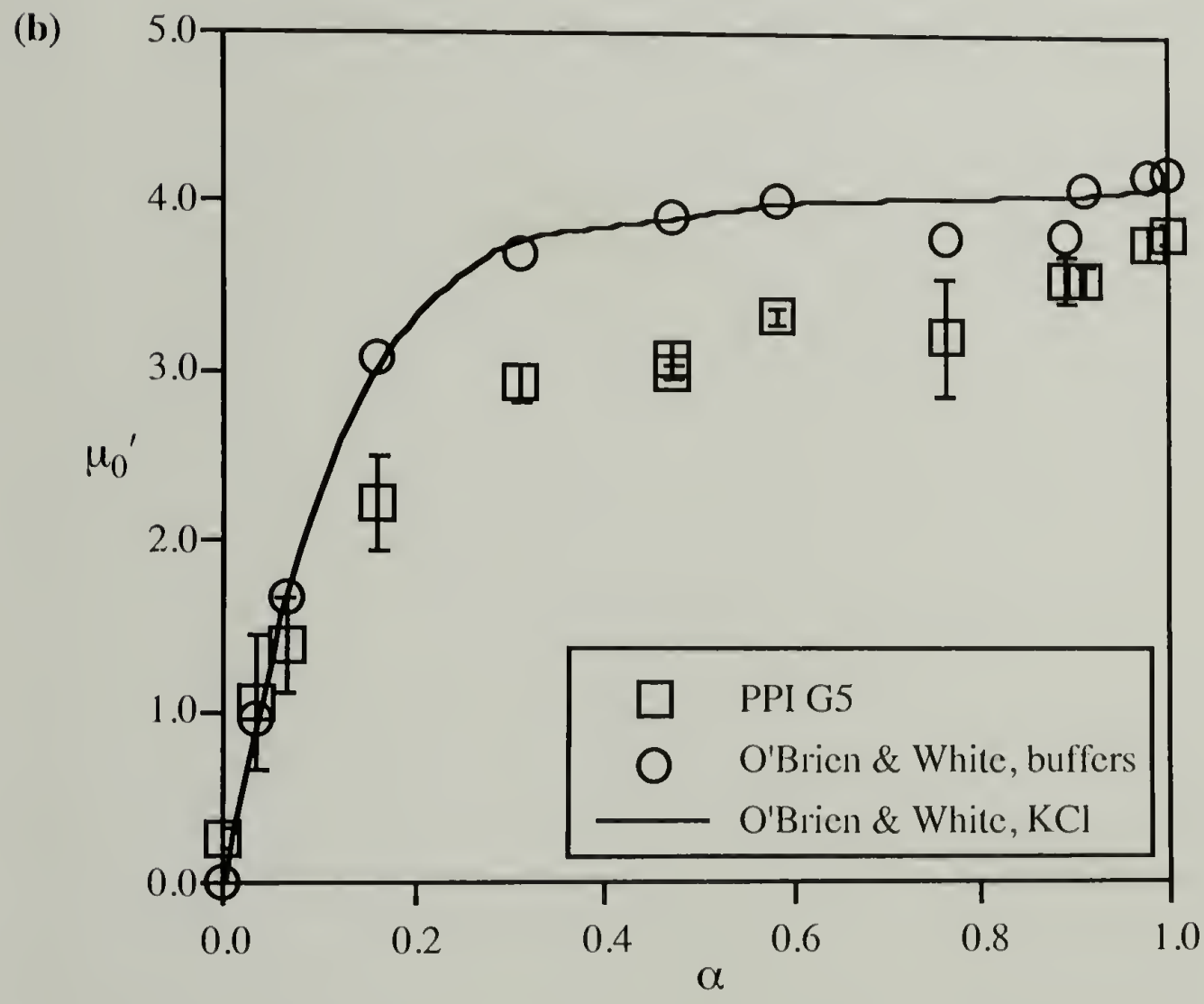

Figure 4.7. The dimensionless mobility $\mu_0'(\alpha)$ for (a) PPI G3 and (b) PPI G5, compared to predictions for charged spheres in KCl solutions vs. various buffer systems (see text).

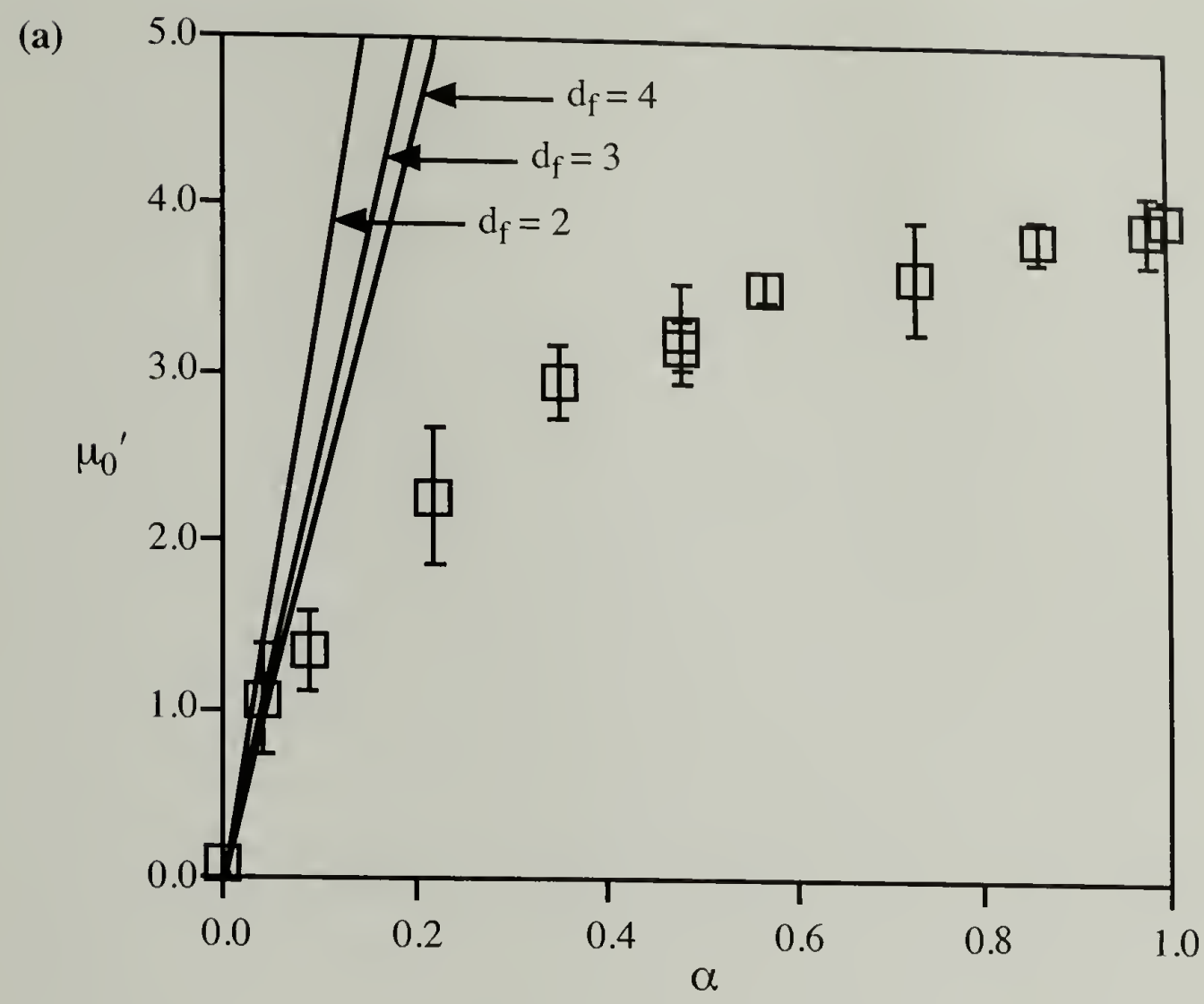

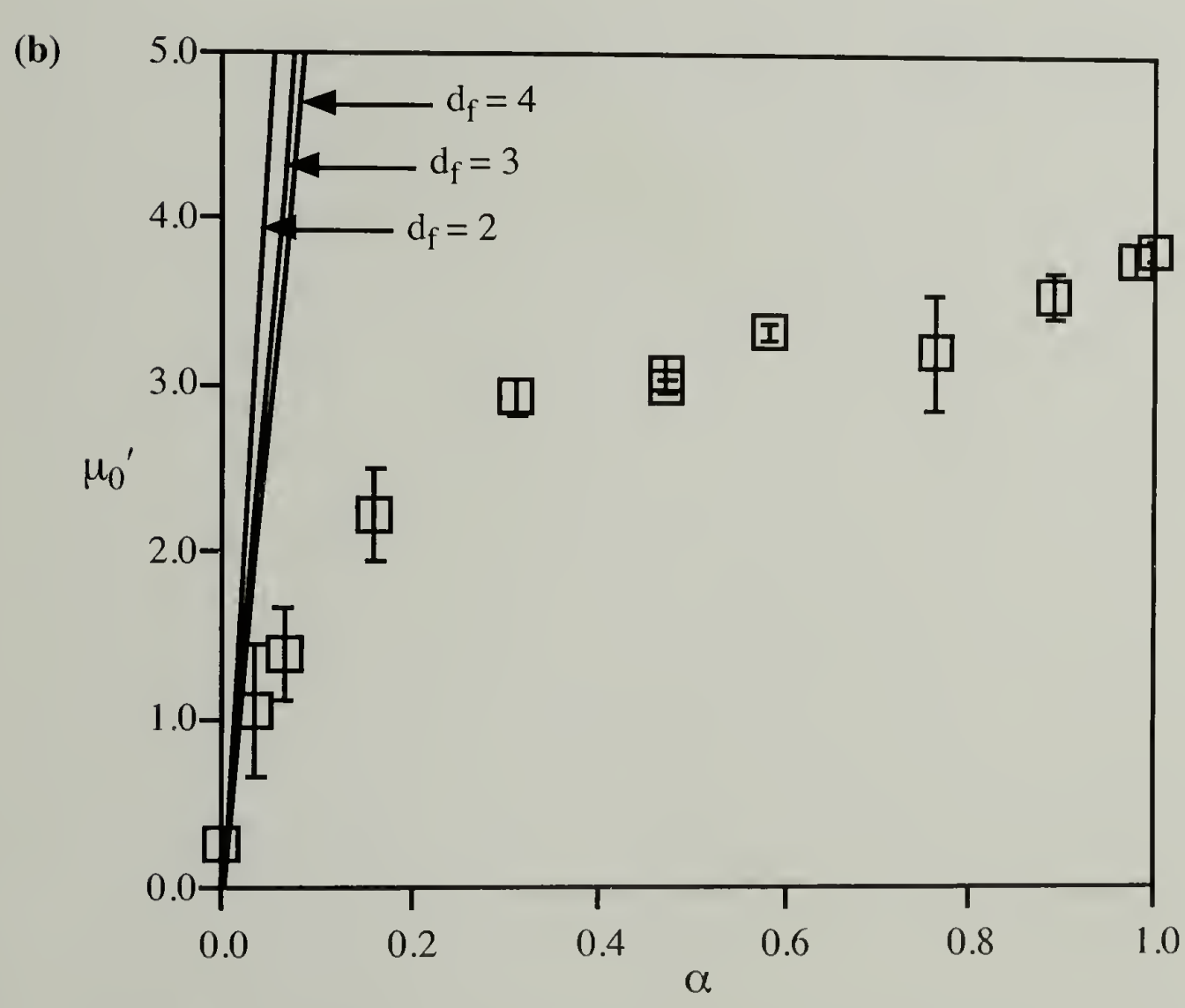

Figure 4.8. The dimensionless mobility $\mu_0'(\alpha)$ for (a) PPI G3 and (b) PPI G5, compared to the Muthukumar predictions for a polyelectrolyte with fractal dimensionality d_f.

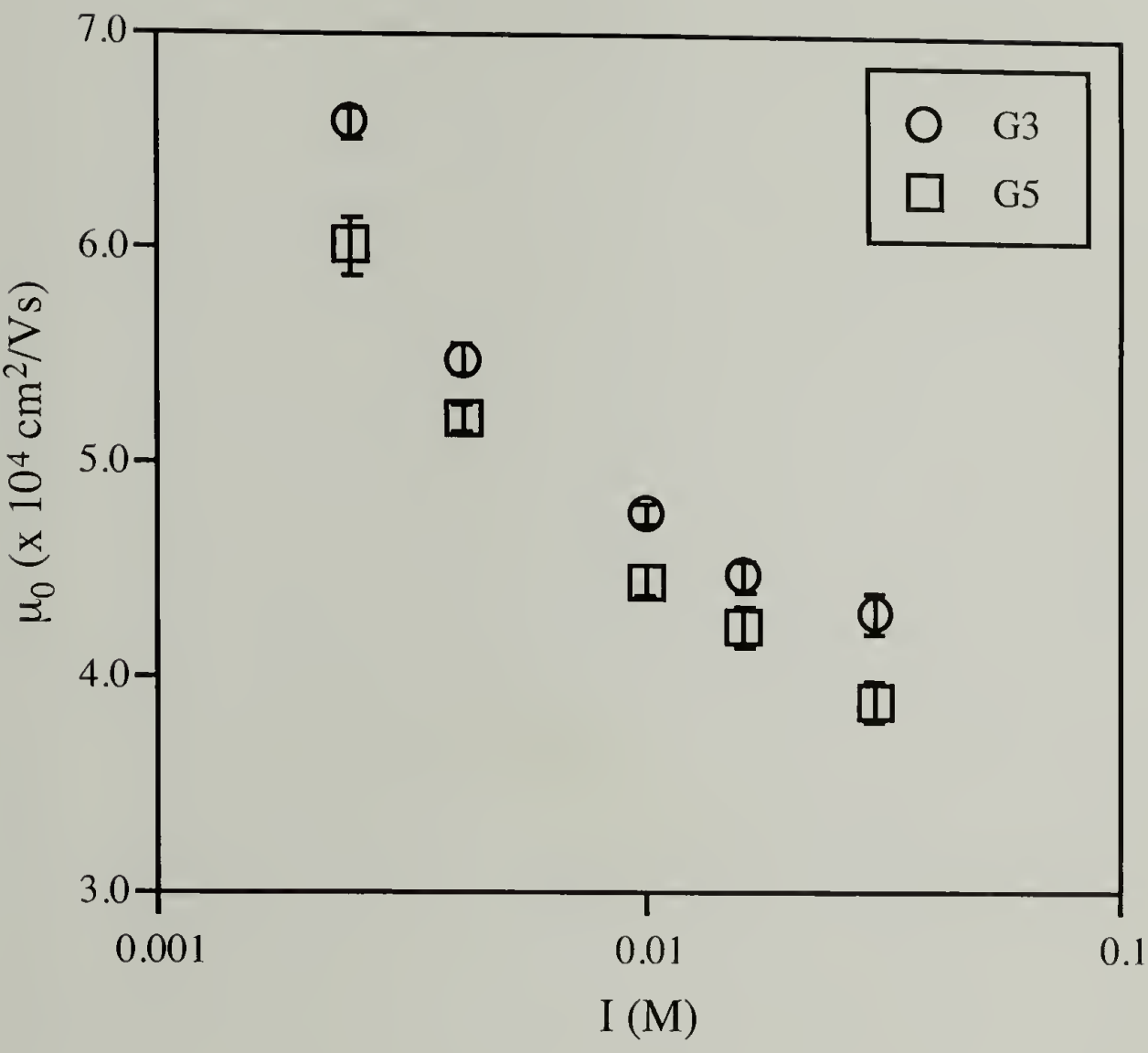

Figure 4.9. Electrophoretic mobility $\mu_0(I)$ for fully charged ($\alpha = 1$) PPI G3 and G5 in formic acid/NaOH buffers.

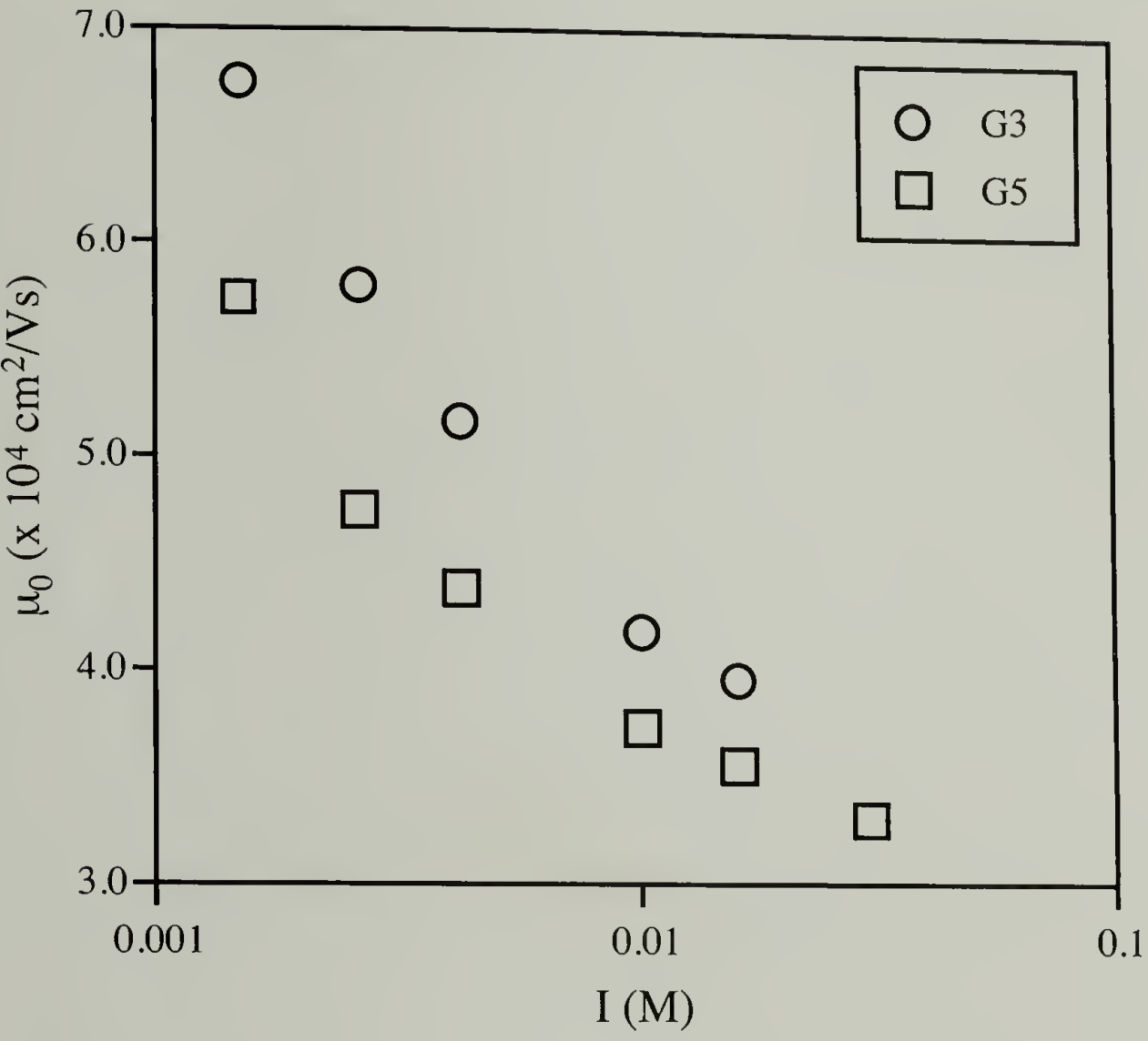

Figure 4.10. Electrophoretic mobility $\mu_0(I)$ for fully charged ($\alpha = 1$) PPI G3 and G5 in KHP/HCl buffers.

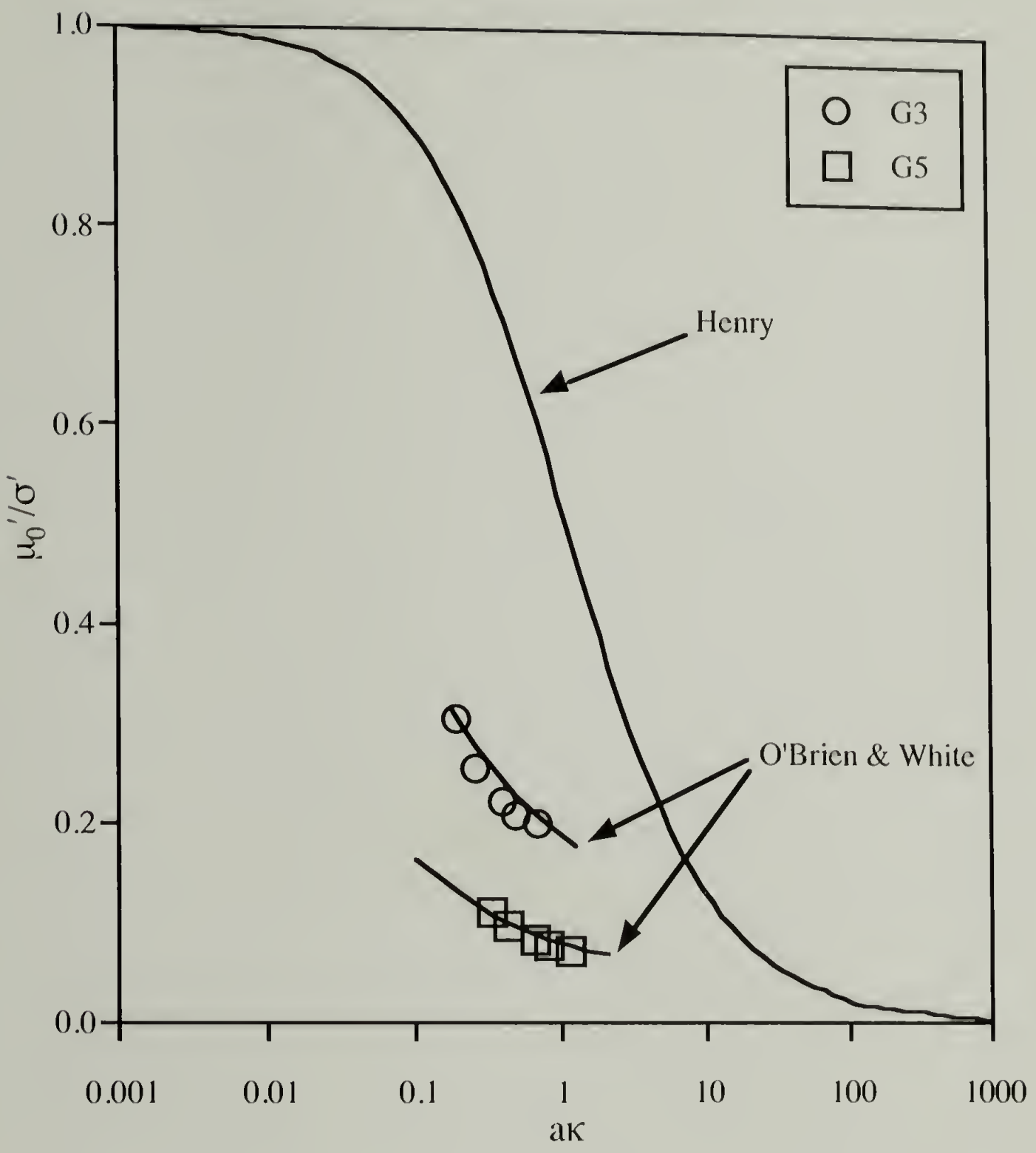

Figure 4.11. Dimensionless plot $\mu_0'/\sigma'(a\kappa)$ to compare fully charged ($\alpha = 1$) PPI G3 and G5 data (in formic acid/NaOH buffers) to predictions for charged spheres. For the O'Brien and White calculations, $\sigma' = 18.1$ ($a = 1.18$ nm, $Q = 30e$) for G3 "sphere," and $\sigma' = 45.3$ ($a = 1.98$ nm, $Q = 126e$) for G5 "sphere."

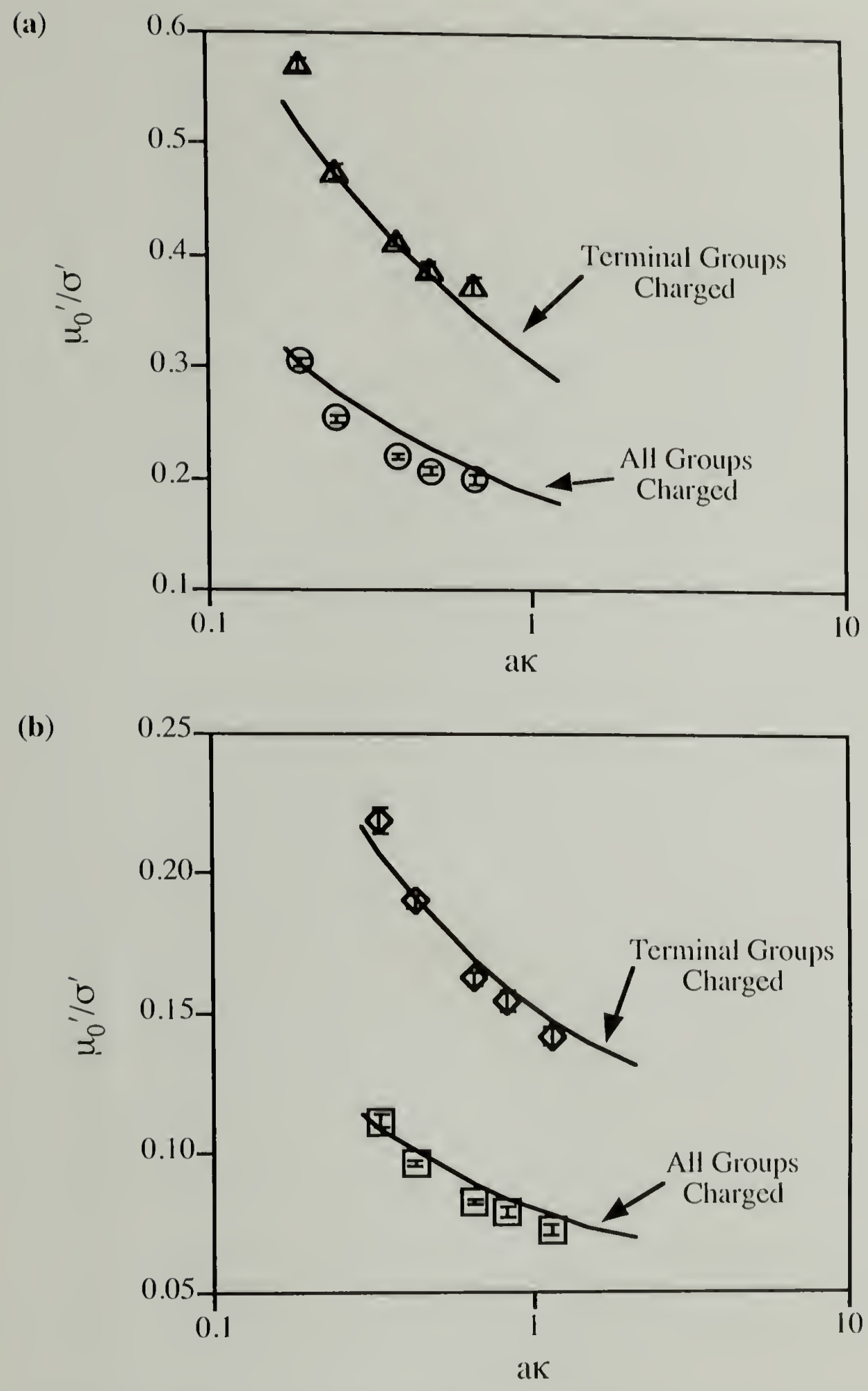

Figure 4.12. Effect of σ' on O'Brien and White calculations for (a) PPI G3 and (b) PPI G5. In (a), $\sigma' = 9.65$ ($Q = 16e$) corresponds to PPI G3 with charged terminal groups only, and $\sigma' = 18.1$ ($Q = 30e$) corresponds to PPI G3 with all amine groups charged. Likewise in (b), $\sigma' = 23.0$ ($Q = 64e$) is for PPI G5 with charged terminal groups, and $\sigma' = 45.3$ ($Q = 126e$) is for PPI G5 with all amine groups charged.

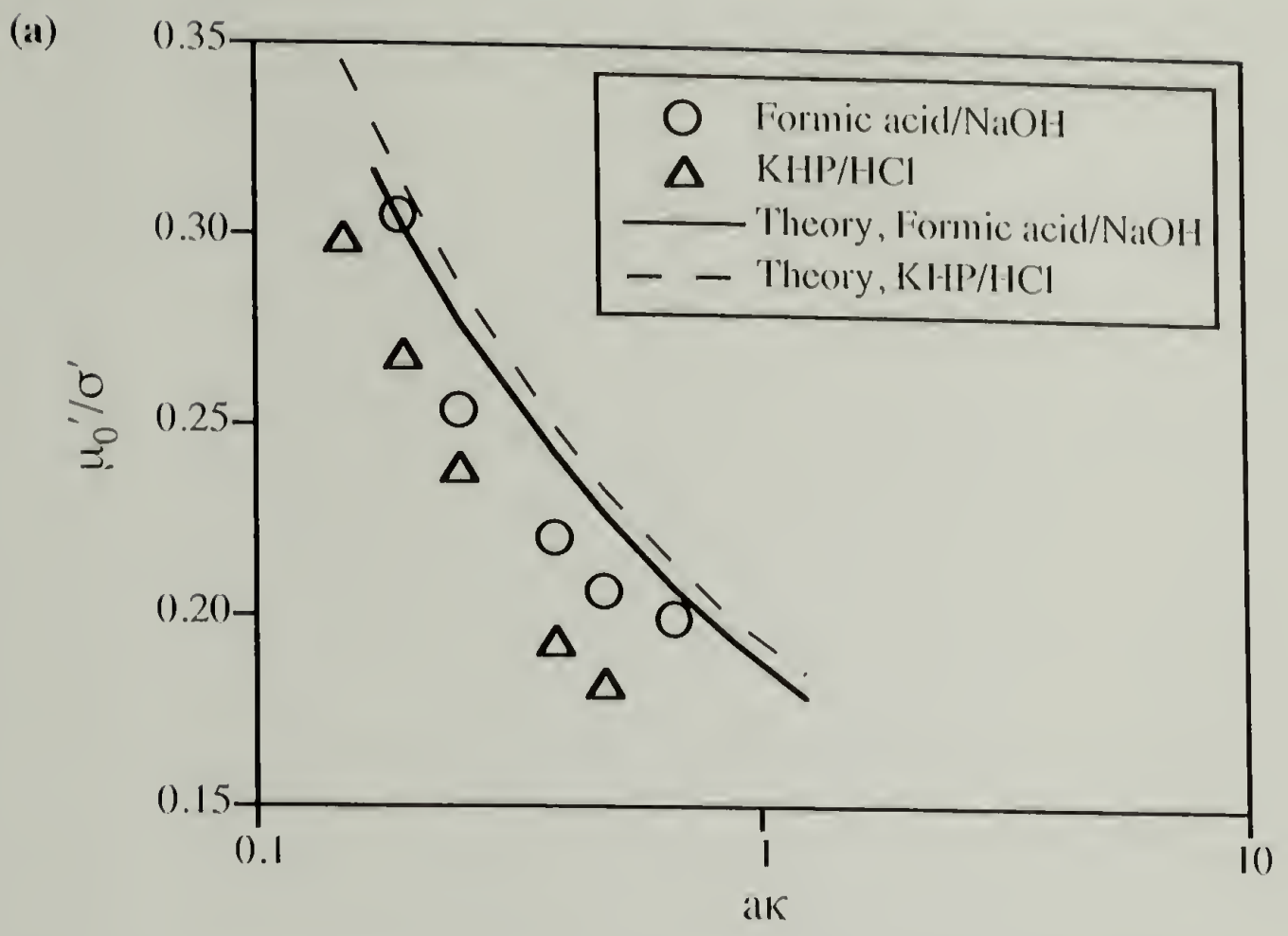

Figure 4.13. O'Brien and White predictions for the two different buffer systems employed in Figures 4.9 (formic acid/NaOH) and 4.10 (KHP/HCl), along with the (a) PPI G3 and (b) PPI G5 data for each buffer system.

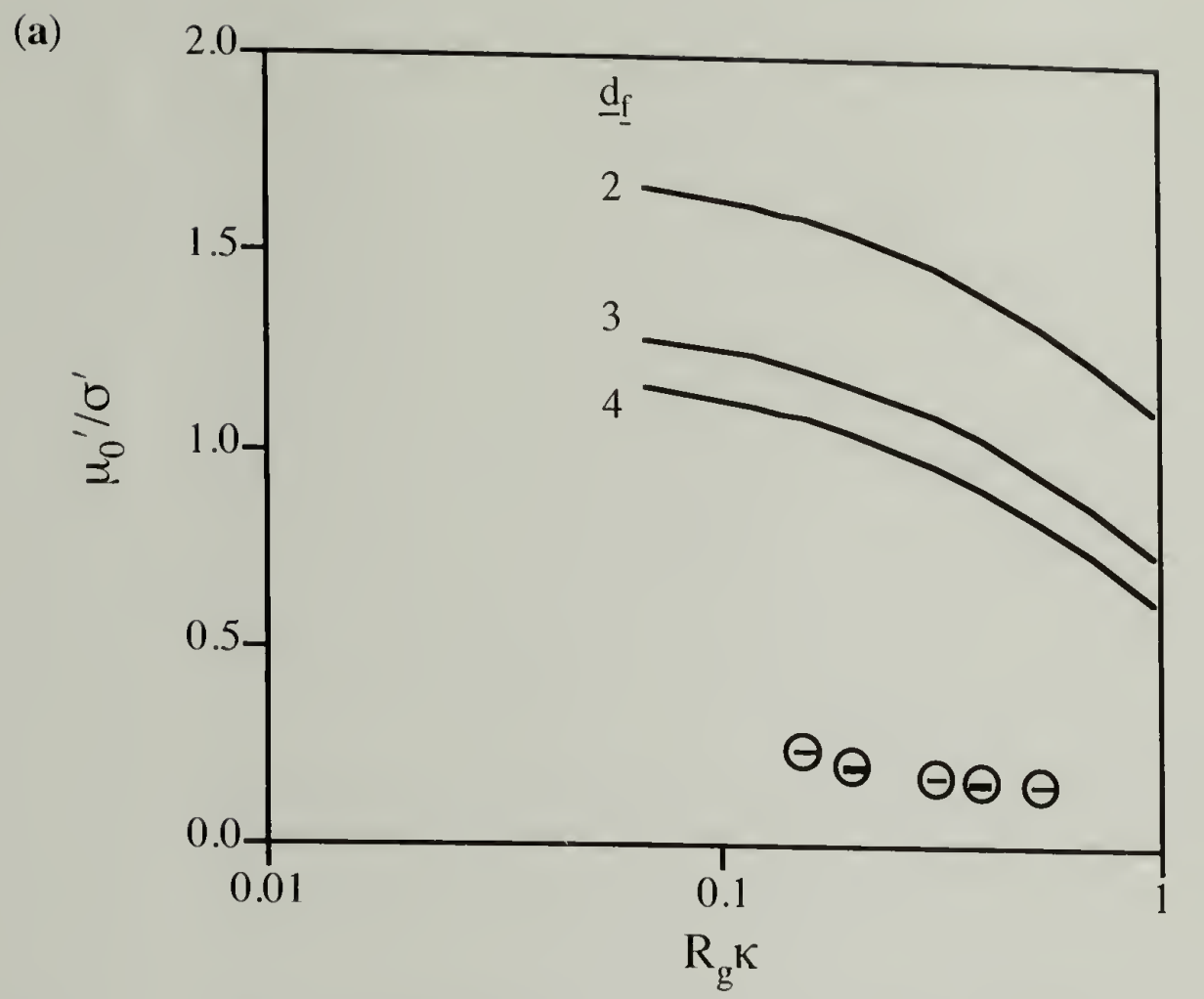

Figure 4.14. Dimensionless plot $\mu_0'/\sigma'(R_g\kappa)$ to compare fully charged ($\alpha = 1$) (a) PPI G3 and (b) PPI G5 data (in formic acid/NaOH buffers) to the Muthukumar predictions for a polyelectrolyte with fractal dimensionality d_f. For G3, $\sigma' = 22.9$ ($R_g = 0.93$ nm, $Q = 30e$); for G5, $\sigma' = 64.5$ ($R_g = 1.39$ nm, $Q = 126e$).

CHAPTER 5

OVERVIEW AND EXTENSIONS

The overall goals of this dissertation were to improve the ability to investigate synthetic polyelectrolytes by electrophoretic techniques and to use these techniques to better our understanding of polyelectrolyte behavior in dilute solution. Comprehensive experimental results have been generated and compared to existing theories, with the aim of identifying which theory correctly captures the physics behind the observed behavior. Most of the experiments reported here were possible only after the technological challenges of polycation electrophoresis were overcome. This new ability to study polycations with capillary electrophoresis has opened the door to many more experimental investigations that can be used to test the validity of current electrophoresis theories.

5.1 Overview

The results presented in Chapter 2 reveal the complexity of the relationship between free solution electrophoretic mobility μ_0 and molecular weight M for charged oligomers. A maximum in μ_0 with respect to M was clearly demonstrated for poly(deoxythymidine) oligomers. The magnitude of this maximum decays with increasing solution ionic strength. A better theoretical understanding of the relationship between μ_0 and M is needed before electrophoresis can be used to separate polyelectrolyte oligomers.

For high molecular weight polyelectrolytes, electrophoretic separation by M cannot be achieved in free solution; rather, some type of matrix material (i.e., neutral polymer solution or gel) must be used to impart a M dependence in the electrophoretic

mobility μ. While these techniques are easily applied for the analysis of polyanions, difficulties are encountered for polycations because of their electrostatic interactions with the electrophoresis medium. Chapter 3 demonstrated how these difficulties can be overcome by using a cationic surfactant solution to create a dynamic capillary coating. The separation of protonated and quaternized poly(2-vinylpyridine)s in dilute neutral polymer solution was easily achieved with high resolution. Further, the high resolution revealed features in the molecular weight distributions of the quaternized polymers that were much less noticeable in GPC results. Taken together, results from the two techniques suggest how poly(2-vinylpyridine)s degrade/crosslink when exposed to quaternizing conditions for an excessive period. The model experiments described in Chapter 3 can be extended for the improved characterization of commercial polycations. Appendix A presents the challenges associated with this extension and provides some possible routes in adapting both capillary and gel electrophoresis techniques for the analysis of high molecular weight polycations with variable charge density.

The ability to use capillary electrophoresis for polycation investigations was further exploited in Chapter 4 with a free solution electrophoresis study of cationic dendrimers. This work centered on the fundamental relationship between a charged solute and its counterions in dilute solution. The electrophoretic mobilty of the dendrimer as a function of charge density, size, and ionic strength was compared to theoretical predictions, and a greater understanding of the counterions' effect on μ_0 resulted. In particular, the relaxation effect clearly played a dominating role in the behavior of charged dendrimers. The similarity of the dendrimers' behavior to that previously seen for linear polyelectrolytes [1-3] suggests that similar mechanisms may be operative in linear polyelectrolyte electrophoresis.

5.2 Extensions

The dendrimer work shows how experiment can be used to test theories, and how a greater understanding can thus be achieved. Further studies of this type could yield a greater understanding of linear polyelectrolyte electrophoresis. The new ability to investigate polycations with capillary electrophoresis will allow for such studies.

Polycations such as ionenes are ideal for testing various theories on polyelectrolyte electrophoresis. Previously, Klein and Ware [4] conducted electrophoretic light scattering experiments on ionenes in mixed solvents; in doing so, they were able to vary the dimensionless charge density parameter ξ through solvent dielectric constant rather than polyion charge density. Their results showed a transition in μ near $\xi = 1$, the point at which Manning's counterion condensation model [5,6] predicts that μ will become independent of ξ. However, the nature of the transition seen experimentally was quite different than that predicted by Manning. Further, the electrophoretic light scattering technique limited the precision of their mobility measurements, giving large error bars for μ.

Capillary electrophoresis experiments on the same system should give more precise results, and experiments with different ionenes will also allow for complementary investigations of μ as a function of polyion charge density. My preliminary experiments with 6,6-ionene indicate that model ionene polymers can be easily synthesized and that the cationic surfactant capillary coating sufficiently prevents adsorption problems so that accurate mobilities may be measured. Once a comprehensive data set is generated, the results can be compared to various polyelectrolyte electrophoresis theories to determine whether the counterion condensation model is correct or whether nonlinear electrostatic effects (i.e., the relaxation effect) are dominating the mobility behavior.

5.3 Summary

The work described in this dissertation reveals the potential of electrophoretic techniques for the characterization and the better understanding of polyelectrolyte solutions. Comparison of my comprehensive results to those predicted by various theories has provided a better understanding of polyelectrolyte solution behavior and demonstrated where existing theories may be improved. The new method developed for polycation electrophoresis studies was an important step in achieving these goals and can be used for many future investigations into polyelectrolyte solution behavior.

5.4 References

1. Hoagland, D. A.; Smisek, D. L.; Chen, D. Y. *Electrophoresis* **1996**, *17*, 1151.

2. Whitlock, L. R. *Isotachophoresis of Synthetic Ion-Containing Polymers*; Jorgenson, J. W. and Phillips, M., Ed.; American Chemical Society: Washington, DC, 1987, pp 222-245.

3. Gao, J. Y.; Dubin, P. L.; Sato, T.; Morishima, Y. *J. Chrom. A* **1997**, *766*, 233.

4. Klein, J. W.; Ware, B. R. *J. Chem. Phys.* **1984**, *80*, 1334.

5. Manning, G. S. *Q. Rev. Biophys.* **1978**, *11*, 179.

6. Manning, G. S. *J. Phys. Chem.* **1981**, *85*, 1506.

APPENDIX

ELECTROPHORETIC SEPARATION OF COMMERCIAL POLYCATIONS

A.1 Introduction

Chapter 3 reported a new capillary electrophoresis (CE) method that provides a high resolution separation of polycations according to molecular weight. Using dilute neutral polymer solutions in coated capillaries, we demonstrated the power of this technique with model polycations. Here, we will focus on our efforts to characterize the molecular weights of commercial polycations (all provided by Nalco Chemical Company). To properly analyze these polycations, many challenges must be overcome. Issues associated with electrostatic adsorption, ultra-high molecular weights, varying degress of charge, and detection must all be addressed. This Appendix describes our various attempts to overcome all of these potential problems, with the overall objective being a routine, rapid, and inexpensive method to separate these polymers by molecular weight. We begin with the capillary electrophoresis technique described in Chapter 3 but also explore the development of a gel electrophoresis method for cationic polymers.

A.2 Capillary Electrophoresis in Neutral Polymer Solutions

A.2.1 Unlabeled Polycations

The fractionation method described in Chapter 3 was attempted for two types of commercial polycations which do not possess any functionality easily detectable by our UV detector. These polymers are poly(dimethylaminoethyl acrylate, methyl chloride quat.) (Poly(DMAEA.MCQ)) and poly(acrylamide-co-dimethylaminoethyl acrylate, methyl chloride quat.) (Poly(Am/DMAEA.MCQ)); their chemical structures are given in

Figure A.1. All CE experiments described in this section were performed in the same manner as described in Chapter 3 (see section 3.3.4); to prevent polycation adsorption to the capillary wall, 0.5 mM CTAB was added to all running buffer (Tris-HCl, pH 7, I=0.01 M) and sample vials.

For the homopolymer poly(DMAEA.MCQ), the main issue to address is detection with the UV detector on our instrument. Three strategies were tested: direct detection of the acrylate functionality, indirect detection, and concurrent dying of the polyelectrolyte. For these experiments, two Nalco poly(DMAEA.MCQ) samples were used: 3918-174-5 ($[\eta]$=1.8 dl/g) and 3918-174-7 ($[\eta]$=0.4 dl/g). Both were supplied as 15% aqueous solutions.

Previous work in our laboratory [1], as well as recent literature [2], indicates that the direct UV detection of the acrylate functionality may be a possibility in CE. For this experimentally straightforward method, relatively large polymer concentrations are required (>1mg/ml), which could cause peak distortions. In free solution electrophoresis, we were able to detect the polycations at wavelengths between 205 - 230 nm for polycation concentrations of 1 mg/ml. Figure A.2 shows a typical result. Though the polymer peak is evident, signal-to-noise is poor. Molecular weight fractionation trials using pullulan as a matrix were also attempted. Figure A.3 compares results obtained for the two polycations (3918-174-5 and 3918-174-7). As expected, 3918-174-5 ($[\eta]$ = 1.8 dl/g) has a lower μ in the pullulan solution than 3918-174-7 ($[\eta]$ = 0.4 dl/g). Though we seem to be successful in separating these two samples by molecular weight, the noisy baseline precludes any meaningful interpretation on the molecular weight distributions.

With the indirect UV detection method, a small cationic chromophore (methylene violet) was added to the running buffer vials but not to the polycation sample vial. As the polycation migrates down the capillary, electrostatic repulsion depletes the small molecule chromophore from the sample band, giving a negative UV absorption as the sample passes the detector. Figure A.4 gives an example of the free solution

electrophoresis of Nalco sample 3918-174-5 at a concentration of 1 mg/ml. Though the polymer sample does create a negative UV absorbance, the dip is small and somewhat distorted. Molecular weight fractionation trials were not attempted, as the probability of measuring molecular weight distributions seems low with this detection method.

The third detection strategy tested was the concurrent dying of the polycation. In this method, a strongly anionic dye (8-hydroxy-1,3,6-pyrenetrisulfonic acid) is added to the polycation sample solution so that it will electrostatically bind to the polycation. This dye absorbs strongly in the UV, so only a small amount is needed. In the free solution experiment (Figure A.5a), we get good signal-to-noise. However, in pullulan solution (Figure A.5b), signal-to-noise is not much better than with the direct detection method. In this system, the anionic dye may also be associating with the cationic surfactant and the pullulan to give a noisy baseline. Therefore, measurement of molecular weight distributions may be problematic.

The second type of unlabelled polymer, poly(Am/DMAEA.MCQ), is a higher molecular weight copolymer with a low degree of charge (nominally 10%). Slight variability in charge density may lead to peak broadening. Furthermore, the smaller number of charge sites will make detection by the indirect UV method and the concurrent dying method more difficult. The direct UV detection method should not be hindered, however, as the amide functionality in the neutral portion of the copolymer should be detectable to the same degree as the acrylate funtionality in the charged portion. Only one copolymer sample was used for these experiments: 3918-174-1 (η_{red} = 17 dl/g); it was supplied as a dry powder and gave somewhat cloudy aqueous solutions at a nominal concentration of 1 mg/ml. Two detection methods were attempted: direct UV detection of the amide/acrylate group and concurrent dying of the copolymer.

The direct UV detection method was not been successful for the Nalco copolymers. As with the cationic homopolymer, a noisy baseline contributed to the difficulties. In this case, however, we were unable to discern a polymer peak above the

noise. The higher molecular weight of these polymers may be prohibiting us from obtaining homogeneous solutions at the required concentration (1 mg/ml).

The detection method involving concurrent dying of the cationic sites did not give good results for the copolymer, either. As with the cationic homopolymer, here we added the anionic dye 8-hydroxy-1,3,6-pyrenetrisulfonic acid to the copolymer sample solution. However, this method did not yield a peak above the noisy baseline for the copolymer. Unfortunately, this copolymer has a much lower number of possible binding sites than the homopolymer. And, as mentioned previously, the high molecular weight may prevent complete dissolution.

A.2.2 Rhodamine-Labeled Polycations

To bypass the detection problems described above, Nalco supplied us with some rhodamine-labeled copolymers (properties given in Table A.1). Using these, we aimed to further develop the CE technique to separate high molecular weight cationic copolymers. For these experiments, the dry, labeled copolymers were added to Tris-HCl buffer (pH 7, I=0.01 M) at a concentration of 1 mg/ml and stirred overnight. CE experiments were conducted as described above, with 0.5 mM CTAB added to all running buffer and sample vials to prevent polycation adsorption to the capillaries. UV-Vis spectra of these labeled copolymers showed a maximum absorption at 562 nm. As we could not find a water-soluble neutral molecule that absorbed at this wavelength, the electroosmotic flow could not be directly measured. Instead, we used a cationic dye (methylene violet) with a known μ value (1.7×10^{-4} cm^2/Vs) to calculate the electroosmotic flow and the electrophoretic mobilities of the cationic copolymers.

The μ distributions of both labeled copolymers in free solution are given in Figure A.6. The first two peaks are attributed to the copolymers, while the peak with the highest μ is that of the methylene violet marker. The marker has a higher mobility than the copolymers because these copolymers only have 10% cationic monomer incorporation.

The first copolymer peak in both cases is fairly broad, likely indicating a distribution in charge density.

Results for the molecular weight fractionation trials of the two copolymers are given in Figure A.7. The neutral polymer was 1.66 x 10^6 g/mol pullulan, at a concentration of 2.8 mg/ml or half of its critical overlap concentration. In comparison to the free solution environment, this pullulan solution shifts the first copolymer peak to lower μ values for each copolymer sample. The second copolymer peak, however, maintains a mobility approximately equal to that in free solution. This second peak may be due to aggregates or an insoluble fraction that cannot entangle with the pullulan chains, while the first peak probably represents single copolymer chains in solution. Comparing the first peaks for the two copolymer samples, little difference is noted, despite their different RSV values. Dynamic light scattering on these two copolymers revealed overlapping distributions of the hydrodynamic radius, though the 4378-132SQ sample (higher RSV) did have a higher maximum hydrodynamic radius. In these CE experiments, the fractionation capability is limited by the combination of the high electroosmotic flow in the CTAB-coated capillary and the low mobilities of the 10% copolymers in free solution. Better separations should be possible with a lower electroosmotic flow, which may be obtainable with a mixed surfactant coating system.

A.3 Agarose Gel Electrophoresis

Given the detection difficulties in CE for P(Am/DMAEA.MCQ), we chose to put some initial efforts into the analytical possibilities of gel electrophoresis for these same materials. Because the mass of solute in the detected volume is much larger, the detection threshold for a gel electrophoresis experiment is much lower than for an analogous CE experiment. However, the agarose gels commonly used for electrophoretic analysis of large molecules contain residual negative charges that hinder analysis of

cationic polymers. Overcoming polycation adsorption could be more difficult than in the CE experiments, given the larger internal surface area of a gel compared to a capillary filled with dilute neutral polymer solutions.

Initial gel electrophoresis experiments were conducted with the rhodamine-labeled cationic copolymers, as the labels make detection of the polymers easy. The dry polymer samples were dissolved in Tris-HCl buffer (pH 7, I=0.01 M) overnight at 10 mg/ml. For some experiments, these stock solutions were diluted with more Tris-HCl buffer.

We have tried two approaches for the gel electrophoresis of these cationic copolymers. In the first approach, we treated the gels with a sacrificial cationic molecule, which adsorbs to the negative sites and renders a slight positive charge to the gel. Cationic molecules we have used include polyethyleneimine (PEI) and the surfactants cetyltrimethylammonium bromide (CTAB) and cetyltrimethylammonium chloride (CTAC). In the second approach, untreated agarose gels were employed, with the expectation that the lightly charged copolymer might not adsorb to the lightly charged agarose gel.

A.3.1 Cationic Composite Gels

In our most successful effort, agarose (0.4 wt. % Bio-Rad Ultrapure DNA grade) is mixed with a 1 wt.% PEI (30-50,000 g/mol)/Tris-HCl buffer solution (pH 7, I=0.01 M); the solution is heated to dissolve/associate the two polymers. On cooling, the agarose gels in the usual fashion but the PEI complexes through the anionic agarose units (presumably sulfates) to create a composite gel of somewhat higher strength than the comparable gel of pure agarose. We have ascertained by measurement of electroosmotic flow that the composite gel is indeed positively charged: the electroosmotic flow is both large and directed toward the anode.

When sample 4378-132SQ (solution less than 1 week old) is loaded in the well and an electric field applied across the gel (20V/15cm), surprisingly, the polymer

migrates toward the anode. We interpret this behavior as revealing that the electroosmotic flow of the gel dominates over the electrophoretic migration of polyelectrolyte. This situation is unusual for gel electrophoresis, but we see no reason that such migration can't be exploited to create molecular weight separation. The cause for the unusual behavior is clear: the quaternization of the polymer is only 10%, a value associated with low μ. We expect that the fully charged homopolymer Poly(DMAEA.MCQ) might migrate in the opposite direction. Detection for this experiment is via the fluorescent label attached on the specially prepared 10% quaternized polymer. When the gels are laid on a standard short wave UV transilluminator, the polymer bands are easily visualized and photographed. The concentration of the sample in the wells has been varied between 1-10 mg/ml in a Tris-HCl buffer (pH 7, I=0.01 M).

Figure A.8a displays a digital photograph of a gel section approximately 5 cm in length in the field direction. Five samples of 4378-132SQ (solution less than 1 week old) were placed in the five discernable wells and then run downfield to various extents based on molecular weight. To generate the different samples, we used a sonicator to degrade the original solution into four additional fractions of lower molecular weight; the sonication times varied from 20 seconds to 5 minutes. The more highly sonicated samples at 1 mg/ml are much less viscous than the original solution. Although the reproduction in Figure A.8a is poor, the greater migration of the more highly sonicated samples is clearly observed, a trend in accord with the expectation that these molecular weights are lowest. In fact, a second band emerges in the downfield region of the highly sonicated samples.

Figure A.8b shows intensity traces for the same gel, with fluorescence intensity plotted vs. downfield position for each sample. The figure reveals more extensive penetration and eventual second peak of the sonicated samples. Without knowledge of molecular weight and its distribution, one cannot easily interpret the intensity traces.

Nevertheless, the poor entry of the original sample (i.e., no sonication) into the gel and the larger fraction of lower molecular weight material in the sonicated samples cannot be missed. To validate the results in a more quantitative fashion, each of the samples was also studied by dynamic light scattering. The dynamic light scattering data was interpreted via CONTIN as a hydrodynamic size distribution. The different size distributions are displayed in Figure A.9. The peak in the distribution for the unsonicated samples is at 75 nm, and the peaks for the sonicated samples shift toward lower size, with an enhanced lower size tail also developed. (The buffer was of high enough ionic strength that the dynamic light scattering experiment was not perturbed by the anomalous secondary relaxations often seen with polyelectrolyte solutions.) The dynamic light scattering data shows that all size distributions are quite broad, leading us to expect broad smears in the electrophoresis scans. In fact, these smears are exactly what we note in Figure A.8.

The results obtained for these gel electrophoresis experiments appear successful, but improvements are needed. The entry of the unsonicated material into the gel appears slow and incomplete, precluding a good analysis. The complexation of agarose with PEI may reduce the pore size of the agarose gel, preventing entry of higher molecular weight polyelectrolyte. Normal agarose gels can accommodate entire chromosomes, a fact implying that entry of molecules of the size of the polycations should not be overly difficult. In an attempt to avoid this pore reduction, we substituted a cationic surfactant (CTAB or CTAC) for the PEI, but similar results were obtained.

A.3.2 Untreated Gels

Since the copolymer only contains 10% positive charge, it may not adsorb too strongly to untreated agarose, especially if the agarose is also only lightly charged. Different commercially available agarose grades claim to have lower levels of electroosmotic flow, and these may contain fewer negative sites. Therefore, we conducted a series of gel electrophoresis experiments using both labeled copolymers

(4378-131SQ and 4378-132SQ) and untreated agarose (either Bio-Rad Ultrapure DNA grade or SeaKem Gold ultralow electroosmotic flow grade). When two-week old copolymer sample solutions are run in 0.2% agarose gel, broad smears migrate toward the cathode and separate completely from the wells. However, a significant portion of each sample remains in the wells. To determine if this portion is due to aggregates or other insoluble material, we compare the gel electrophoresis of the supernatant of centrifuged samples to that of the original, uncentrifuged samples. Figure A.10 shows that the centrifuged samples leave no material in the wells, unlike the original, uncentrifuged samples. In this experiment, then, we achieve a successful molecular weight separation of the 10% labeled copolymers and demonstrate the presence of some insoluble material that cannot enter the gel.

Unfortunately, further investigations revealed that the copolymers analyzed above had actually hydrolyzed to some extent such that they were less positively charged than the original 10% copolymers. As the samples continued to age, they even began to behave as polyanions. When new samples were prepared, our experiments showed that the unhydrolyzed 10% copolymer does adsorb to the untreated agarose gels used above.

We believe a valid strategy is to deliberately hydrolyze the Nalco cationic copolymers in a controlled fashion to transform them to polyanions with similar, known charge densities. Standard base hydrolysis reactions can be used to convert both monomer types in the copolymer to acrylic acid units; a preference toward reaction at the cationic sites may be expected. In a first attempt, the rhodamine-labeled copolymers were hydrolyzed in a 0.23 M sodium hydroxide/0.09 M sodium chloride solution at 50°C for 1 hour. Under these conditions, we expect the products to contain approximately 20-30% acrylic acid units [3]. Gel electrophoresis in 0.2% untreated agarose (BioRad Ultrapure DNA grade) indicates these deliberately hydrolyzed samples are negatively charged: the samples broke the gel while migrating toward the anode. Unfortunately, the

hydrolysis reaction also removed all of the rhodamine label such that the separation of the copolymers in the gel could not be so easily detected.

Based on our gel electrophoresis studies with the rhodamine-labeled poly(Am/DMAEA.MCQ) samples, we believe the best strategy for analyzing cationic, acrylamide-type copolymers is to convert them to polyanions by hydrolysis prior to analysis. The acrylic acid units of the hydrolyzed polymers can be readily labeled to a low substitution level with fluorescein, enabling detection at low polymer concentrations (0.1 mg/ml or less). As demonstrated by previous work on poly(Am/AA)s, gel electrophoresis provides a good molecular weight-based separation for this class of polymers, provided the relative charge densities of all polymers are high [4]. Fortunately, exhaustive hydrolysis will produce polymers of comparable, high charge density.

Hydrolysis, of course, reverses polyion charge and thereby eliminates adsorption to the gel. Modification of a sample prior to analysis, as advised here for polycations, always raises concerns about how the modification might itself be influenced by sample characteristics, in this case, the composition and molecular weight of the starting polycation. Any influence would invalidate the analytical procedure, as observed differences might not be inherent to the actual sample. Fortunately, the proposed electrophoretic approach has much robustness; even if the reversal of charge is not uniform between samples, no impact on mobility is expected. Previous work has shown that above acrylic acid composition near 30%, the mobility is insensitive to this composition [4]. The development of charge density by hydrolysis to the range of 50-60% is straightforward. Thus, the proposed modification procedure does not need to be quantitative in order to ensure reliable molecular weight data for the modified polymers. Furthermore, hydrolysis reactions are not accompanied by molecular weight degradation.

A.4 Summary

We have investigated both CE in neutral polymer solutions and gel electrophoresis for the fractionation of polycations. For the CE experiments, polycation adsorption to the silica capillaries was easily prevented with a dynamic, cationic surfactant coating. High resolution separations of model polycations in dilute pullulan solutions were easily accomplished; however, improvements in detection optics are needed to obtain meaningful molecular weight distributions for the Nalco polycations. Detection is much easier in gel electrophoresis due to the larger mass of solute and increased pathlength. Furthermore, unlabeled polymers may be stained with an anionic dye after electrophoretic separation. Polycation adsorption to the agarose gel is not easily overcome, though a pre-analysis conversion of the polycation to a polyanion may bypass this difficulty. Although conditions for the proposed analytical procedure are suggested by the current results, several steps will require further study before the procedure can be reliably implemented. Specifically, appropriate conditions for hydrolysis and electrophoresis are not known. Although the full approach has not been integrated and optimized, each isolated step has been demonstrated as feasible.

A.5 References

1. Hoagland, D. A.; Smisek, D. L.; Chen, D. Y. *Electrophoresis* **1996**, *17*, 1151.
2. Gao, J. Y.; Dubin, P. L.; Sato, T.; Morishima, Y. *J. Chromatogr. A* **1997**, *766*, 233.
3. Truong, N. D.; Galin, J. C.; François, J.; Pham, Q. T. *Polymer* **1986**, *27*, 459.
4. Smisek, D. L.; Hoagland, D. A. Unpublished results.

Sample	Am:DMAEA.MCQ	% Rhodamine B	η_{red} (dl/g)
4378-131SQ	90:10	0.1	14
4378-132SQ	90:10	0.06	21

Table A.1. Properties of rhodamine-labeled poly(Am/DMAEA.MCQ)s.

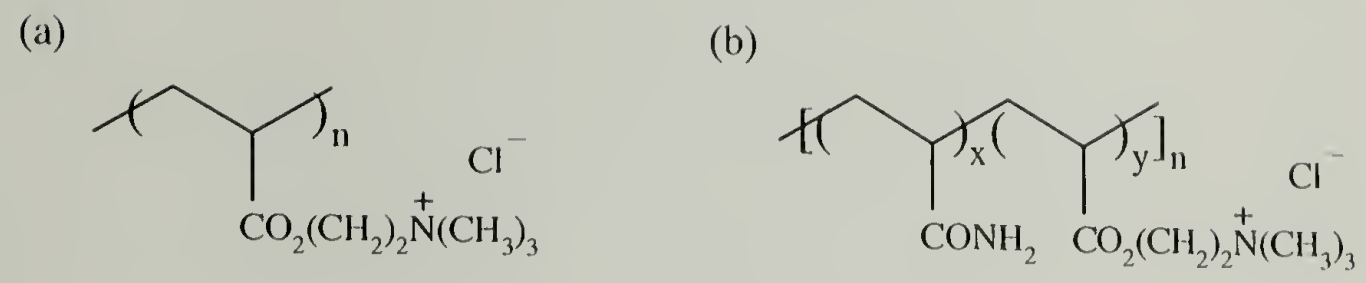

Figure A.1. Chemical structures of commercial polycations (a) poly(DMAEA.MCQ) and (b) poly(Am/DMAEA.MCQ).

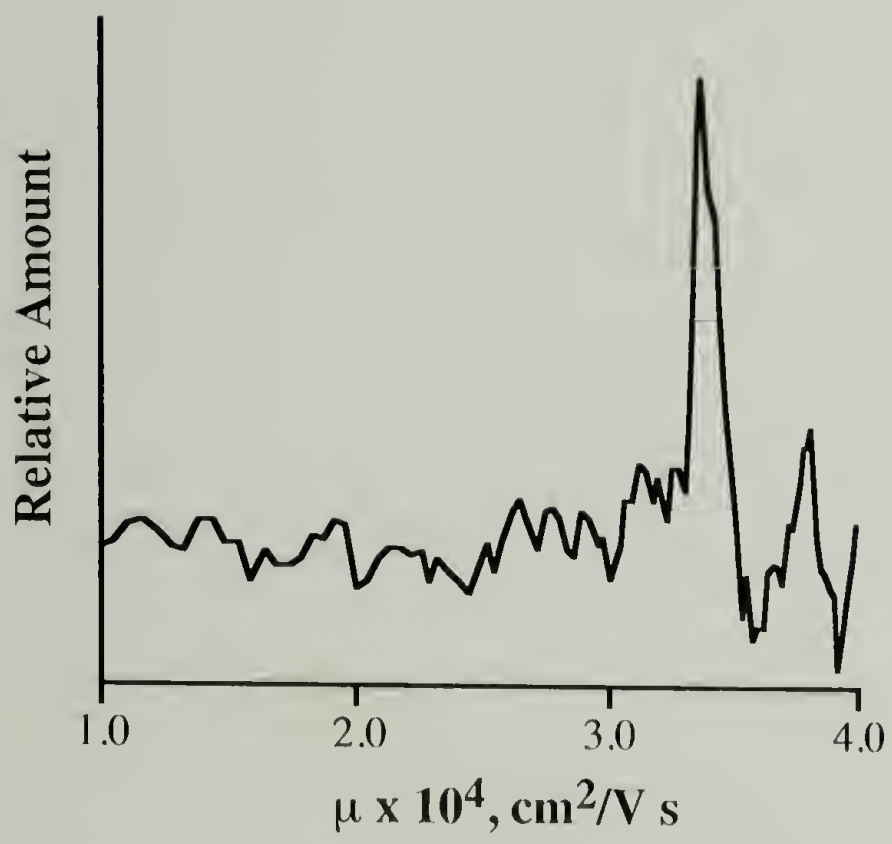

Figure A.2. Electrophoretic mobility μ for poly(DMAEA.MCQ) (sample 3918-174-5) in free solution, using direct detection at 205 nm.

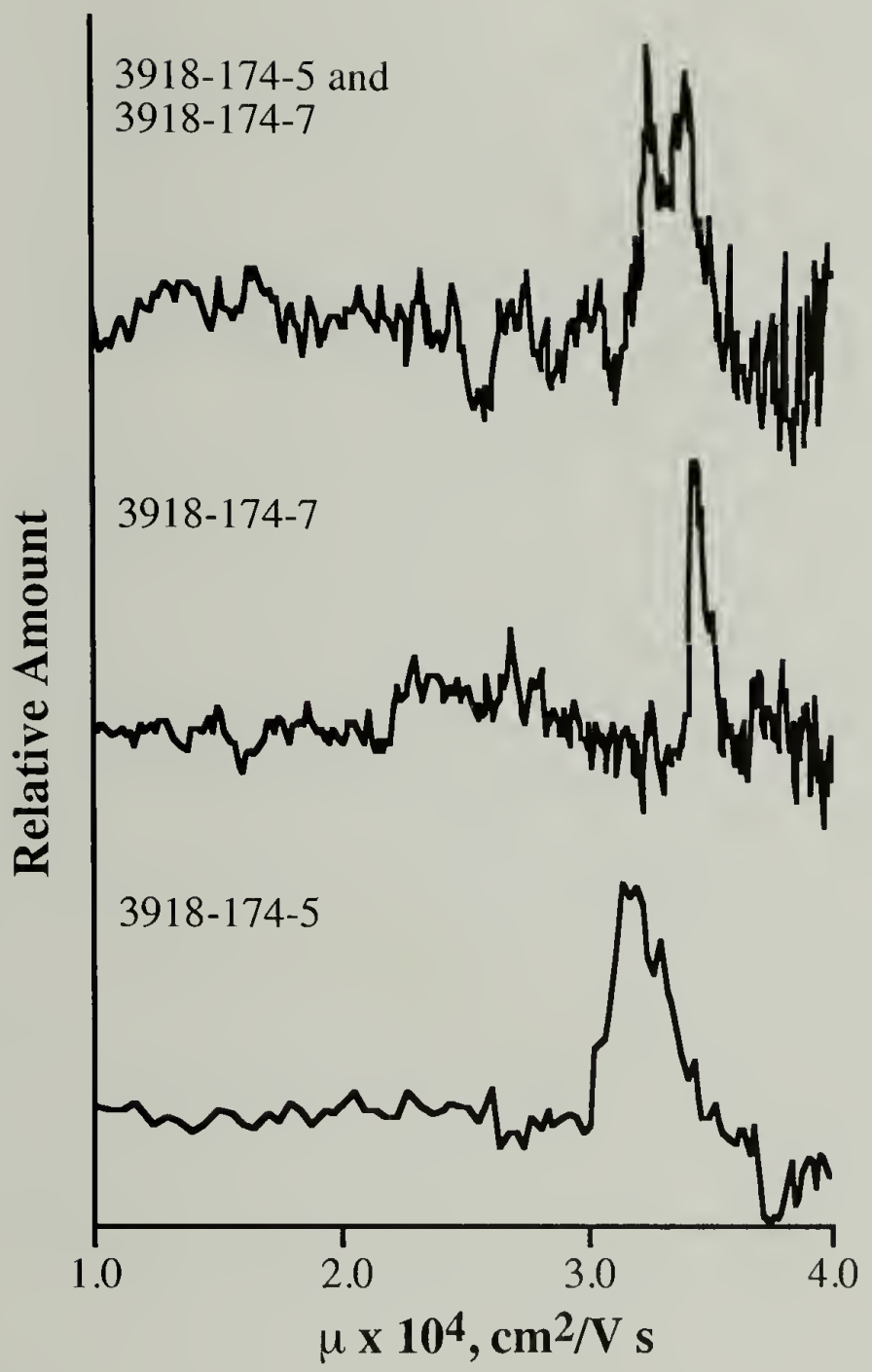

Figure A.3. Electrophoretic mobility μ for two samples of poly(DMAEA.MCQ) in 2.0 mg/ml 5-10 x 10^4 g/mol pullulan, using direct detection at 205 nm.

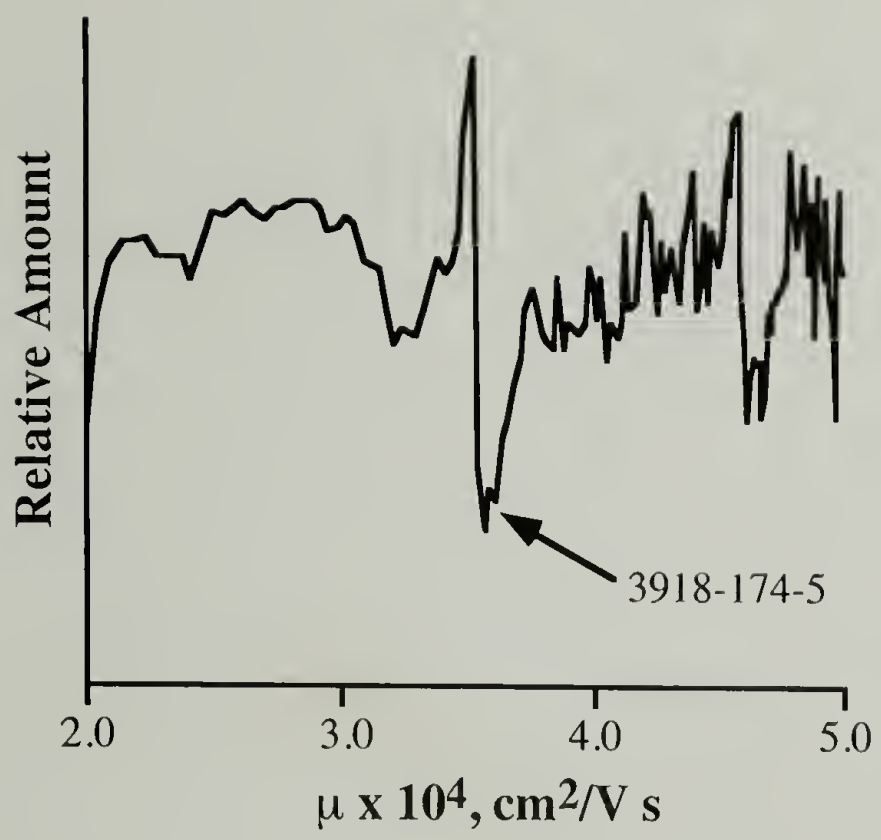

Figure A.4. Electrophoretic mobility μ for poly(DMAEA.MCQ) (sample 3918-174-5) in free solution, using indirect detection.

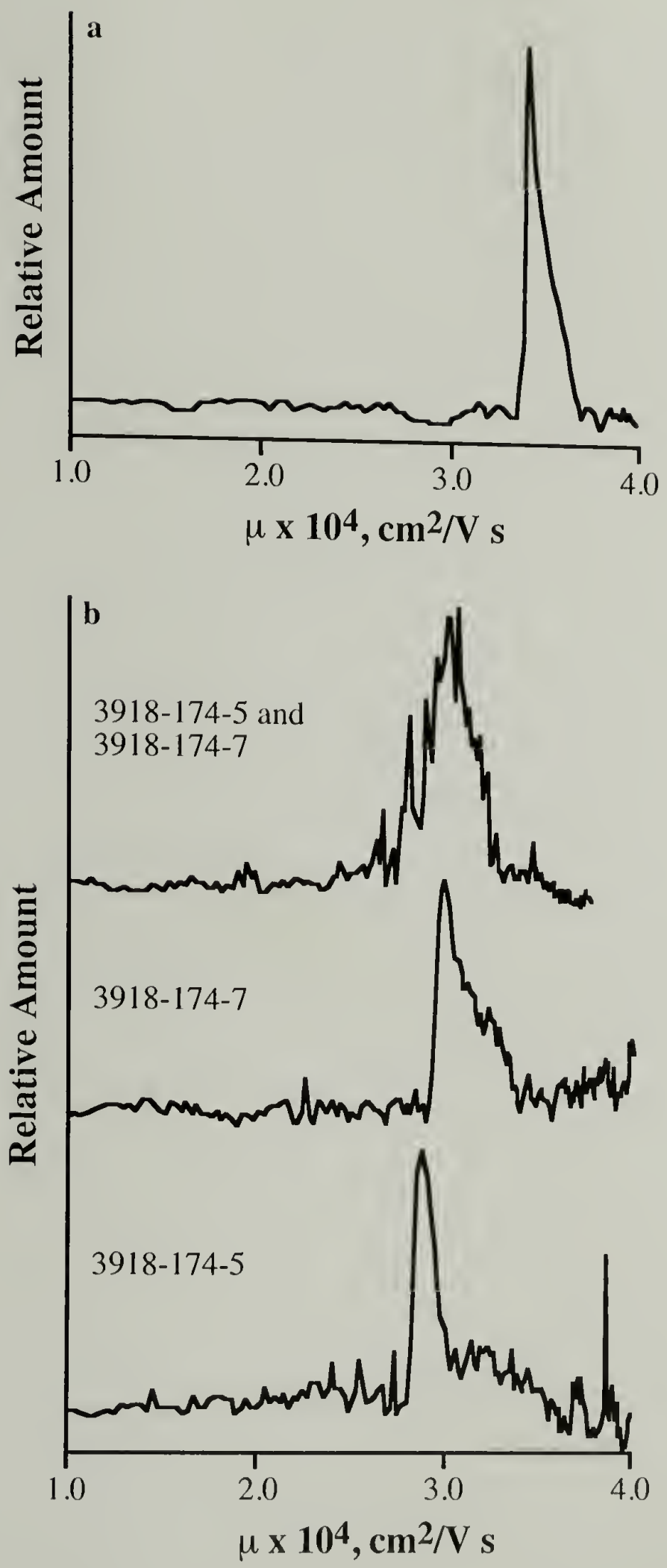

Figure A.5. Electrophoretic mobility μ for two samples of poly(DMAEA.MCQ) in (a) free solution and (b) 10 mg/ml 5-10 x 10^4 g/mol pullulan. An added anionic dye (8-hydroxy-1,3,6-pyrenetrisulfonic acid) binds to the polycations for detection at 247 nm.

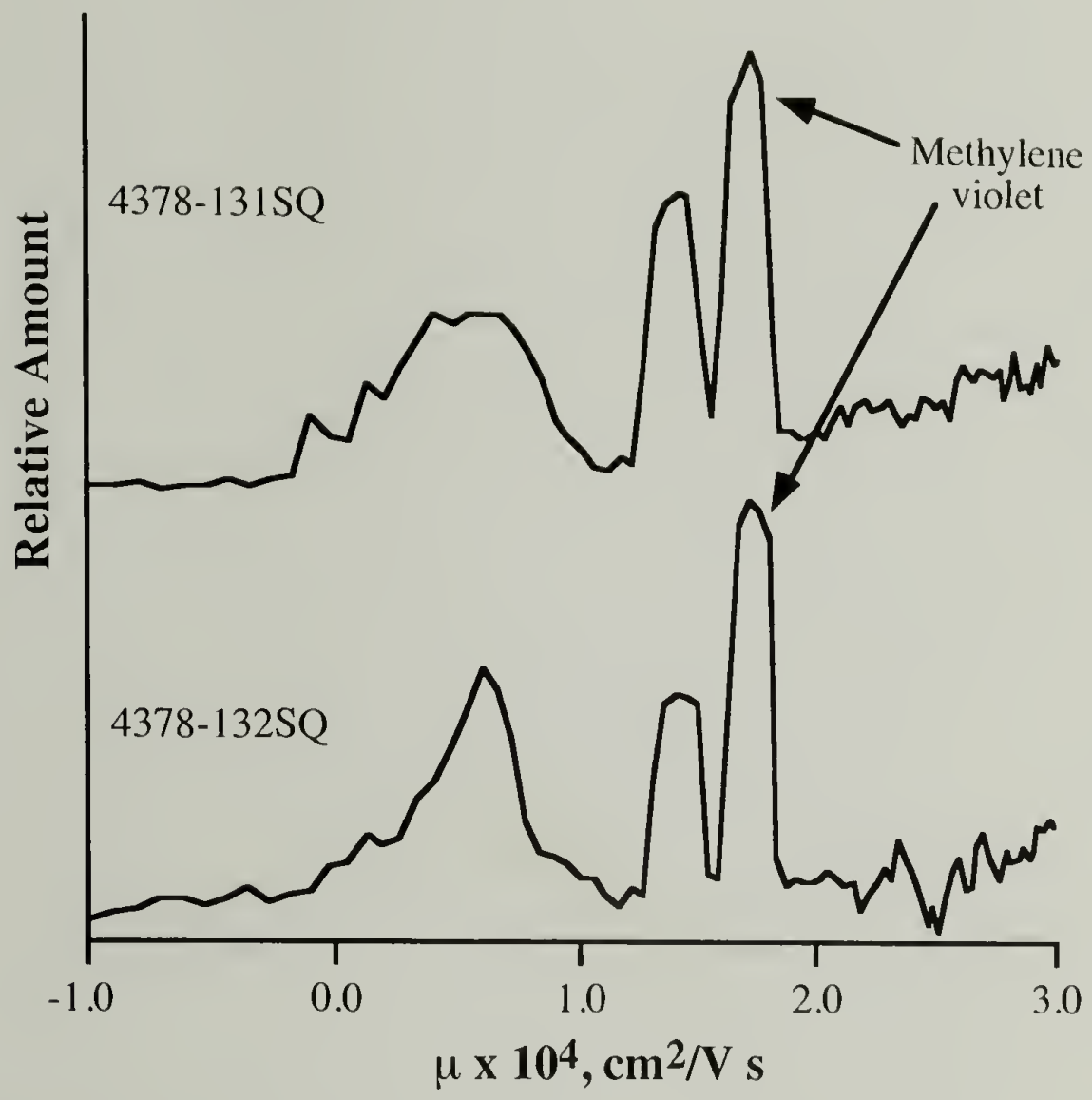

Figure A.6. Electrophoretic mobility μ for rhodamine-labeled poly(Am/DMAEA.MCQ)s in free solution.

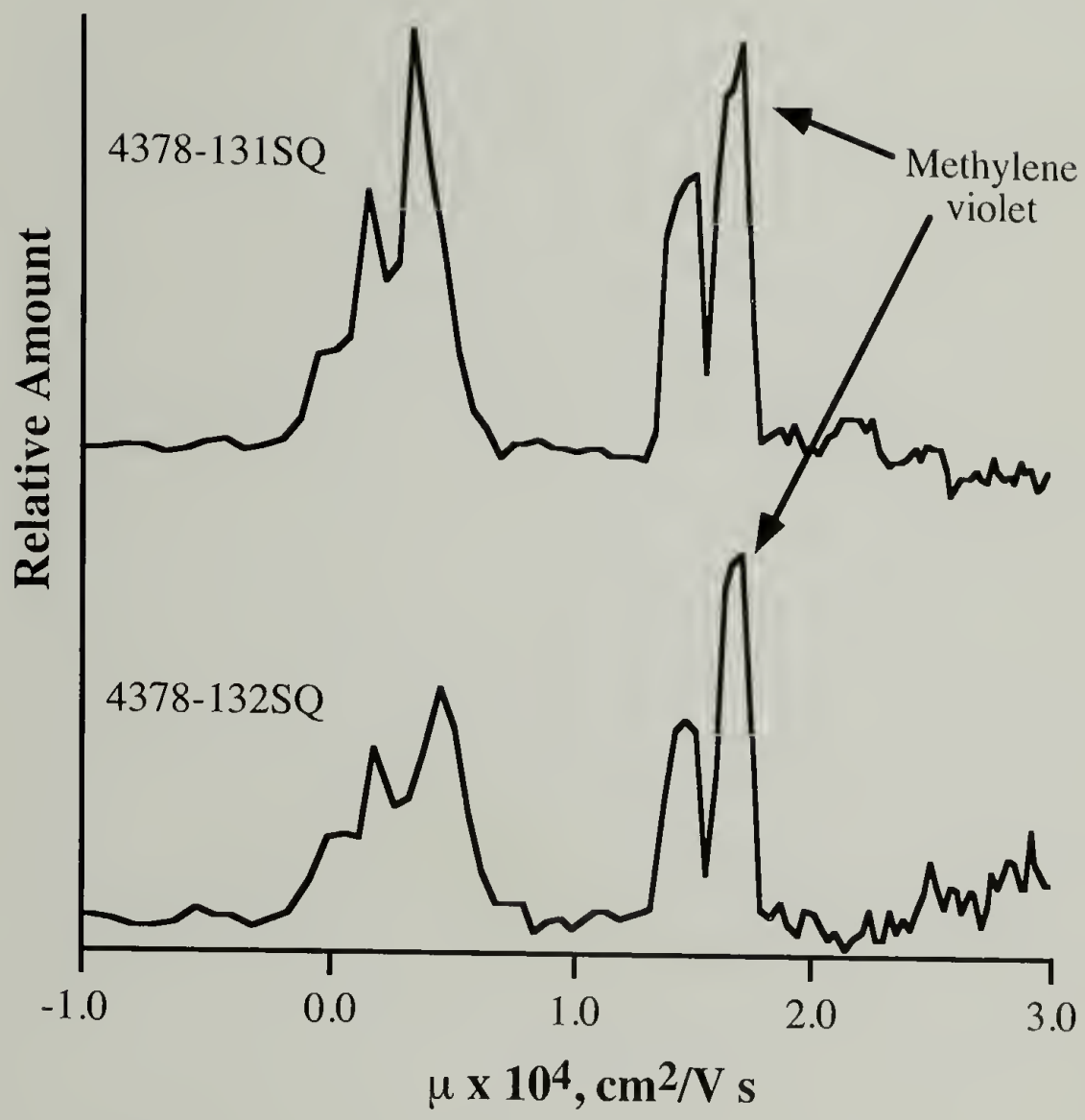

Figure A.7. Electrophoretic mobility μ for rhodamine-labeled poly(Am/DMAEA.MCQ)s in c*/2 1.66 x 10^6 g/mol pullulan.

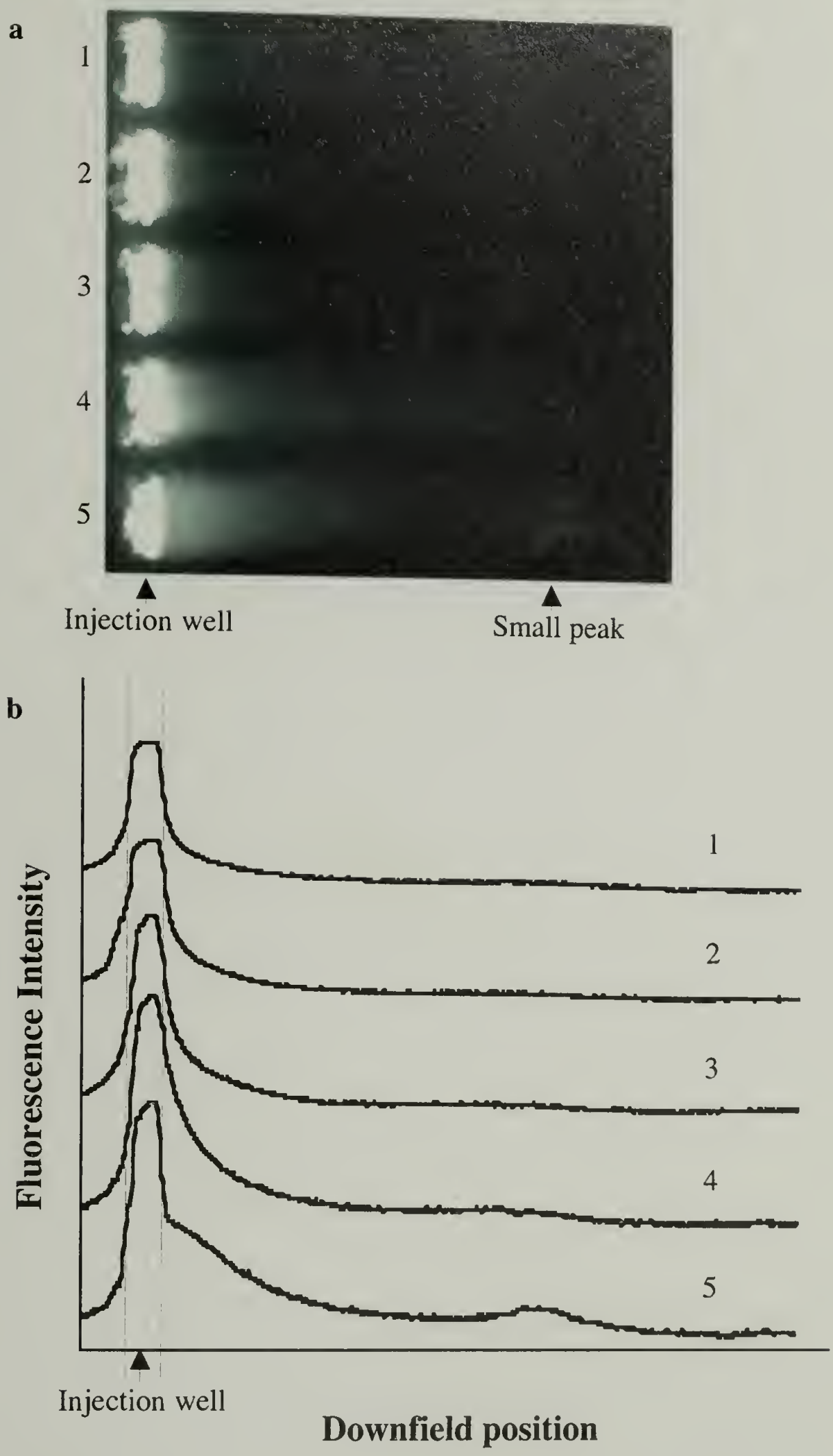

Figure A.8. Gel electrophoresis of rhodamine-labeled poly(Am/DMAEA.MCQ)s (4378-132SQ). **1**=unsonicated, **2**=sonicated 20 s, **3**=sonicated 1 min, **4**=sonicated 2 min, **5**=sonicated 5 min.

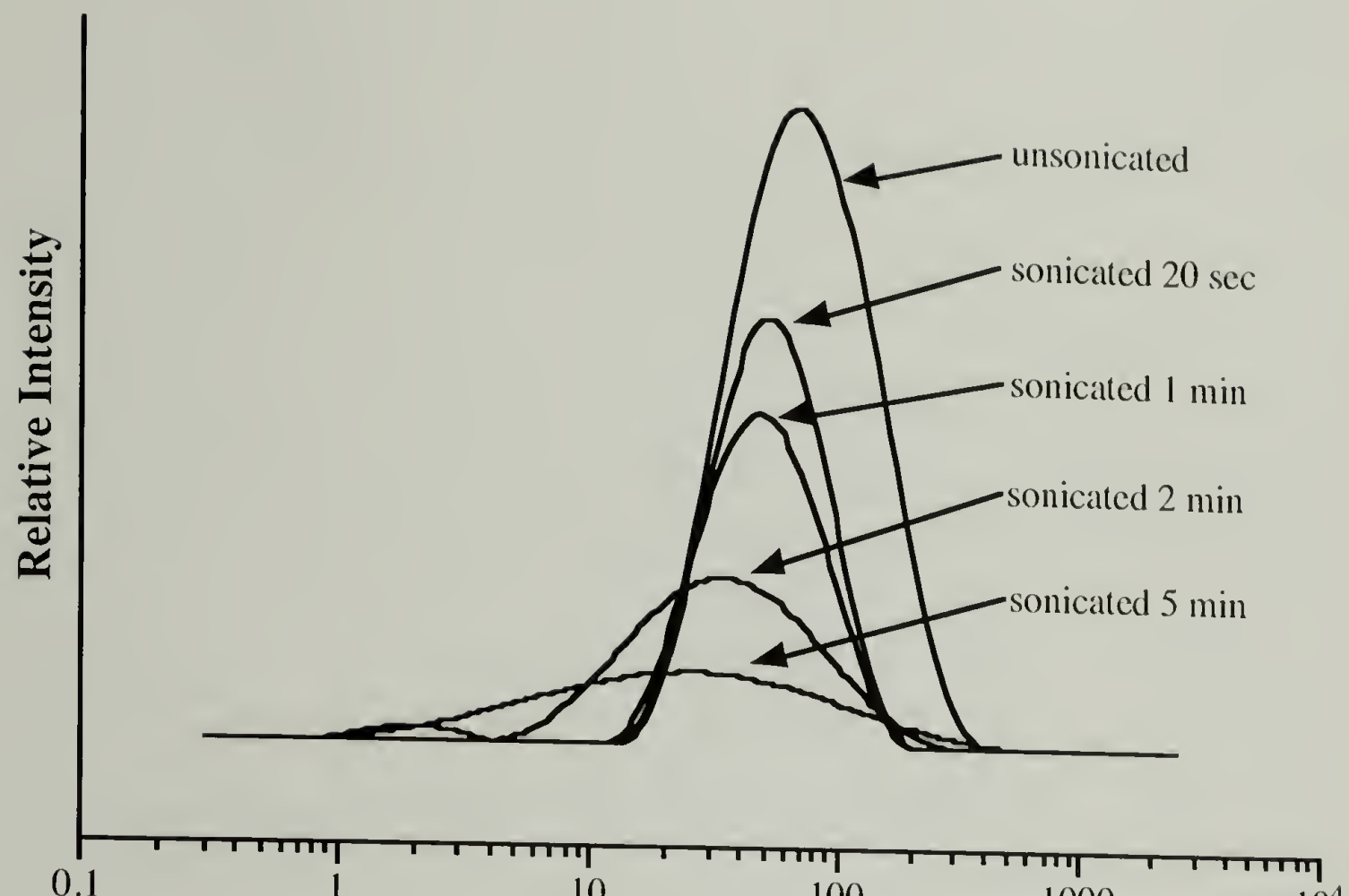

Figure A.9. Hydrodynamic radius distributions for sonicated samples of rhodamine-labeled poly(Am/DMAEA.MCQ) (4378-132SQ).

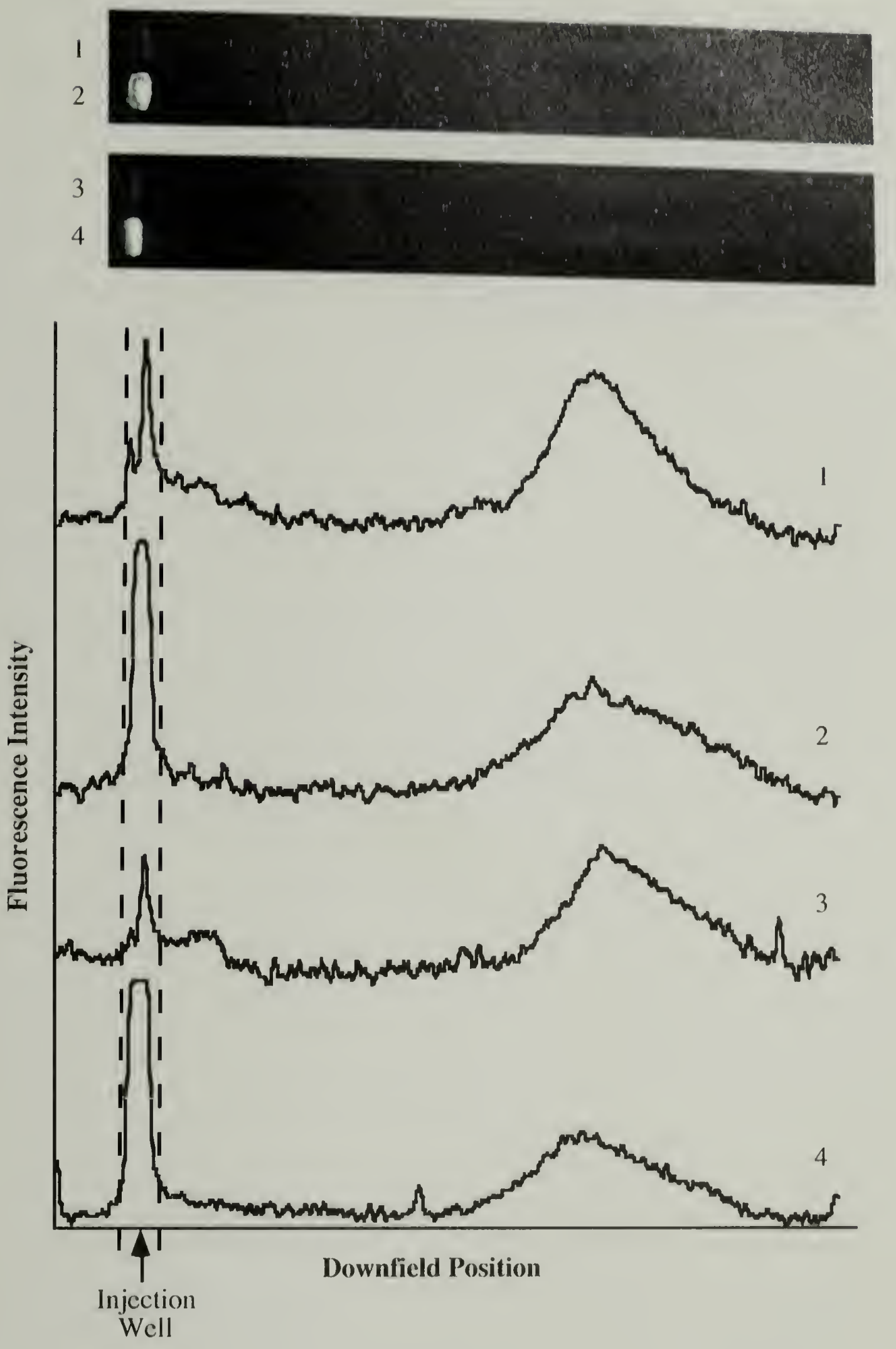

Figure A.10. Gel electrophoresis of rhodamine-labeled poly(Am/DMAEA.MCQ)s. **1**=centrifuged 4378-131SQ (supernatent), **2**=4378-131SQ, **3**=centrifuged 4378-132SQ (supernatent), **4**=4378-132SQ.

BIBLIOGRAPHY

1. Abramson, H. A.; Moyer, L. S.; Gorin, M. H. *Electrokinetic Theory and the Migration of Charged Particles*; Reinhold: New York, 1942, pp 105-142.

2. Alfrey, T., Jr.; Morawetz, H.; Fitzgerald, E. B.; Fuoss, R. M. *J. Am. Chem. Soc.* **1950**, *72*, 1864.

3. Allison, S. A.; Nambi, P. *Macromolecules* **1992**, *25*, 3971-3978.

4. Allison, S. A.; Nambi, P. *Macromolecules* **1994**, *27*, 1413-1422.

5. Allison, S. A.; Mazur, S. *Biopolymers* **1998**, *46*, 359-373.

6. Amankwa, L. N.; Scholl, J.; Kuhr, W. G. *Anal. Chem.* **1990**, *62*, 2189-2193.

7. Antonietti, M.; Vorwerg, L. *Colloid Polym. Sci.* **1997**, *275*, 883.

8. Anzuino, G.; Costantino, L.; Gallo, R.; Vitagliano, V. *Polym. Lett.* **1966**, *4*, 459-462.

9. Arvanitidou, E. S. Electrophoretic Transport Mechanisms of Highly Charged Polyelectrolytes; University of Massachusetts: Amherst, 1993.

10. Attard, P.; Antelmi, D.; Larson, I. *Langmuir* **2000**, *16*, 1542.

11. Barchini, R.; Saville, D. A. *Langmuir* **1996**, *12*, 1442.

12. Barchini, R.; van Leeuwen, H. P.; Lyklema, J. *Langmuir* **2000**, *16*, 8238.

13. Barrat, J.-L.; Joanny, J.-F. *Theory of Polyelectrolyte Solutions*; Prigogine, I. and Rice, S. A., Ed.; John Wiley: New York, 1996; Vol. 94, pp 1-62.

14. Barron, A. E.; Soane, D. S.; Blanch, H. W. *J. Chromatogr. A* **1993**, *652*, 3-16.

15. Barron, A. E.; Blanch, H. W.; Soane, D. S. *Electrophoresis* **1994**, *15*, 597-615.

16. Barron, A. E.; Blanch, H. W. *Separation and Purification Methods* **1995**, *24*, 1-118.

17. Bernard, O.; Turq, P.; Blum, L. *J. Phys. Chem.* **1991**, *95*, 9508-9513.

18. Borkovec, M.; Behrens, S. H.; Semmler, M. *Langmuir* **2000**, *16*, 5209.

19. Braud, C.; Vert, M. *Polym. Bull.* **1992**, *29*, 177-183.

20. Brothers, H. M.; Pichler, L. T.; Tomalia, D. A. *J. Chromatogr. A* **1998**, *814*, 233.

21. Bullock, J. *J. Chrom.* **1993**, *645*, 169-177.

22. Burgi, D. S.; Salomon, K.; Chien, R.-L. *J. Liq. Chrom.* **1991**, *14*, 847-867.

23. Butterman, M.; Tietz, D.; Orban, L.; Chrambach, A. *Electrophoresis* **1988**, *9*, 293-298.

24. Carney, S. L.; Osborne, D. J. *Anal. Biochem.* **1991**, *195*, 132-140.

25. Cha, C. Y.; Folger, R. L.; Ware, B. R. *J. Polym. Sci.: Polym. Phys. Ed.* **1980**, *18*, 1853-1857.

26. Chen, W.; Tomalia, D. A.; Thomas, J. L. *Macromolecules* **2000**, *33*, 9169.

27. Chiari, M.; Nesi, M.; Sandoval, J. E.; Pesek, J. J. *J. Chromatogr. A* **1995**, *717*, 1-13.

28. Chin, A. M.; Colburn, J. C. *Am. Biotech. Lab., News Ed.* **1989**, *7*, 16.

29. Cleland, R. L. *Macromolecules* **1991**, *24*, 4386-4390.

30. Cleland, R. L. *Macromolecules* **1991**, *24*, 4391-4402.

31. Clos, H. N.; Engelhardt, H. *J. Chromatogr. A* **1998**, *802*, 149-157.

32. Cohen, A. S.; Terabe, S.; Smith, J. A.; Karger, B. L. *Anal. Chem.* **1987**, *59*, 1021-1027.

33. Cohen, A. S.; Najarian, D.; Smith, J. A.; Karger, B. L. *J. Chrom.* **1988**, *458*, 323-333.

34. Cosgrove, T.; Obey, T. M.; Ryan, K. *Coll. Surf.* **1992**, *65*, 1-7.

35. Costantino, L.; Liquori, A. M.; Vitagliano, V. *Biopolymers* **1964**, *2*, 1-8.

36. Cottet, H.; Gareil, P.; Viovy, J.-L. *Electrophoresis* **1998**, *19*, 2151-2162.

37. Cottet, H.; Gareil, P.; Theodoly, O.; Williams, C. E. *Electrophoresis* **2000**, *21*, 3529.

38. Creeth, J. M.; Jordan, J. O.; Gulland, J. M. *J. Chem. Soc. (London)* **1949**, 1406-1409.

39. Creeth, J. M.; Jordan, D. O. *J. Chem. Soc. (London)* **1949**, 1409-1413.

40. Dalbiez, J. P.; Tabti, K.; Derian, P. J.; Drifford, M. *Revue Phys. Appl.* **1987**, *22*, 1013-1024.

41. Davis, R. M.; Russel, W. B. *Macromolecules* **1987**, *20*, 518-525.

42. Decher, G.; Hong, J. D.; Schmitt, J. *Thin Solid Films* **1992**, *210/211*, 831.

43. Dolnik, V.; Liu, J.; Banks, J. F., Jr.; Novotny, M. V.; Bocek, P. *J. Chrom.* **1989**, *480*, 321-330.

44. Drifford, M.; Menez, R.; Tivant, P.; Nectoux, P.; Dalbiez, J. P. *Revue Phys. Appl.* **1981**, *16*, 19-33.

45. Drifford, M.; Tivant, P.; Bencheikh-Larbi, F.; Tabti, K.; Rochas, C.; Rinaudo, M. *J. Phys. Chem.* **1984**, *88*, 1414-1420.

46. Drifford, M.; Dalbiez, J. P.; Tabti, K.; Tivant, P. *J. Chim. Phys.* **1985**, *82*, 571-577.

47. Dubin, P. L.; Tecklenburg, M. M. *Anal. Chem.* **1985**, *57*, 275-279.

48. Dubin, P. L. *Electrostatic Effects*; Dubin, P. L., Ed.; Elsevier: Amsterdam, 1988, pp 55-75.

49. Dukhin, S. S.; Derjaguin, B. V. *Electrokinetic Phenomena*; John Wiley & Sons: New York, 1974; Vol. 7.

50. Elimelech, M.; O'Melia, C. R. *Coll. Surf.* **1990**, *44*, 165.

51. Engelhardt, H.; Cuñat-Walter, M. A. *J. Chromatogr. A* **1995**, *716*, 27-33.

52. Fair, M. C.; Anderson, J. L. *J. Colloid Int. Sci.* **1989**, *127*, 388.

53. Fernández Barbero, A.; Martínez García, R.; Cabrerizo Vílchez, M. A.; Higaldo-Alvarez, R. *Coll. Surf. A* **1994**, *92*, 121.

54. Fitzgerald, E. B.; Fuoss, R. M. *J. Polym. Sci.* **1954**, *14*, 329-339.

55. Flygare, W. H.; Hartford, S. L. *Electrophoretic Light Scattering*; O'Konski, C. T., Ed.; Marcel Dekker: New York, 1976, pp 321-364.

56. Folkersma, R.; van Diemen, A. J. G.; Stein, H. N. *Langmuir* **1998**, *14*, 5973.

57. Förster, S.; Schmidt, M.; Antonietti, M. *Polymer* **1990**, *31*, 781.

58. Gao, J. Y.; Dubin, P. L.; Sato, T.; Morishima, Y. *J. Chrom. A* **1997**, *766*, 233-236.

59. Gao, J. Y.; Dubin, P. L.; Sato, T.; Morishima, Y. *J. Chromatogr. A* **1997**, *766*, 233-236.

60. Garcia, F.; Henion, J. D. *Anal. Chem.* **1992**, *64*, 985-990.

61. Gittings, M. R.; Saville, D. A. *Langmuir* **1995**, *11*, 798.

62. Gordon, M. J.; Huang, X.; Pentoney, S. L., Jr.; Zare, R. N. *Science* **1988**, *242*, 224-228.

63. Grossman, P. D.; Soane, D. S. *Anal. Chem.* **1990**, *62*, 1592-1596.

64. Grossman, P. D.; Soane, D. S. *J. Chrom.* **1991**, *559*, 257-266.

65. Grossman, P. D. *Free-Solution Capillary Electrophoresis*; Grossman, P. D. and Colburn, J. C., Ed.; Academic Press: San Diego, CA, 1992.

66. Guttman, A.; Cohen, A. S.; Heiger, D. N.; Karger, B. L. *Anal. Chem.* **1990**, *62*, 137-141.

67. Hartford, S. L.; Flygare, W. H. *Macromolecules* **1975**, *8*, 80-83.

68. Heegaard, N. H. H.; Robey, F. A. *American Laboratory* **1994**, 28T-28X.

69. Heiger, D. N.; Cohen, A. S.; Karger, B. L. *J. Chrom.* **1990**, *516*, 33-48.

70. Henry, D. C. *Proc. Roy. Soc., Ser. A* **1931**, *133*, 106-140.

71. Hermans, J. J.; Overbeek, J. T. G. *Rec. Trav. Chim.* **1948**, *67*, 761.

72. Hermans, J. J.; Fujita, H. *Proc. Akad. Amsterdam* **1955**, *B58*, 182-187.

73. Hermans, J. J. *J. Polym. Sci.* **1955**, *18*, 527-534.

74. Higaldo-Álvarez, R.; Martín, A.; Fernández, A.; Bastos, D.; Martínez, F.; de las Nieves, F. J. *Adv. Coll. Int. Sci.* **1996**, *67*, 1.

75. Hjertén, S. *J. Chromatogr.* **1985**, *347*, 191-198.

76. Hjertén, S.; Elenbring, K.; Kilar, F.; Liao, J.-L. *J. Chrom.* **1987**, *403*, 47-61.

77. Hoagland, D. A.; Smisek, D. L.; Chen, D. Y. *Electrophoresis* **1996**, *17*, 1151-1160.

78. Hoagland, D. A.; Smisek, D. L.; Chen, D. Y. *Electrophoresis* **1996**, *17*, 1151-1160.

79. Hoagland, D. A.; Arvanitidou, E.; Welch, C. *Macromolecules* **1999**, *32*, 6180.

80. Holmes, D. L.; Stellwagen, N. C. *Electrophoresis* **1990**, *11*, 5-15.

81. Hoss, U.; Batzill, S.; Deggelmann, M.; Graf, C.; Hagenbuchle, M.; Johner, C.; Kramer, H.; Martin, C.; Overbeck, E.; Weber, R. *Macromolecules* **1994**, *27*, 3429-3431.

82. Huang, Q. R.; Dubin, P. L.; Moorefield, C. N.; Newkome, G. R. *J. Phys. Chem. B* **2000**, *104*, 898.

83. Hückel, E. *Phys. Z.* **1924**, *25*, 204.

84. Imai, N.; Iwasa, K. *Israel J. of Chem.* **1973**, *11*, 223-233.

85. Jorgenson, J. W.; Lukacs, K. D. *Anal. Chem.* **1981**, *53*, 1298-1302.

86. Jorgenson, J. W.; Lukas, K. D. *Science* **1983**, *222*, 266-272.

87. Kasper, T. J.; Melera, M.; Gozel, P.; Brownlee, R. G. *J. Chrom.* **1988**, *458*, 303-312.

88. Kato, T.; Okamoto, T.; Tokuya, T.; Takahashi, A. *Biopolymers* **1982**, *21*, 1623-1633.

89. Kato, Y.; Matsuda, T.; Hashimoto, T. *J. Chromatogr.* **1985**, *332*, 39-46.

90. Khaledi, M. G. *Micellar Electrokinetic Chromatography*; Khaledi, M. G., Ed.; John Wiley & Sons: New York, 1998; Vol. 146, pp 77.

91. Klein, J. W.; Ware, B. R. *J. Chem. Phys.* **1984**, *80*, 1334-1338.

92. Koper, G. J. M.; van Genderen, M. H. P.; Elissen-Román, C.; Baars, M. W. P. L.; Meijer, E. W.; Borkovec, M. *J. Am. Chem. Soc.* **1997**, *119*, 6512.

93. LeBret, M.; Zimm, B. H. *Biopolymers* **1984**, *23*, 287-312.

94. Li, J.; Swanson, D. R.; Qin, D.; Brothers, H. M.; Piehler, L. T.; Tomalia, D.; Meier, D. J. *Langmuir* **1999**, *15*, 7347.

95. Lide, D. R. *CRC Handbook of Chemistry and Physics*; 76 ed.; CRC Press: Boca Raton, 1995.

96. Liu, J.; Shirota, O.; Novotny, M. *J. Chrom.* **1991**, *559*, 223-235.

97. Loeb, A. L.; Overbeek, J. T. G.; Wiersema, P. H. *The Electrical Double Layer Around a Spherical Colloid Particle*; MIT Press: Cambridge, 1961.

98. Long, D.; Viovy, J.-L.; Ajdari, A. *J. Phys.: Condens. Matter* **1996**, *8*, 9471-9475.

99. Long, D.; Viovy, J.-L.; Ajdari, A. *Phys. Rev. Lett.* **1996**, *76*, 3858-3861.

100. Lozada-Cassou, M.; González-Tovar, E.; Olivares, W. *Phys. Rev. E* **1999**, *60*, R17.

101. Lucy, C. A.; Underhill, R. S. *Anal. Chem.* **1996**, *68*, 300-305.

102. Magdelenat, H.; Turq, P.; Tivant, P.; Chemla, M.; Menez, R.; Drifford, M. *Biopolymers* **1979**, *18*, 187-201.

103. Mandel, M.; Leyte, J. C. *J. Polym. Sci.: Part A* **1964**, *2*, 3771-3780.

104. Manning, G. S. *Q. Rev. Biophys.* **1978**, *11*, 179-246.

105. Manning, G. S. *J. Phys. Chem.* **1980**, *84*, 1059.

106. Manning, G. S. *J. Phys. Chem.* **1981**, *85*, 1506-1515.

107. Manning, G. S. *J. Chem. Phys.* **1988**, *89*, 3772-3777.

108. Mathieson, A. R.; McLaren, J. V. *J. Chem. Soc. (London)* **1956**, 303-307.

109. Meullenet, J. P.; Schmitt, A.; Drifford, M. *J. Phys. Chem.* **1979**, *83*, 1924-1927.

110. Mikkers, F. E. P.; Everaerts, F. M.; Verheggen, T. P. E. M. *J. Chrom.* **1979**, *169*, 11-20.

111. Mills, R. A. *Biopolymers* **1970**, *9*, 1511-1530.

112. Misra, G. S.; Battacharya, S. N. *Eur. Polym. J.* **1979**, *15*, 125.

113. Moller, W. J. H. M.; van Os, G. A. J.; Overbeek, J. T. G. *Trans. Faraday Soc.* **1961**, *57*, 312-324.

114. Moller, W. J. H. M.; van Os, G. A. J.; Overbeek, J. T. G. *Trans. Faraday Soc.* **1961**, *57*, 325.

115. Mondescu, R.; Muthukumar, M. *To be submitted for publication* **1999**.

116. Muller, G.; Ripoll, C.; Selegny, E. *European Polym. J.* **1971**, *7*, 1373-1392.

117. Muthukumar, M. *Macromol. Theory Simul.* **1994**, *3*, 61-71.

118. Muthukumar, M. *Electrophoresis* **1996**, *17*, 1167-1172.

119. Nagasawa, M.; Soda, A.; Kagawa, I. *J. Polym Sci.* **1958**, *31*, 439-451.

120. Nagasawa, M.; Noda, I.; Takahashi, T.; Shimamoto, N. *J. Phys. Chem.* **1972**, *76*, 2286-2294.

121. Nakatani, M.; Shibukawa, A.; Nakagawa, T. *Electrophoresis* **1996**, *17*, 1210-1213.

122. Napjus, P. J.; Hermans, J. J. *J. Coll. Sci.* **1959**, *14*, 252-267.

123. Nierlich, M.; Boué, F.; Lapp, A.; Oberthur, R. *J. Physique* **1985**, *46*, 649-655.

124. Nisato, G.; Ivkov, R.; Amis, E. J. *Macromolecules* **2000**, *33*, 4172.

125. Noda, I.; Nagasawa, M.; Ota, M. *J. Am. Chem. Soc.* **1964**, *86*, 5075-5079.

126. Novotny, M.; Cobb, K. A.; Liu, J. *Electrophoresis* **1990**, *11*, 735-749.

127. O'Brien, R. W.; White, L. R. *J. Chem. Soc. Faraday Trans. II* **1978**, *74*, 1607.

128. O'Brien, R. W.; Ward, D. N. *J. Coll. Int. Sci.* **1988**, *121*, 402-413.

129. Offord, R. E. *Nature* **1966**, *211*, 591-593.

130. Olivera, B. M.; Baine, P.; Davidson, N. *Biopolymers* **1964**, *2*, 245-257.

131. Overbeek, J. T. G.; Stigter, D. *Rec. Trav. Chim. Pays Bas* **1956**, *75*, 543-554.

132. Overbeek, J. T. G.; Wiersema, P. H. *The Interpretation of Electrophoretic Mobilities*; Bier, M., Ed.; Academic Press: New York, 1967.

133. Paulus, A.; Gassmann, E.; Field, M. J. *Electrophoresis* **1990**, *11*, 702-708.

134. Pesak, D. J.; Moore, J. S.; Wheat, T. E. *Macromolecules* **1997**, *30*, 6467.

135. Poli, J. B.; Schure, M. R. *Anal. Chem.* **1992**, *64*, 896-904.

136. Prokopová, E.; Vitagliano, V. *Eur. Polym J.* **1972**, *8*, 851-859.

137. Prokopová, E.; Ciferri, A. *Biopolymers* **1972**, *11*, 1621-1626.

138. Radko, S. P.; Stastna, M.; Chrambach, A. *Anal. Chem.* **2000**, *72*, 5955.

139. Ramzi, A.; Scherrenberg, R.; Brackman, J.; Joosten, J.; Mortensen, K. *Macromolecules* **1998**, *31*, 1621.

140. Rasmusson, H. T.; McNair, H. M. *J. Chrom.* **1990**, *516*, 223-231.

141. Rasmusson, M.; Åkerman, B. *Langmuir* **1998**, *14*, 3512-3516.

142. Rasmusson, M.; Wall, S. *J. Coll. Int. Sci.* **1999**, *209*, 312.

143. Rasmusson, M.; Vincent, B.; Marston, N. *Coll. Polym. Sci.* **2000**, *278*, 253.

144. Record, M. T.; Woodbury, C. P.; Lohman, T. M. *Biopolymers* **1976**, *15*, 893-915.

145. Rhee, K. W.; Ware, B. R. *J. Chem. Phys.* **1983**, *78*, 3349-3353.

146. Rietveld, I. B.; Smit, J. A. M. *Macromolecules* **1999**, *32*, 4608.

147. Ripoll, C.; Muller, G.; Selegny, E. *European Polym. J.* **1971**, *7*, 1393-1409.

148. Ross, P. D. *Biopolymers* **1964**, *2*, 9-14.

149. Ross, P. D.; Scruggs, R. L. *Biopolymers* **1964**, *2*, 79-89.

150. Ross, P. D.; Scruggs, R. L. *Biopolymers* **1964**, *2*, 231-236.

151. Ruponen, M.; Yla-Herttuala, S.; Urtti, A. *Biochim. Biophys. Acta - Biomembranes* **1999**, *1415*, 331.

152. Russel, W. B.; Saville, D. A.; Schowalter, W. R. *Colloidal Dispersions*; Cambridge University Press: Cambridge, 1989.

153. Russell, A. S.; Scales, P. J.; Mangelsdorf, C. S.; Underwood, S. M. *Langmuir* **1995**, *11*, 1112.

154. Schellman, J. A.; Stigter, D. *Biopolymers* **1977**, *16*, 1415-1434.

155. Scherrenberg, R.; Coussens, B.; van Vliet, P.; Edouard, G.; Brackman, J.; de Brabender, E. *Macromolecules* **1998**, *31*, 456.

156. Schmalzing, D.; Piggee, C. A.; Foret, F.; Carrilho, E.; Karger, B. L. *J. Chromatogr. A* **1993**, *652*, 149-159.

157. Schmitt, A.; Meullenet, J. P.; Varoqui, R. *Biopolymers* **1978**, *17*, 413-423.

158. Schmitt, A.; Meullenet, J. P.; Varoqui, R. *Biopolymers* **1978**, *17*, 1249-1255.

159. Schofield, K. Hetero-Aromatic Nitrogen Compounds: Pyrroles and Pyridines; Butterworths: London, 1967.

160. Schurr, J. M.; Smith, S. B. *Biopolymers* **1990**, *29*, 1161-1165.

161. Seebergh, J. E.; Berg, J. C. *Coll. Surf. A* **1995**, *100*, 139.

162. Shaaban, A. H.; Behilo, K.; Ander, P. *Electric Transport of Polyelectrolytes in Aqueous Salt-Free Solutions*; Schmitz, K. S., Ed.; American Chemical Society: Washington, DC, 1994.

163. Shaw, J. N.; Ottewill, R. H. *Nature* **1965**, *208*, 681.

164. Shaw, D. J. *Introduction to Colloid and Surface Chemistry*; 3rd ed.; Butterworths: London, 1980.

165. Sherwood, J. D. *J. Chem. Soc., Faraday Trans. 2* **1982**, *78*, 1091-1100.

166. Smisek, D. L.; Hoagland, D. A. , Unpublished results.

167. Smisek, D. L.; Hoagland, D. A. *Macromolecules* **1989**, *22*, 2270-2277.

168. Smith, S. B.; Bendich, A. J. *Biopolymers* **1990**, *29*, 1167-1173.

169. Starkweather, M. E.; Muthukumar, M.; Hoagland, D. A. *Macromolecules* **1998**, *31*, 5495-5501.

170. Starkweather, M. E.; Muthukumar, M.; Hoagland, D. A. *Macromolecules* **1999**, *32*, 6837-6840.

171. Starkweather, M. E.; Hoagland, D. A.; Muthukumar, M. *Macromolecules* **2000**, *33*, 1245-1253.

172. Stellwagen, N. C.; Gelfi, C.; Righetti, P. G. *Electrophoresis* **1997**, *42*, 687-703.

173. Stigter, D.; Mysels, K. J. *J. Phys. Chem.* **1955**, *59*, 45.

174. Stigter, D. *J. Electroanal. Chem.* **1972**, *37*, 61.

175. Stigter, D. *J. Phys. Chem.* **1978**, *82*, 1424-1429.

176. Stigter, D. *J. Phys. Chem.* **1978**, *82*, 1603-1606.

177. Stigter, D. *J. Phys. Chem.* **1978**, *82*, 1417-1423.

178. Stigter, D. *J. Phys. Chem.* **1979**, *83*, 1663-1670.

179. Stigter, D. *J. Phys. Chem.* **1979**, *83*, 1670-1675.

180. Strauss, U. P.; Gershfeld, N. L.; Spiera, H. *J. Am. Chem. Soc.* **1954**, *76*, 5909-5911.

181. Strauss, U. P.; Woodside, D.; Wineman, P. *J. Phys. Chem.* **1957**, *61*, 1353-1356.

182. Strege, M.; Lagu, A. *Anal. Chem.* **1991**, *63*, 1233-1236.

183. Takahashi, T.; Noda, I.; Nagasawa, M. *J. Phys. Chem.* **1970**, *74*, 1280-1284.

184. Tinland, B.; Pluen, A.; Sturm, J.; Weill, G. *Macromolecules* **1997**, *30*, 5763-5765.

185. Tiselius, A. *Trans. Faraday Soc.* **1937**, *33*, 524-531.

186. Topp, A.; Bauer, B. J.; Prosa, T. J.; Scherrenberg, R.; Amis, E. J. *Macromolecules* **1999**, *32*, 8923.

187. Towns, J. K.; Regnier, F. E. *J. Chromatogr.* **1990**, *516*, 69-78.

188. Truong, N. D.; Galin, J. C.; François, J.; Pham, Q. T. *Polymer* **1986**, *27*, 459.

189. Tuffile, F. M.; Ander, P. *Macromolecules* **1975**, *8*, 789-792.

190. Tuin, G.; Senders, J. H. J. E.; Stein, H. N. *J. Coll. Int. Sci.* **1996**, *179*, 522.

191. Turco, G. P. Polyelectrolyte Dynamics; Diffusion and Electrophoresis in Complex Media; Univ. of Wisconsin, 1992.

192. van der Drift, W. P. J. T.; Overbeek, J. T. G. *J. Coll. Int. Sci.* **1979**, *71*, 79-92.

193. van der Drift, W. P. J. T.; de Keizer, A.; Overbeek, J. T. G. *J. Coll. Int. Sci.* **1979**, *71*, 67-78.

194. van Duijvenbode, R. C.; Borkovec, M.; Koper, G. J. M. *Polymer* **1998**, *39*, 2657.

195. Venkatarao, K.; Santappa, M. *J. Polym. Sci. A1* **1970**, *8*, 1785.

196. von Smoluchowski, M. *Z. Phys. Chem.* **1918**, *92*, 129.

197. Vorwerg, L.; Antonietti, M.; Tauer, K. *Coll. Surf. A* **1999**, *150*, 129.

198. Völkel, A. R.; Noolandi, J. *Macromolecules* **1995**, *28*, 8182-8189.

199. Völkel, A. R.; Noolandi, J. *J. Chem. Phys.* **1995**, *102*, 5506-5511.

200. Welch, P.; Muthukumar, M. *Macromolecules* **1998**, *31*, 5892.

201. Welch, C. F.; Hoagland, D. A. *Polymer Preprints* **1998**, *39(2)*, 771-772.

202. Whitlock, L. R.; Wheeler, L. M. *J. Chrom.* **1986**, *368*, 125-134.

203. Whitlock, L. R. *Isotachophoresis of Synthetic Ion-Containing Polymers*; Jorgenson, J. W. and Phillips, M., Ed.; American Chemical Society: Washington, DC, 1987, pp 222-245.

204. Wiersema, P. H.; Loeb, A. L.; Overbeek, J. T. G. *J. Coll. Int. Sci.* **1966**, *22*, 78-99.

205. Wilcoxon, J. P.; Schurr, J. M. *J. Chem. Phys.* **1983**, *78*, 3354-3364.

206. Xia, J.; Dubin, P. L.; Kukufuta, E. *Macromolecules* **1993**, *26*, 6688-6690.

207. Xia, J.; Dubin, P. L.; Havel, H. A. *Macromolecules* **1993**, *26*, 6335-6337.

208. Xia, J.; Dubin, P. L.; Izumi, T.; Hirata, M.; Kokufuta, E. *J. Polym. Sci.: Part B: Polym. Phys. Ed.* **1996**, *34*, 497-503.

209. Yamaguchi, M.; Yamaguchi, Y.; Matsushita, Y.; Noda, I. *Polymer J.* **1990**, *22*, 1077-1083.

210. Yen, W. S.; Rhee, K. W.; Ware, B. R. *J. Phys. Chem.* **1983**, *87*, 2148-2152.

211. Yoon, B. J.; Kim, S. *J. Coll. Int. Sci.* **1989**, *128*, 275-288.

212. Yoon, B. J. *J. Coll. Int. Sci.* **1997**, *192*, 503.

213. Zero, K.; Ware, B. R. *J. Chem. Phys.* **1984**, *80*, 1610-1615.

214. Zhu, M.; Hansen, D. L.; Burd, S.; Gannon, F. *J. Chromatogr.* **1989**, *480*, 311-319.

215. Zimm, B.; Stockmayer, W. *J. Chem. Phys.* **1949**, *17*, 1301.